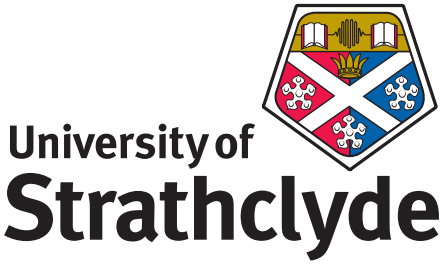

Reaction-Diffusion Equations with Saturating Flux Arising in the Theory of Solid-Solid Phase Transitions

Martin Burns

Department of Mathematics and Statistics

University of Strathclyde

Glasgow, UK

June 2011

This thesis is submitted to the University of Strathclyde for the degree of Doctor of Philosophy in the Faculty of Science.

This thesis is the result of the author's original research. It has been composed by the author and has not been previously submitted for examination which has led to the award of a degree.

Signed: Date:

Acknowledgements

I am indebted to EPSRC for the three and a half years of funding I received from them. I am also obliged to my supervisor Dr Michael Grinfeld who supported me throughout my PhD with his patience, knowledge and resolute dedication to ensuring that this thesis met with the high standards that he keeps. The numerous discussions I had with him on mathematics and philosophy in general proved to be invaluable. I am grateful to Dr John Mackenzie and Prof. Gabriel Lord for their help and advice on some of the numerical aspects of the thesis. Sincere thanks (and, in some cases, apologies) must go also to those with whom I have had the privilege of sharing an office. Their humour and optimism rescued me from peril and self-doubt more times than I care to recall. In fact, The Department of Mathematics and Statistics as a whole deserves huge credit for creating a pleasant and friendly working environment in which to carry out research. I would also like to thank my family and in particular my parents Ian and Linda to whom I owe all that I am and all that I can ever be.

Abstract

This thesis is concerned with two new one-dimensional models for solid-solid phase transitions. The models, the idea of which is due to P. Rosenau, are proposed to extend the Allen-Cahn and Cahn-Hilliard equations, which arise from the Ginzburg-Landau theory, to the case of large spatial gradients in the order parameter. The new models incorporate saturation of the diffusion flux, which should be expected of a physical process involving high gradients. We will study the effect that a saturating diffusion flux has on the ensuing morphology of the system and contrast this with the situation in the case of previous models. We show for example that, unlike the situation for the Allen-Cahn and Cahn-Hilliard equations, discontinuous equilibria are now admissible and we discuss questions of structure and stability of equilibria, stabilisation and the dynamics of coarsening in the new models.

Contents

Chapter 1

Introduction

1.1 Phase transitions

Phase transitions are of great academic interest and considerable technological importance. In many contexts, it is essential to describe how a (mixture of) phase(s) in a physical system changes into a new (mixture of) phase(s). Examples of phase transitions include metal casting, crystal growth, glass formation and the phase separation in alloys. We can speak of a solid-solid phase transition whenever there is a transition from one solid state to another solid state, as in phase separation in a metallic alloy or in the conversion of a metal (e.g. iron) from a paramagnetic state, in which the material is not magnetised in the absence of an applied magnetic field, to a ferromagnetic state, in which the material is magnetised even when no field is applied. The second of these two examples of solid-solid phase transitions is known as the phenomenon of **ferromagnetism**.

Assume that we have a physical system occupying a domain $\Omega \subset \mathbb{R}^n$, $n \geq 1$. Then the state of a system undergoing a phase transition over time t can be described by an **order parameter** $u(x,t)$, $x \in \Omega$, which distinguishes different phases. In this thesis, we are concerned with the simplest case of a **scalar** order parameter which takes values in a bounded interval on the real line since we are only interested in

materials which can exist in two phases. If, for instance, one were interested in modelling the phase separation of an alloy consisting of three or more components then one would need to consider taking the order parameter to be a vector [28, 35]. We think of the order parameter as a measure of the local microscopic order of a material which can exist in two phases and the order parameter varies between one value u_1, which represents one phase, and another value u_2 which represents the other phase. If the phase transition is governed by a conservation law then we are in the case of a **conserved order parameter**. We have a **non-conserved order parameter** whenever there are no global constraints on the order parameter. An example of a conserved order parameter phase transition is the phase separation of a binary alloy in which the order parameter may be taken to be the local concentration of one of the two components of the alloy or the difference between the local concentrations of each of the two components of the alloy (see (1.2) and (1.3) respectively). An example of a non-conserved order parameter phase transition is the phenomenon of ferromagnetism which we discuss in detail below in order to introduce the necessary concepts.

Often there exists a **critical** temperature T_c such that for temperatures $T > T_c$, the material exists in a stable uniform state $u(x,t) = \bar{u}$ and for $T < T_c$ (the **subcritical temperature regime**), the uniform state can lose stability. By the mathematical study of phase transitions we mean the study of the evolution of $u(x,t)$ in the subcritical temperature regime. In the case of a ferromagnet (as described in, for example, [8, Chapter 1]), in the absence of an applied magnetic field, the material undergoes a spontaneous transition from a disordered (paramagnetic) phase, in which there is no net magnetisation (this is the uniform state), to an ordered (ferromagnetic) phase, in which the material has non-zero magnetisation, at some critical transition temperature T_c known in this context as the **Curie temperature**. Conversely, as one heats a sample of a ferromagnetic material through the critical temperature T_c, the material's mean magnetisation steadily decreases

as T_c is approached and vanishes entirely at T_c and for all higher temperatures as in Figure 1.1.

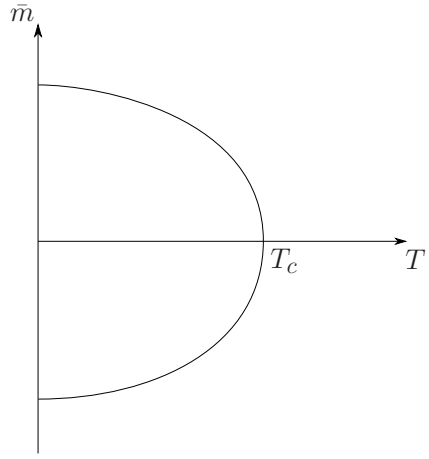

Figure 1.1: Average magnetisation $\bar{m}$ of a ferromagnet in the absence of an applied field against temperature T. For $T < T_c$, there is a spontaneous average magnetisation $\pm\bar{m}(T)$.

Hence the uniform state is no longer stable once $T < T_c$. From the microscopic point of view, the system consists of a lattice populated by two sorts of spins ("up" and "down"). In the paramagnetic state ($T > T_c$), there is no preferred direction for the magnetic moments of the spins, hence no net magnetisation. Below the critical temperature T_c, some spins flip in such a way as to become aligned with their nearest neighbours in the lattice as the material becomes magnetised. This type of dynamics is commonly referred to as **Glauber dynamics** [33]. Suppose we assign to a site i an occupation variable s_i, with $s_i = +1$ if the spin at site i is up and $s_i = -1$ if the spin at site i is down. At the *continuum* level, we take the order parameter $u(x,t)$ at some $x \in \Omega$ and time t, to be the **instantaneous mean magnetisation** in a small ball $B(x,r)$ of radius r centred at x. That is, we take

$$u(x,t) = \lim_{r\to 0} \frac{1}{r} \sum_{i\in B(x,r)} s_i(t), \tag{1.1}$$

so that $u(x,t)$ represents the average of the spins in the vicinity of the point $x \in \Omega$ at a particular time t.

To relate this to the conserved order parameter situation, consider the phase separation of a binary alloy which is experimentally seen to occur if the high temperature, at which alloys are prepared (so that the material is in a homogeneous disordered phase), is reduced rapidly to a temperature below a critical value T_c at which the material is seen to separate into regions of predominantly one component or the other. Once again the uniform mixed state is no longer stable once the temperature T is less than some critical temperature T_c. At the atomic level, we now consider a lattice populated by two sorts of atoms, say A and B, and the occupation variable s_i is now such that $s_i = +1$ if we find an A-atom at site i and $s_i = -1$ if we find a B-atom at site i. This time the "spins" do not flip from one sign to the other since flipping a single "spin" in this model would correspond to converting an A-atom into a B-atom (or vice versa), which is inadmissible. Instead, there is a direct interchange between two neighbouring "spins" in the material below the critical temperature T_c. This type of dynamics is known as **Kawasaki dynamics** [41]. At the *continuum* level, the order parameter in this case may be taken to be the concentration of one of the two components of the binary mixture or the difference between the local concentrations of each of the two species of the alloy. For example, suppose that the binary alloy under consideration is the iron-nickel (Fe-Ni) alloy. Then we can take the order parameter to be

$$\frac{[Fe](x,t)}{[Ni](x,t) + [Fe](x,t)} = v(x,t), \quad x \in \Omega, \tag{1.2}$$

where $[Fe](x,t)$ and $[Ni](x,t)$ are respectively the number of iron and the number of nickel atoms in a small ball around $x \in \Omega$ at some time t, in which case

$v(x,t) \in [0,1]$. Alternatively, we can can take the order parameter to be

$$\begin{aligned} u(x,t) &= 1 - 2v(x,t) \\ &= \frac{[Ni](x,t) - [Fe](x,t)}{[Ni](x,t) + [Fe](x,t)}, \end{aligned} \tag{1.3}$$

so that $u(x,t)$ is restricted to lie in the interval $[-1,1]$ and positive (negative) values of u correspond to Ni (Fe)-rich regions. If $u = +1$ then we are in the pure Ni-phase and $u = -1$ means that we are in the pure Fe-phase. When $u = 0$, we have a one-to-one composition. Also, since the total order parameter is to be conserved, the following constraint is imposed

$$\frac{1}{|\Omega|} \int_{\Omega} u(x,t)\, dx = M \quad \forall t,$$

where $|\Omega|$ denotes the volume of the domain and $|M| \leq 1$ is a constant.

As mentioned, below some critical temperature T_c, the alloy can no longer exist in equilibrium in its homogeneous state and the alloy tends to separate and order over time into a coarse mixture of its original materials. The order parameter u, i.e. the difference between the local concentrations of each of the two species, changes as the system is quenched below T_c from the homogeneous mixed state ($u = 0$) to that of a spatially separated two-phase structure where each phase is characterised by a different value of u which is either -1 or 1. For more details on phase separation, one can consult the survey paper [29] of Fife.

We postulate the existence of a **bulk free energy** which is defined in terms of the order parameter and the change in the bulk free energy with temperature T is used to explain the dynamics of a system following a quench from a disordered phase to an ordered phase. As explained in [59, Chapter 4], Landau theory is concerned with the phenomenological description of phase transitions and is based on the assumption that in the vicinity of the critical temperature T_c, the bulk free energy of the system is an analytic function of the order parameter u where only

those terms compatible with the symmetry of the system are retained. In the case of a simple ferromagnet in zero external field, the Landau theory predicts that the paramagnetic ($u = 0$) to ferromagnetic ($u \neq 0$) transition can be described by an expansion of the bulk free energy $E(u, T)$ in powers of the order parameter u

$$E(u, T) = \alpha(T) + \beta(T)u^2 + \gamma(T)u^4, \tag{1.4}$$

where, because of the up-down spin symmetry of the system, the expansion contains only even powers of u. In (1.4), the phenomenological parameters $\alpha(T)$, $\beta(T)$ and $\gamma(T)$ are assumed to be smooth functions of the temperature T where $\alpha(T)$ and $\gamma(T)$ are positive for all T and $\beta(T)$ is positive for $T > T_c$ and negative for $T < T_c$.

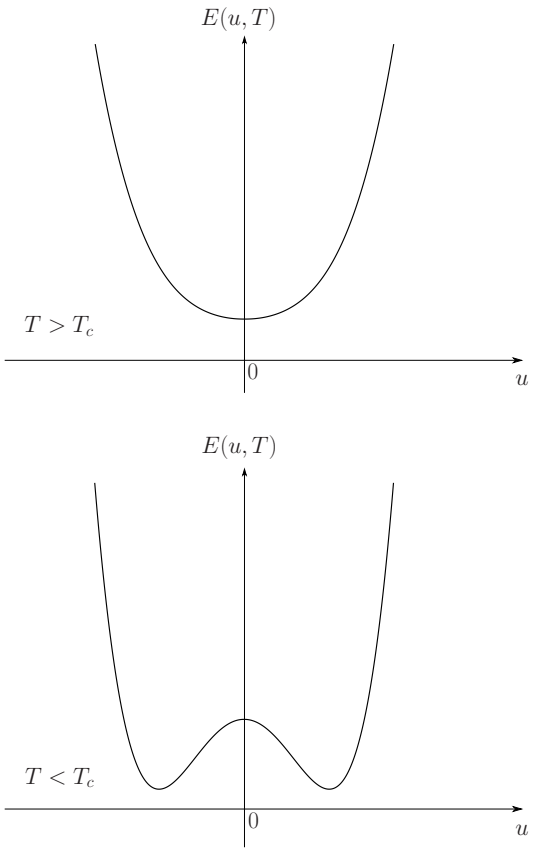

Figure 1.2: The bulk free energy $E(u, T)$ for some temperature $T > T_c$ and for some temperature $T < T_c$.

Hence at high temperatures ($T > T_c$), the bulk free energy $E(u,T)$ is a convex function of u and is minimised by $u = 0$ which corresponds to the disordered paramagnetic state. The state of the system undergoes a sudden change when we reach $T = T_c$ at which $\beta(T) = 0$ in (1.4). Below the critical temperature T_c, the minima of $E(u,T)$ occur at $u = \pm\sqrt{\frac{-\beta(T)}{2\gamma(T)}}$ and these correspond to the equilibrium states in the ordered phase. The bulk free energy for $T < T_c$ also has a local maximum at $u = 0$ corresponding to the disordered state which is unstable in the subcritical temperature regime. In summary, the bulk free energy is to be convex for $T > T_c$ and to have two symmetric wells at $u = \pm\sqrt{\frac{-\beta(T)}{2\gamma(T)}}$ for $T < T_c$ as in Figure 1.2.

That the wells arising in the subcritical temperature regime are symmetric makes sense in this situation since the two equilibrium states for $T < T_c$ are identical in all aspects except in the direction of the magnetisation. Note that assuming $\gamma(T) > 0$ in (1.4) corresponds to the physical condition that the magnetisation be finite. Also, the series is truncated after the term $O(u^4)$ since, as argued in [59], if $\gamma(T) > 0$, subsequent terms in (1.4) cannot alter the critical behaviour of the system.

As we have discussed, we are only interested in the evolution of the order parameter $u(x,t)$ in the subcritical temperature regime and we therefore fix T in (1.4) such that $T < T_c$ so that we can then take

$$\beta(T) = -b, \quad \gamma(T) = c,$$

in (1.4) for some constants $b, c > 0$. Denote $W(u,T) = E(u,T) - \alpha(T)$ and scale the order parameter $u \in \left[-\sqrt{\frac{b}{2c}}, \sqrt{\frac{b}{2c}}\right]$ as $u \mapsto \sqrt{2b}u$ so that $u \in \left[-\sqrt{\frac{b^2}{c}}, \sqrt{\frac{b^2}{2}}\right]$ and

$$W(u,T) = -\frac{u^2}{2} + \frac{cu^4}{4b^2}, \tag{1.5}$$

from (1.4). Without loss of generality, we choose constants b and c such that $\frac{c}{b^2} = 1$ in (1.5) since physically, in both the case of the ferromagnet and the binary

alloy, we require the order parameter to be restricted to $[-1, 1]$. Therefore, in the subcritical temperature regime, we may regard the bulk free energy $W = W(u)$ as a double-well function, e.g. $W(u) = \frac{u^4}{4} - \frac{u^2}{2}$, of the order parameter u only which has minima at $u = \pm 1$.

In order to account for energy contributions from phase boundaries, Ginzburg and Landau (see [44]) augmented the bulk free energy $W(u)$ with a gradient term $\frac{\epsilon}{2}|\nabla u|^2$ where $\epsilon > 0$ is a small parameter. The total free energy of the system at a fixed temperature below T_c over a domain Ω is then given by

$$E[u](t) = \int_\Omega \left[W(u) + \frac{\epsilon}{2}|\nabla u|^2 \right] dx, \tag{1.6}$$

where $\Omega \subset \mathbb{R}^n$, $n \geq 1$, corresponds to the region occupied by the material under consideration and $W(u)$ is of double-well type. The functional in (1.6) is often referred to as the Ginzburg-Landau free energy functional and it will be also be discussed in Section 2.1.1. The free energy (1.6) at a constant temperature is derived in [44] (and also in [13] under the constraint that the total order parameter u be conserved) by assuming that the local free energy per unit volume is a smooth function of u *and* its derivatives so that it can be expanded in Taylor series about the uniform composition $\bar{u}$ where only leading terms are retained. Hence the theory is based on the assumption of small gradients in the order parameter.

The Allen-Cahn [2] and Cahn-Hilliard [13] equations have been used to simulate many phase transition phenomena in solids. The Cahn-Hilliard equation models conserved order parameter processes such as the phase separation in binary alloys and the Allen-Cahn equation models non-conserved order parameter processes such as phase transitions in a ferromagnetic material. The equations may be obtained by considering **gradient flows** of the associated free energy of the system which in the case of both of these equations is given by the Ginzburg-Landau free energy functional (1.6). We will see how these and other equations can be obtained in

this way in the next chapter.

In the Ginzburg-Landau framework for solid-solid phase transitions, equilibrium states with sharp interfaces are not permitted. Focussing on the one-dimensional situation (since this will be the setting of interest to us in subsequent chapters) we can see this from the point of view of the Ginzburg-Landau free energy functional in (1.6) in which we take $\Omega \equiv (0, L) \subset \mathbb{R}$ for some $L > 0$. Suppose we consider only the interacting part of the free energy functional by setting $W(u) \equiv 0$ in (1.6). The one-dimensional Sobolev space $H^1(0, L)$ is embedded in the space $C([0, L])$ of continuous functions. In fact, according to the Sobolev embedding theorem (see [1])

$$H^1(0, L) \subset C^{0,\frac{1}{2}}([0, L]),$$

where $C^{0,\frac{1}{2}}([0, L])$ is the Hölder space of all functions $u \in C([0, L])$ for which

$$\sup_{x,y\in(0,L),\, x\neq y} \left\{ \frac{|u(x) - u(y)|}{|x - y|^{\frac{1}{2}}} \right\} < \infty.$$

The interacting part of the free energy in (1.7) grows quadratically in the norm of the gradient and this implies unbounded energy across a sharp interface in this one-dimensional situation since if u is not continuous then u is not an $H^1(\Omega)$ function by the above arguments and therefore the quantity $\int_\Omega u_x^2\, dx$ is not finite. Consequently such interfaces must be precluded.

Philip Rosenau [52] looked to extend the Ginzburg-Landau small-gradient theory in the one-dimensional setting to domains of higher gradients in the order parameter by modifying the free energy functional (1.6) in such a way as to ensure that the interaction energy across a sharp interface be finite. In other words, he considered the more general free energy functional

$$E_{\mathcal{R}}[u] = \int_\Omega [W(u) + \epsilon\Psi(u_x)]\, dx, \tag{1.7}$$

and imposed the condition that $\int_\Omega \Psi(u_x)\,dx$ in (1.7) remains bounded for arbitrarily large gradients. The main step lies in choosing a form for Ψ in (1.7) which interpolates between the small gradient regime and the large gradient limit. We will discuss this in more detail in Section 2.1.4 but we note here that with Rosenau's choice for Ψ, the free energy functional (1.7) has a linear growth rate in the spatial gradient of the order parameter (which allows for equilibrium states with genuinely sharp interfaces). Additionally [53], an initial state endowed with sharp interfaces does not become smooth immediately and discontinuities persist for a finite time after which they disappear. It is natural to view $-\Psi'(u_x)$ as a flux of u which, since $\Psi(s)$ has linear growth at infinity, is monotone, bounded and saturates at a finite value as $|u_x| \to \infty$. Note that although saturation of the flux is a necessary condition in delaying the resolution of discontinuities, it is not sufficient and an appropriate saturation rate is needed to sustain discontinuities [53]. If initial discontinuities persist for a finite time, we say that the saturation is **strong**. Otherwise, the discontinuity disappears immediately and the saturation is said to be **weak**. Equations with a strongly saturating flux are the ones that we will consider in the subsequent chapters. The purpose of this thesis is to investigate in the one-dimensional setting the consequences of taking the Rosenau saturating flux theory for phase transitions in solids instead of the more usual Ginzburg-Landau framework.

1.2 Thesis outline

The thesis is organised as follows. Chapter 2 contains necessary background material on models for solid-solid phase transitions and the mathematical tools that we will employ. Chapters 3 to 5 comprise the original material of this thesis. In Chapter 3 we discuss a one-dimensional model which has the saturating diffusion mechanism introduced in [52] to replace the Allen-Cahn equation in the case of large gradients. We prove a well-posedness result for (weak) solutions to this model

and then present numerical simulations pertaining to the asymptotic behaviour of solutions to this new model. This work has led to a publication [11] which is to appear in the journal Communications in Applied Analysis.

In Chapter 4 we study the stationary problem associated with the model discussed in Chapter 3. After defining what we mean by a solution to this problem, we prove some results relating to its classical solutions. We first prove local bifurcation results for solutions to the stationary problem and then show that as the bifurcation parameter (which physically corresponds to the reciprocal of the diffusion coefficient) is increased, solutions to the stationary problem develop infinite gradient in the interior of the space interval and classical solutions cease to exist. We will see that these bifurcation results depend on the length of the space interval as well as on the bifurcation parameter. We prove that the non-constant classical solutions are unstable and then discuss non-classical (discontinuous) solutions to the problem. We derive a formal construction for non-classical solutions to the problem through phase plane arguments and then establish that this formal construction satisfies our definition of a solution and delivers an uncountable number of solutions to the stationary problem. We conclude this chapter with a presentation of numerical simulations for non-classical solutions to the problem which suggest that the non-classical solutions possess certain stability properties. The work contained in this chapter has led to a publication [12] to appear in the European Journal of Applied Mathematics.

Chapter 5 deals with a mass-conserving version of the Rosenau model described in Chapter 3. This equation can also be viewed as a quasilinear analogue of the semilinear equation introduced by Rubinstein and Sternberg in [54]. We are interested in the stationary solutions to this (non-local) quasilinear model. We establish local bifurcation results similar to those for the semilinear (Cahn-Hilliard) case considered in [26] except that our results depend on the length of the space

interval as well as on the bifurcation parameter (which again corresponds to the reciprocal of the diffusion coefficient) and the average mass of a solution to the problem. We then show that for a given length of the space domain and for each average mass of a solution within a certain prescribed range, we have non-existence of classical solutions whenever the bifurcation parameter is large enough. These results are illustrated numerically using path-following methods. We conclude this chapter with a derivation of a numerical scheme for the full evolution problem and prove that this numerical scheme conserves mass. We then use this scheme to present and discuss numerical simulations for the full evolution problem. The thesis concludes with a summary of our main results and suggestions for further work.

Chapter 2

Preliminary Material

2.1 Gradient flows

We are concerned in this section with the derivation of evolution equations describing phase transitions in solids such as ferromagnetic phase transitions or phase separation in binary alloys. In order to do this, one assumes that the behaviour of the system can be described by a free energy functional defined as a function of an order parameter. We take the point of view that the material structure changes in such a way as to decrease the free energy of the system as required by thermodynamic principles. On a simple level of understanding, the total energy of a physical system at a constant temperature can be considered as the sum of the free energy and the entropy in the system. That is, it is the sum of the energy available to do work and the energy unavailable to do work. According to the second law of thermodynamics, the entropy in a physical system that does not interact with its surroundings (i.e. a system that is isolated) will tend to increase with time. Hence in order to preserve the conservation of energy principle, the free energy of the mixture must counterbalance this by decreasing over time. Thus we expect the system to evolve in such a way that the free energy decreases with time.

The approach we take here to achieve this follows the approach of Fife in [29]

which postulates the evolution of a state as a **gradient flow** of the free energy functional $E[u]$ which is defined by

$$\frac{\partial u}{\partial t} = -\text{grad}\, E[u], \tag{2.1}$$

so that u evolves in the direction opposite to the gradient of the free energy functional. Note that for each t, $u(t)$ is a function of position i.e. $u(t)$ belongs to some function space X defined on a spatial domain so that $\frac{\partial u}{\partial t} \in X$ for all $t > 0$. On the other hand, $E : X \to \mathbb{R}$ is a nonlinear functional and $\text{grad}\, E[u]$ in (2.1) is a linear functional on X defined by

$$\frac{d}{dh} E[u + hv]|_{h=0} = \langle \text{grad}\, E[u], v \rangle \quad \forall v \in X,$$

where $< \cdot, \cdot >$ denotes the duality pairing in X. So for (2.1) to make sense we must be able to identify $\text{grad}\, E[u]$, which is an element of the dual space of X, with an element of X and therefore it makes sense to choose X to be a Hilbert space. We make our definitions more formal now that we know that we are going to be working in a Hilbert space setting.

Definition 2.1. *For a Hilbert space H, let $\langle \cdot, \cdot \rangle$ denote the H^*, H pairing and $(\cdot, \cdot)$ the H inner product. A functional E on H is said to be Gateaux differentiable at $u \in H$ with derivative (or first variation) $E'[u] \in H^*$ if*

$$\lim_{h \to 0} \frac{E[u + hv] - E[u]}{h} = \langle E'[u], v \rangle \quad \forall v \in H,$$

i.e. if

$$\frac{d}{dh} E[u + hv]|_{h=0} = \langle E'[u], v \rangle \quad \forall v \in H.$$

So if E is Gateaux differentiable at $u \in H$ it then follows from the Riesz Representation Theorem that there exists a *unique* $w(u) \in H$ such that

$$\langle E'[u], v \rangle = (w(u), v) \quad \forall v \in H. \tag{2.2}$$

Definition 2.2. *The $w(u)$ in (2.2) is the classical or unconstrained gradient of E at u which we denote by* $\operatorname{grad} E[u]$ *i.e.*

$$\frac{d}{dh}E[u+hv]|_{h=0} = (\operatorname{grad} E[u], v) \ \ \forall v \in H.$$

Now let $\mathcal{M}$ be an affine linear subspace (or linear manifold) of the Hilbert space H. Hence $\mathcal{M}$ is a translate of some linear subspace of H, that is, there exists $\hat{u} \in H$ and a linear subspace $\mathcal{N}$ of H such that

$$\mathcal{M} = \hat{u} + \mathcal{N} = \{\hat{u} + v : v \in \mathcal{N} \subset H\}.$$

Definition 2.3. *We denote the constrained gradient of $E[u]$ in H by* $\operatorname{grad}_{\mathcal{M}} E[u]$ *defined as an element in $\overline{\mathcal{N}}$ such that*

$$\frac{d}{dh}E[u+hv]|_{h=0} = (\operatorname{grad}_{\mathcal{M}} E[u], v) \ \ \forall v \in \mathcal{M},$$

when such an element exists.

So Definition 2.2 is the same as Definition 2.3 when $\mathcal{M} = H$.

2.1.1 The free energy

Suppose, as in Section 1.1 we have a physical system which can locally be described by a scalar order parameter $u \in [-1, 1]$ which depends on space and time. The system may, for example, consist of a sample of ferromagnetic material which, at the atomic level, has two possible spins ± 1 as described in Section 1.1. It may instead consist of a crystalline material with two possible lattice structures which are represented by the order parameter assuming either the value $+1$ or the value -1. The order parameter taking values in the interval $(-1, 1)$ then corresponds, in case of the ferromagnet, to a local mean magnetisation which may be obtained by a coarse graining (as in (1.1)) or, in the case of the model of the crystal, to mixtures of the two lattice structures. To model such a situation, a

possible first step would be to derive a free energy associated with a configuration u. In either the case of the ferromagnetic material or the case of the crystalline structure, it is more favourable for the sample to attain values close to ± 1 than to attain an intermediate value in $(-1, 1)$. This is true in the case of the coarse grained ferromagnet if one considers the microscopic dynamics since, as discussed in Chapter 1, it is energetically favourable for an atom to have the same spin as its neighbours and in the case of the crystal because the pure lattice structures are the most favourable. This effect is accounted for by the potential energy

$$E_0[u] = \int_\Omega W(u(x))\, dx, \tag{2.3}$$

where $\Omega \subset \mathbb{R}^n$ with $n \geq 1$ denotes the spatial domain occupied by the material under consideration and, as explained in Chapter 1,

$$W(u) = \frac{u^4}{4} - \frac{u^2}{2} = -\int_0^u f(s)\, ds, \tag{2.4}$$

represents the bulk energy of the system, i.e. the free energy density that the material would have if each of its components had a uniform spatial distribution. So $W(u)$ is a smooth double-well potential whose wells $u = -1$ and $u = 1$ define the two phases of the system and $f(u) = -W'(u)$ is a (dissipative) bistable non-linearity. This means that $f(u)$ is assumed to have three simple zeros at u_1, u_2 and at u_0 with u_0 situated between u_1 and u_2. Hence $f(u)$ is such that

$$\begin{aligned} &f(u) = 0 \Leftrightarrow u = u_1 \text{ or } u_0 \text{ or } u_2, \\ &f'(u) < 0 \text{ if } u < u_1^* \text{ or } u > u_2^*, \\ &f'(u) > 0 \text{ if } u_1^* < u < u_2^*, \end{aligned}$$

where $u_1 < u_1^* < u_0 < u_2^* < u_2$ as in Figure 2.1.

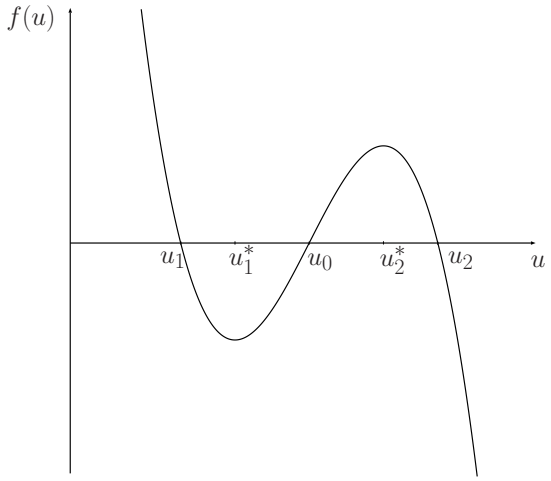

Figure 2.1: The bistable function $f(u)$.

The three intermediate intervals are given the following names

(u_1, u_1^*) is called metastable interval 1;

(u_1^*, u_2^*) is called the spinodal interval;

(u_2^*, u_2) is called metastable interval 2.

In particular, if we take $f(u) = u - u^3$ then $u_1 = -1$, $u_0 = 0$ and $u_2 = 1$, the spinodal interval is $(u_1^*, u_2^*) = \left(-\frac{1}{\sqrt{3}}, \frac{1}{\sqrt{3}}\right)$ and the metastable interval is $(u_1, u_1^*) \cup (u_2^*, u_2) = \left(-1, -\frac{1}{\sqrt{3}}\right) \cup \left(\frac{1}{\sqrt{3}}, 1\right)$.

Suppose we take the free energy functional to be given by (2.3). Then one would be tempted to model the evolution of u by letting u evolve in such a way that the functional E_0 decreases with time. This would mean that the appropriate minimum of E_0 would be taken up by functions u which assume only the two values -1 and 1 (as desired) where -1 and 1 are the preferred states of u in the sense that they ensure that free energy will be of moderate size. As discussed in Section 2.1, one method to ensure that u evolved in such a way that E_0 decreases in time would be to let u evolve in the direction opposite to that of the gradient of E_0 at u.

One objection to this approach with the free energy as it is in (2.3) would be that

u could oscillate wildly between -1 and 1 in space but the energy in (2.3) remains unaffected. We would expect the energy to penalise these large transitions in phase and, as explained in Chapter 1, this is done by including some small gradient term

$$\frac{\epsilon}{2}\int_{\Omega}|\nabla u(x)|^2\,dx, \tag{2.5}$$

in the free energy functional (2.3) where ϵ is a small positive parameter. The gradient term in (2.5) is the contribution to the free energy of creating interfaces which roughly speaking are the sets separating regions where the order parameter u is positive from regions where u is negative.

This produces the Ginzburg-Landau free energy functional introduced in Chapter 1 and given by

$$E_\epsilon[u] = E[u] = \int_{\Omega}\left[W(u(x)) + \frac{\epsilon}{2}|\nabla u(x)|^2\right]\,dx, \tag{2.6}$$

so that ϵ is a measure of the relative strength of the two terms in (2.6). Hence the contribution to the free energy from (2.5) tends to spread the interface region and thereby reduce the gradient as the order parameter changes between its stable values -1 and 1. So we think of the first term in (2.6) as penalising states which take values other than -1 and 1 and of the second term as penalising spatial non-uniformity. Hence one would expect to observe competition between the effects of an attraction of the material towards either one of the "pure" states -1 or 1 and a tendency for the material to become spatially homogeneous. We say more on this competition and its effects on the dynamics in Secton 2.1.3.

2.1.2 Gradient flows of the Ginzburg-Landau functional

The Allen-Cahn equation is a semilinear elliptic equation which was introduced in [2] to model the growth of grains in crystalline materials near their melting point. It is one of the simplest conceivable models describing order-disorder kinetics and the evolution of interfaces between phases which does not preserve the total order parameter. The equation is given by

$$\frac{\partial u}{\partial t} = \epsilon \Delta u + f(u), \quad x \in \Omega, \quad (\Delta \equiv \nabla^2), \tag{2.7}$$

where ϵ is a small positive parameter, Ω is a bounded domain in $\mathbb{R}^n$, $n \geq 1$ and $u(x,t) \in [-1,1]$ is the order parameter representing the state of the system at position x and time t as described at the start of Section 2.1.1. The equation is a prototype for the continuous modelling of phase transition phenomena of two-phase systems such as the phase transitions in a ferromagnetic material described in Chapter 1 or the motion of "phase-antiphase" boundaries between two grains in a solid. As we will show, it is an example of an equation which can be written as the gradient flow of the free energy functional $E[u]$ in (2.6) with respect to a suitable inner product. Let $\Omega \subset \mathbb{R}^n$ denote the vessel (spatial domain) containing the material under consideration so that Ω is open and bounded. Consider the homogeneous Neumann conditions on the boundary $\partial\Omega$,

$$\nabla u \cdot \mathbf{n} = 0 \quad \text{for } x \in \partial\Omega, \tag{2.8}$$

where $\mathbf{n}$ denotes the outward unit normal to $\partial\Omega$. The no-flux boundary conditions in (2.8) are certainly the natural ones to take in the order parameter conserving situation of the phase separation in a binary alloy discussed in Chapter 1 since in that case we physically do not want there to be any mass loss occurring at the boundary walls. For mathematical consistency, we choose the same boundary conditions in the present situation of a non-conserved order parameter where (2.8) have the same implication of there being no exchange of material with the surroundings. We see that another consequence of having Neumann boundary conditions is that the free energy functional decreases with time (as required). Indeed, we have that formally

$$\begin{aligned}
\frac{d}{dt}E[u] &= \int_\Omega \left[W'(u)u_t + \epsilon \nabla u \cdot \nabla u_t\right] dx \\
&= \int_\Omega W'(u)u_t \, dx + \epsilon \left(\int_{\partial\Omega} u_t \left(\nabla u \cdot \mathbf{n}\right) dS - \int_\Omega \Delta u u_t \, dx \right) \\
&= \int_\Omega \left[W'(u) - \epsilon \Delta u\right] u_t \, dx = -\int_\Omega u_t^2 \, dx \\
&= -||u_t||^2_{L_2(\Omega)} \leq 0,
\end{aligned} \tag{2.9}$$

where the boundary terms have vanished because of the Neumann boundary conditions on u in (2.8). Hence as desired, the free energy functional in (2.6) evaluated at a solution $u = u(t)$ of (2.7) is non-increasing in time and this means that $E[u]$ is a Liapunov functional for solutions to the Allen-Cahn equation.

It follows from Definition 2.2 with $H = L^2(\Omega)$ that for any $v(x) \in H$ we should have

$$\frac{d}{dh}E[u + hv]|_{h=0} = (\text{grad}\, E[u], v)\,, \tag{2.10}$$

where, and hereafter, $(\cdot, \cdot)$ denotes the L^2-inner product on Ω. Hence using the form for $E[u]$ in (2.6), Green's identity and the Neumann boundary conditions on u, we have

$$\begin{aligned}\frac{d}{dh}E[u + hv]|_{h=0} &= \int_\Omega [W'(u)v + \epsilon \nabla u.\nabla v]\, dx \\ &= \int_\Omega [W'(u) - \epsilon\Delta u]v\, dx \\ &= (W'(u) - \epsilon\Delta u\,,\, v)\,. \end{aligned} \tag{2.11}$$

Thus from (2.10) and (2.11) we identify

$$\text{grad}\, E[u] \equiv -\epsilon\Delta u + W'(u),$$

in the space $L^2(\Omega)$ and from (2.1) we obtain

$$\frac{\partial u}{\partial t} = \epsilon\Delta u + f(u), \;\; x \in \Omega,$$

as the L^2-gradient flow of (2.6) as in (2.7). The Allen-Cahn equation is the simplest dynamics that one can associate with the Ginzburg-Landau form of the free energy functional (2.6) and is the gradient system defined by (2.6) which by (2.9), serves as the Liapunov functional for the equation - see [38, 40] for details on gradient systems. Being a gradient system means that the dynamics are such that equilibrium points of (2.7) are the only limit points for (2.7). We shall say more

on the Allen-Cahn equation in Section 2.1.3.

We have noted that the Allen-Cahn equation does not preserve the total amount of the order parameter u. This is not a problem if we are modelling phase transitions in ferromagnetic materials but it does become an issue if we are modelling the phase separation in a binary alloy since the total amount of each species in the system must be conserved and consequently, the evolution equation which models the phenomenon must posses this property. One can derive equations for which the order parameter is conserved by imposing a mass constraint on the order parameter and considering constrained gradient flows of the free energy functional (2.6). Consider the case of a molten binary alloy with species A and B. For the interpretation of the order parameter in this context see (1.3). We consider a constrained gradient flow of (2.6) by taking

$$\mathcal{N} = L_0^2(\Omega) = \left\{ v \in L^2(\Omega) : \int_\Omega v(x)\, dx = 0 \right\},$$

in Definition 2.3 and, for some $\hat{u} \in L^2(\Omega)$, we introduce the affine linear subspace

$$\mathcal{M} = \hat{u} + \mathcal{N}$$

of $H = L^2(\Omega)$. We now find the constrained gradient $\mathrm{grad}_{\mathcal{M}} E[u]$ of $E[u]$ as an element in $\overline{\mathcal{N}} = \mathcal{N}$. From (2.11), we have for all $v \in \mathcal{M}$ and $c \in \mathbb{R}$ constant that

$$\begin{aligned} (\mathrm{grad}_{\mathcal{M}} E[u], v) &= (W'(u) - \epsilon\Delta u, v) \\ &= (W'(u) - \epsilon\Delta u + c, v), \end{aligned} \tag{2.12}$$

since $\int_\Omega v\, dx = 0$ so that $(c, v) = 0$. In order to obtain an evolution law over $L_0^2(\Omega)$ we must be able to guarantee that $\mathrm{grad}_{\mathcal{M}} E[u] \in \mathcal{N} = L_0^2(\Omega)$. Hence we require that

$$\begin{aligned} &\int_\Omega [W'(u) - \epsilon\Delta u + c]\, dx = \int_\Omega [W'(u) + c]\, dx = 0 \\ &\Rightarrow c = -\frac{1}{|\Omega|} \int_\Omega W'(u)\, dx, \end{aligned}$$

where $|\Omega|$ is the total volume of our domain. Thus we identify

$$\text{grad}_{\mathcal{M}} E[u] \equiv -\epsilon\Delta u + W'(u) - \frac{1}{|\Omega|}\int_\Omega W'(u)\,dx,$$

in the space $L^2_0(\Omega)$ and the ansatz (2.1) gives us the law of motion

$$\frac{\partial u}{\partial t} = \epsilon\Delta u - W'(u) + \frac{1}{|\Omega|}\int_\Omega W'(u)\,dx, \quad x \in \Omega \tag{2.13}$$

which, with the boundary conditions in (2.8), is the model for phase separation introduced by Rubinstein and Sternberg in [54] as an alternative to the classical Cahn-Hilliard equation (given by (2.16)) since, for example, stationary solutions of (2.13) will also be stationary solutions to (2.16).

Equation (2.13) may be regarded as being physically unrealistic since it violates a physical principle namely that there should be "no action at a distance". In brief, this means that the evolution law for the distribution u should be local but in (2.13), the term $\frac{1}{|\Omega|}\int_\Omega W'(u)\,dx$, which arose from an enforcement of the conservation of mass, is an integral operator and hence non-local in nature so in this sense the model (2.13) could be regarded as unreasonable.

A better choice of metric is that of the Hilbert space $H_0^{-1}(\Omega)$ where $H^{-1}(\Omega)$ is the dual of the Sobolev space $H^1(\Omega)$ of L^2 functions whose weak first derivatives are also L^2 functions and the subscript 0 refers to mean value zero. For any function $v \in L^2(\Omega)$ satisfying

$$\int_\Omega v(x)\,dx = 0,$$

there is a unique function ϕ which is a solution to the Neumann problem

$$\begin{aligned} \Delta\phi &= v(x), \quad \text{in } \Omega, \\ \nabla\phi \cdot \mathbf{n} &= 0, \quad \text{on } \partial\Omega, \end{aligned} \tag{2.14}$$

and satisfies $\int \phi(x)\,dx = 0$. As in [29], the inner product in $H_0^{-1}(\Omega)$ can be defined by

$$\langle v_1, v_2 \rangle_{H_0^{-1}} := (\nabla\phi_1, \nabla\phi_2),$$

where ϕ_i and v_i for $i = 1, 2$ are related to each other via (2.14) so that we may write this as

$$\langle \Delta\phi_1, \Delta\phi_2 \rangle_{H_0^{-1}} = (\nabla\phi_1, \nabla\phi_2). \tag{2.15}$$

Hence from (2.11), (2.14) and (2.15) we have

$$\begin{aligned}
\frac{d}{dh}E[u+hv]|_{h=0} &= \frac{d}{dh}E[u+h\Delta\phi]|_{h=0} \\
&= \int_\Omega [W'(u) - \epsilon\Delta u]\Delta\phi \, dx \\
&= -\int_\Omega \nabla[W'(u) - \epsilon\Delta u] \cdot \nabla\phi \, dx \\
&= (-\nabla[W'(u) - \epsilon\Delta u], \nabla\phi) \\
&= \langle -\Delta[W'(u) - \epsilon\Delta u], \Delta\phi \rangle_{H_0^{-1}} \\
&= \langle \operatorname{grad} E[u], v \rangle_{H_0^{-1}} .
\end{aligned}$$

Thus we obtain the Cahn-Hilliard equation [13]

$$\frac{\partial u}{\partial t} = \Delta[W'(u) - \epsilon\Delta u], \quad x \in \Omega \tag{2.16}$$

which also conserves mass and, as discussed in Chapter 1, describes the process of phase separation by which the two components of a binary alloy subject to a sharp drop in temperature spontaneously separate and form domains which are pure in each component. The Cahn-Hilliard equation is usually considered with the following boundary conditions

$$\nabla u \cdot \mathbf{n} = 0 \text{ and } \nabla[W'(u) - \epsilon\Delta u] \cdot \mathbf{n} = 0 \quad \text{on } \partial\Omega, \tag{2.17}$$

the first of which corresponds to there being no exchange of material at the boundary of Ω and the second is necessary in order to have global conservation of the order parameter. Note that equilibria of the Cahn-Hilliard equation with the boundary conditions in (2.17) do correspond to the equilibria of the non-local bistable diffusion equation in (2.13) with Neumann boundary conditions. This is seen by considering the stationary problem

$$\Delta[W'(u) - \epsilon\Delta u] = 0, \quad x \in \Omega, \tag{2.18}$$

associated with (2.16) and integrating (2.18) over Ω twice using the boundary conditions in (2.17).

2.1.3 The local and non-local Allen-Cahn equations

Suppose, instead of considering the Ginzburg-Landau form of the free energy (2.6), we take the free energy functional

$$E[u] = \frac{\epsilon}{4}\int_\Omega\int_\Omega J(|x-y|)(u(y)-u(x))^2\,dy\,dx + \int_\Omega W(u)\,dx, \tag{2.19}$$

known as the van der Waals free energy functional where $J(\cdot) \in L^1(\Omega)$ is a smooth weight function which measures the interaction between particles at position x and particles at position y and as before $W(u) = \frac{u^4}{4} - \frac{u^2}{2}$. A derivation of (2.19) from elementary statistical mechanics can be found in [5]. As with the Ginzburg-Landau free energy functional in (2.6), the first term in (2.19) penalises spatial non-uniformity while the second term penalises states which take values other than ± 1. As shown in [30], the associated unconstrained gradient flow of (2.19) with respect to the L^2-inner product is the integro-differential equation

$$\frac{\partial u}{\partial t} = \epsilon\int_\Omega J(|x-y|)(u(y)-u(x))\,dy + f(u), \quad x \in \Omega. \tag{2.20}$$

The functional in (2.19) is a natural generalisation of the Ginzburg-Landau free energy functional given in (2.6). For simplicity, we illustrate this in the one-dimensional situation so that $\Omega \subset \mathbb{R}$ for the moment. Consider just the interacting part $I(u)$ of the free energy functional (2.19) so that

$$I(u) = \frac{\epsilon}{4}\int_\Omega\int_\Omega J(|x-y|)(u(y)-u(x))^2\,dy\,dx. \tag{2.21}$$

We change variables in (2.21) to $\xi = \frac{x+y}{2}$ and $\eta = \frac{x-y}{2}$ and Taylor expand the expression about $\eta = 0$ to obtain

$$\begin{aligned}&\frac{\epsilon}{4}\int_\Omega\int_\Omega J(2|\eta|)(u(\xi-\eta)-u(\xi+\eta))^2\,d\eta\,d\xi\\ &= \epsilon\int_\Omega\int_\Omega J(2|\eta|)\left(\sum_{k=1}^{\infty}\frac{\eta^{2k-1}}{(2k-1)!}D^{2k-1}u(\xi)\right)^2 d\eta\,d\xi.\end{aligned}$$

We now truncate the series at $k = 1$ so that

$$\begin{aligned} I(u) &= \epsilon \int_\Omega \int_\Omega J(2|\eta|) \left(\eta Du(\xi)\right)^2 \, d\eta \, d\xi, \\ &= \epsilon \int_\Omega J(2|\eta|)\eta^2 \, d\eta \int_\Omega [Du(\xi)]^2 \, d\xi \\ &= c \, \frac{\epsilon}{2} \int_\Omega [Du(\xi)]^2 \, d\xi \end{aligned}$$

for $c = 2\int_\Omega J(2|\eta|)\eta^2 \, d\eta$ which gives the interacting part of the free energy functional in (2.6) up to a constant c which can be absorbed by a further change of variable. Thus one can view (2.20) as a non-local analogue for the Allen-Cahn equation (2.7) and one advantage it has over (2.7) lies in the fact that the diffusion term in (2.20) can account for more general types of interactions between two nearby states.

If we set the parameter $\epsilon = 0$ in either (2.7) or (2.20) we obtain the kinetic equation

$$u_t = f(u), \quad x \in \Omega, \tag{2.22}$$

and this ordinary differential equation has stable equilibria at $u = \pm 1$ and an unstable equilibrium at $u = 0$ where clearly

$$\begin{aligned} u(0) > 0 \Rightarrow u(t) \to +1 \text{ as } t \to \infty, \\ u(0) < 0 \Rightarrow u(t) \to -1 \text{ as } t \to \infty. \end{aligned}$$

The kinetic equation also admits an uncountable set of equilibria which can be characterised as follows. If we take any disjoint sets A, B and C such that $A \cup B \cup C = \Omega$ then any function $u(x)$ such that $u = 1$ in A, $u = 0$ in B and $u = -1$ in C is a steady state solution of (2.22) and clearly there will be an uncountable number of these.

Fife in [30] was particularly interested in characterising the differences between equations (2.7) and (2.20). We mentioned in Section 2.1.2 that in some nonlinear reaction-diffusion equations, solutions can develop internal transition layers

or interfaces which separate the spatial domain into regions with different phase. Typically this occurs when the diffusion coefficient ϵ is small. The motion of these interfaces is then driven by their curvature. The Allen-Cahn equation (2.7) is an example of an equation exhibiting such qualities. The situation for the Allen-Cahn equation in one space dimension is well understood (see the pioneering work of Carr and Pego [14] and also Fusco and Hale [32]): starting with smooth initial data with a finite number of simple zeros and a sufficiently small ϵ, the orbit of (2.7) quickly evolves to a state which is approximately a step function that takes values in the set $\{-1, +1\}$ where regions in which $u \approx 1$ are separated from regions in which $u \approx -1$ by transition layers or interfaces. Diffusive effects tending to decrease the area of the interfaces then take hold and drive these transition layers towards one another or towards the boundary $\partial\Omega$ of Ω at an extremely slow speed ($O(e^{-\frac{C}{\sqrt{\epsilon}}})$ for a constant C which depends on the distance between the layers). When some of the layers are close enough to each other or to $\partial\Omega$, they disappear quickly and the system once again enters this regime of extremely slow migration of the transition layers. For ϵ sufficiently small, the process repeats finitely many times until finally all the transition layers have been annihilated and the solution converges either to $+1$ or to -1 depending on the precise nature of the initial condition $u_0(x)$. So for small enough ϵ, what one should theoretically see is a spatially homogeneous state but the time for settling down to this state is so long that what one actually observes is "the motion towards a stable state". This phenomenon can be referred to as "dormant instability" or "coarsening of solutions" and it means that in the case of the Allen-Cahn equation (2.7), the only stable equilibria are the constant stable solutions of the kinetic equation (2.22) i.e. $u \equiv \pm 1$

The situation is different in the case of the non-local Allen-Cahn equation (2.20). It is shown in [36] that a "Conway-Hoff-Smoller" kind of result holds for (2.20): if the diffusion coefficient ϵ is sufficiently large then the only stable steady state solutions in, for example, $L^\infty(\Omega)$ of (2.20) are the constant solutions $u = +1$ and

$u = -1$. However, as shown in [25], for sufficiently small ϵ, the solution does not converge to either of the stable homogeneous states $u = +1$ or to $u = -1$. Instead, for every initial condition $u_0(x)$ that changes sign in Ω, there is a value $\epsilon_0 > 0$ which depends upon $u_0(x)$, such that the non-local Allen-Cahn equation admits an uncountable number of non-constant steady state solutions which are in one-to-one correspondence with the (uncountable) steady state solutions of the kinetic equation (2.22). This is because, as shown in [25] using the implicit function theorem, for each solution $\hat{u}$ of $f(u) = 0$, there exists a locally unique continuation $u(\epsilon)$ of $\hat{u}$ (with $u(0) = \hat{u}$) to the steady state solutions of (2.20) provided ϵ is small enough. Hence in the case of the non-local Allen-Cahn equation (2.20) with sign-changing initial data $u_0(x)$, for $0 < \epsilon < \epsilon_0$, the initial condition will be in the domain of attraction of some non-constant (not necessarily smooth) equilibrium solution of (2.20).

To summarise, for all $\epsilon > 0$, solutions to the Allen-Cahn equation (2.7) will (eventually) coarsen either to $+1$ or to -1 and for sufficiently small values of ϵ, solutions to the non-local Allen-Cahn equation (2.20) cannot coarsen and the equilibrium solutions of (2.20) are in one-to-one correspondence with equilibrium solutions of the kinetic equation (2.22). This makes (2.7) a singular perturbation of (2.22) since an approximation to (2.22) cannot be made simply by setting ϵ close to zero in (2.7), while (2.20) is a regular perturbation of (2.22) and this is essentially a consequence of the boundedness in $L^\infty(\Omega)$ of the non-local operator A in (2.20) defined by

$$Au = \int_\Omega J(|x - y|)(u(y) - u(x))\, dy.$$

Another consequence of the boundedness of the operator A is that the non-local Allen-Cahn equation is well-posed both forwards and backwards in time hence defines a flow in $L^\infty(\Omega)$ while the local Allen-Cahn equation (2.7) is well-posed only forwards in time and as such defines only a nonlinear semi-flow in for example

the function space $H^1(\Omega)$. As mentioned in Section 2.1.2, the Allen-Cahn is the gradient system defined by the Liapunov functional given by (2.6). It possesses a global attractor $\mathcal{A}$, that is, a compact connected invariant set which for this equation consists of equilibria and the orbits connecting them - see [38]. This set $\mathcal{A}$ contains all the essential information about the asymptotic behaviour of the semi-flow for the Allen-Cahn equation. On the other hand, it is shown in [25] that the set of equilibria of the non-local Allen-Cahn equation is not compact in $L^\infty(\Omega)$ and so it is not possible for the dynamical system generated by (2.20) to possess a compact attractor in this setting.

The local (2.7) and non-local (2.20) Allen-Cahn equations do however share some common features. They are both unconstrained L^2-gradient flows of their respective natural free energy functionals (2.6) and (2.19) which also serve as Liapunov functionals for the equations. Both (2.7) and (2.20) have been shown to admit monotone travelling wave solutions, see [31] in the Allen-Cahn case and [6] in the case of the non-local Allen-Cahn equation. The most important similarity that the local and non-local Allen-Cahn equations share is the comparison principle: if $u_0(x) \geq v_0(x)$ then corresponding solutions satisfy $u(x,t) \geq v(x,t)$ for both equations (2.7) and (2.20) under the condition in the case of (2.20) that the kernel $J(\cdot)$ be non-negative. Also, the total amount of the order parameter is not conserved over time in either of the two equations.

Both equations have their shortcomings: many people have been concerned by the non-locality of the diffusion term in (2.20). With regards to considering discontinuous solutions to the equations, the fact that (2.20) generates a dynamical system in $L^\infty(\Omega)$ means that propagation of discontinuities is impossible. On the other hand, the Laplacian term in (2.7) which comes from the small-gradient Ginzburg-Landau theory is not really justified as the flux function in that case is linear in gradients and so the flux response to a sharp interface is for it to

become unbounded and fail to represent the physical reality. It contradicts the important global constraint of having an upper bound on the speed of propagation.

2.1.4 An alternative model

One would like to have a diffusion mechanism that is both local and does not have an infinite speed of propagation of perturbations (i.e. a diffusion mechanism which does not have immediate smoothing properties). To this end Philip Rosenau [42, 52, 53] suggested an alternative model for solid-solid phase transitions

$$\frac{\partial u}{\partial t} = \epsilon \nabla\cdot(\psi(\nabla u)) + f(u), \quad x \in \Omega, \tag{2.23}$$

where $\Omega \subset \mathbb{R}^n$, $n \geq 1$ and as we will see, the flux function ψ is a bounded increasing smooth function of the gradient and such that $\psi(0) = 0$ and $\psi'(s) \to 0$ as $|s| \to \infty$. Of course (2.23) must be supplemented with an initial condition and some boundary conditions which as above we take to be the no-flux boundary conditions

$$\psi(\nabla u) \cdot \mathbf{n} = 0 \quad \text{for } x \in \partial\Omega,$$

and these guarantee that there is no exchange of material at the boundary of the region Ω occupied by the material under consideration.

We can obtain (2.23) as the unconstrained L^2-gradient flow of the free energy functional given as

$$E_{\mathcal{R}}[u] = \int_\Omega [W(u) + \epsilon\Psi(\nabla u)]\, dx. \tag{2.24}$$

where $W(u)$ is the double-well potential given in (2.4) and as we will show, suitable choices for the functions Ψ in (2.24) and ψ in (2.23) are

$$\Psi(\nabla u) = \sqrt{1 + |\nabla u|^2} - 1,$$

and

$$\psi(\nabla u) = \frac{\nabla u}{\sqrt{1+|\nabla u|^2}}.$$

With the above choices for Ψ and ψ we have, from Definition 2.2 with $H = L^2(\Omega)$,

$$\begin{aligned}
(\text{grad}\, E_{\mathcal{R}}[u], v) &= \frac{d}{dh} E_{\mathcal{R}}[u+hv]|_{h=0} \\
&= \frac{d}{dh}\int_\Omega [W(u+hv) + \epsilon\Psi(\nabla u + h\nabla v)\, dx|_{h=0} \\
&= \int_\Omega \left[W'(u)v + \epsilon \frac{\nabla u \cdot \nabla v}{\sqrt{1+|\nabla u|^2}} \right] dx \\
&= \int_\Omega W'(u)v\, dx + \epsilon \int_\Omega \psi(\nabla u)\cdot \nabla v\, dx \\
&= \int_\Omega W'(u)v\, dx + \epsilon \left\{ \int_{\partial\Omega} v\ [\psi(\nabla u)\cdot \mathbf{n}]\, dS - \int_\Omega v\nabla\cdot(\psi(\nabla u))\, dx \right\} \\
&= \int_\Omega [W'(u) - \epsilon\nabla\cdot(\psi(\nabla u))]\, v\, dx, \\
&= (W'(u) - \epsilon\nabla\cdot(\psi(\nabla u)), v),
\end{aligned}$$

for all $v \in L^2(\Omega)$ where we have used Green's identity:

$$\int_\Omega v\Delta u\, dx = \int_{\partial\Omega} v\frac{\partial u}{\partial n}\, dS - \int_\Omega \nabla u\cdot\nabla v\, dx,$$

but taken $\nabla u = \psi(\nabla u)$. As in the situation for the local and non-local Allen-Cahn equations and their respective free energy functionals, the free energy functional in (2.24) serves as a Liapunov functional for (2.23) as one can easily check.

We will be restricting ourselves, as Rosenau did in [42, 52, 53], to one space dimension so that $\Omega \subset \mathbb{R}$ and from the point of view of the free energy functional

$$E_{\mathcal{R}}[u] = \int_\Omega [W(u) + \epsilon\Psi(u_x)]\ dx, \quad x \in \Omega \subset \mathbb{R}, \tag{2.25}$$

we can determine the properties that the functions Ψ and ψ must possess in order for (2.23) to be able to admit discontinuous solutions. As discussed in Chapter 1, if large gradients occur then the Ginzburg-Landau form for the free energy functional (2.6) cannot be correct. Rosenau [52] generalised the Ginzburg-Landau form

of the free energy functional to domains of larger gradients by modifying the free energy functional in (2.6) and considering the free energy functional in the form of (2.25).

The L^2 gradient flow of the free energy functional in (2.25) is given by

$$\begin{aligned} u_t &= \epsilon(\Psi'(u_x))_x - W'(u) \\ &= \epsilon\Psi''(u_x)u_{xx} - W'(u), \end{aligned} \tag{2.26}$$

assuming u is smooth enough. Hence one sees immediately that we must have that Ψ is convex, i.e.

$$\Psi''(s) \geq 0 \quad \forall s.$$

since if $\Psi''(u_x)$ were to become negative then (2.26) would describe the dynamics of *backwards* diffusion and this problem is not well-posed as we do not have continuous dependence on the initial data. We also require $\Psi(u_x)$ to have linear growth at infinity so that the flux $\Psi'(u_x) = \psi(u_x)$ will saturate as $|u_x| \to \infty$.

This provides a means to control the growth of the flux as gradients become infinite and we thereby depart from the previous nonphysical linear dependence of the flux on the gradients in which an overestimate of the speed of propagating fronts can occur. Therefore,

$$\Psi(s) = \sqrt{1+s^2} - 1, \tag{2.27}$$

being a convex function with linear growth at infinity, is indeed a suitable choice for Ψ and the free energy functional (2.25) becomes

$$E_{\mathcal{R}}[u] = \int_\Omega \left[\frac{u^4}{4} - \frac{u^2}{2} + \epsilon(\sqrt{1+u_x^2} - 1) \right] dx, \tag{2.28}$$

which reduces to the Landau-Ginzburg free energy functional (2.6) in the case of small gradients since

$$\sqrt{1+s^2} - 1 \sim \frac{1}{2}s^2,$$

for small s. We therefore take the flux function ψ to be given by

$$\psi(s) = \frac{s}{\sqrt{1+s^2}}, \tag{2.29}$$

which corresponds to the well-known mean-curvature operator.

We note that the flux in (2.29) is *strongly* saturating since

$$\int_0^\infty s\psi'(s)\,ds < \infty,$$

and so the saturation rate is sufficiently fast and initially imposed discontinuities persist for a finite time as shown in [53]. There are other possibilities for a flux with strong saturation. For example, one could take

$$\psi(s) = \frac{1}{2}\tan^{-1}(s) + \frac{1}{2}\frac{s}{1+s^2},$$

or

$$\psi(s) = \tanh(s),$$

however, we will proceed with the choice of flux (2.29) which is taken in [18, 42, 52, 53]. An example of a flux with weak saturation is

$$\psi(s) = \tan^{-1}(s),$$

since in that case

$$\int_0^\infty s\psi'(s)\,dx = \int_0^\infty \frac{s}{1+s^2}\,ds = \infty,$$

and initially imposed discontinuities are resolved instantaneously [53].

With the choice for $\Psi(s)$ in (2.27), the evolution equation (2.26) becomes

$$u_t = \epsilon\left(\frac{u_x}{\sqrt{1+u_x^2}}\right)_x + u - u^3, \quad x \in \Omega \equiv (0, L), \tag{2.30}$$

where $L > 0$ is the length of the space domain. Equation (2.30) with Neumann boundary conditions and suitable initial data will be the subject of discussion in the next two chapters. In Chapter 3 we will prove that (2.30) is well-posed in the space of functions of bounded variation (see Section 2.2 for a discussion on functions of bounded variation). In Chapter 4, we study the one-dimensional stationary problem associated with (2.30) and obtain results for classical and non-classical solutions to that problem. We will also be interested in determining in what ways the effects of the quasilinear diffusion mechanism in (2.30) can be related to the effects of the semilinear and non-local diffusion mechanisms of (2.7) and (2.20) respectively.

As an aside, we note that (2.30) as it stands is dimensionless. In the most general dimensional form, we would have

$$\frac{\partial \hat{u}}{\partial \hat{t}} = \frac{\partial}{\partial \hat{x}} \left(\frac{\hat{\kappa}}{\sqrt{1 + \hat{\alpha} \left(\frac{\partial \hat{u}}{\partial \hat{x}} \right)^2}} \frac{\partial \hat{u}}{\partial \hat{x}} \right) + \hat{\beta}\hat{u} - \hat{\gamma}\hat{u}^3 \quad \text{on} \quad 0 \leq \hat{x} \leq \hat{L},$$

where carets denote dimensional quantities and where $\hat{\kappa}$, $\hat{\alpha}$, $\hat{\beta}$ and $\hat{\gamma}$ are physical parameters. The nondimensionalisation that yields (2.30) is

$$\hat{u} = \sqrt{\frac{\hat{\beta}}{\hat{\gamma}}} u, \qquad \hat{x} = \sqrt{\frac{\hat{\alpha}\hat{\beta}}{\hat{\gamma}}} x, \qquad \hat{t} = \frac{1}{\hat{\beta}} t, \qquad \epsilon = \frac{\hat{\kappa}\hat{\gamma}}{\hat{\alpha}\hat{\beta}^2}, \qquad L = \hat{L}\sqrt{\frac{\hat{\gamma}}{\hat{\alpha}\hat{\beta}}}.$$

If we take $\hat{u}$ to be a dimensionless quantity initially, then both $\hat{\beta}$ and $\hat{\gamma}$ become inverse timescales while $\sqrt{\hat{\alpha}}$ is a lengthscale representing the inverse of the typical gradient at which the flux starts to saturate. The dimensionless parameter L then represents the ratio of the domain length to this saturation lengthscale, while the dimensionless parameter ϵ represents the ratio of the saturation lengthscale to a diffusive lengthscale defined in terms of the rate parameters and the diffusion coefficient. Hence we have shown that (2.30) contains two irreducible dimensionless parameters L and ϵ and we will see in Chapter 4 that the bifurcation behaviour of the stationary problem associated (2.30) depends in a non-trivial way on the parameter ϵ as well as on the length L of the space domain Ω.

We conclude this section by noting that one obtains a quasilinear version of the Rubinstein-Sternberg equation (2.13) by taking the constrained L^2-gradient flow of (2.24) to give the following mass-conserving equation

$$u_t = \epsilon \nabla\cdot(\psi(\nabla u)) + f(u) - \frac{1}{|\Omega|}\int_\Omega f(u)\,dx, \quad x \in \Omega,$$

whose one-dimensional stationary problem with Neumann boundary conditions we will study in Chapter 5.

2.2 Functions of bounded variation

In Chapter 3, we consider a problem of the form

$$u_t = \epsilon(\psi(u_x))_x + f(u), \tag{2.31}$$

where $x \in \Omega = (0, L) \subset \mathbb{R}$, $L > 0$, $\epsilon \in (0, \infty)$, $\psi(s) = \frac{s}{\sqrt{1+s^2}}$ and $f(u) = u - u^3$. We explained in Section 2.1.4 that (2.31) can be obtained as the L^2-gradient flow of the free energy functional in (2.28).

In studying this problem, we will not be able to work in the function space $L^p(\Omega)$ since in general

$$f(u) : L^p(\Omega) \nrightarrow L^p(\Omega).$$

For example, take $p = 1$ and $u(x) = x^{-\frac{1}{2}}$ so that $u(x) \in L^1(\Omega)$ but $u^3(x) = x^{-\frac{3}{2}} \notin L^1(\Omega)$. Nor will we be able to work in any classical Sobolev space such as $H^1(\Omega)$ of L^2-functions whose weak first derivatives are also L^2-functions since (2.31) admits discontinuous solutions and in particular, in the one-dimensional setting of interest to us, $H^1(\Omega) \subset C(\bar{\Omega})$ (as discussed in Chapter 1). When u is discontinuous, the gradient of u has to be understood as a measure.

Therefore as we shall see, the space of functions of bounded variation (BV) is a reasonable candidate in which to study solutions to (2.31). To define BV in the

modern way we need some measure theory and what follows can be found in, for example [3, 27, 58, 60]. We need a measure space $(X, \mathcal{E})$ where X is any set and $\mathcal{E}$ is a σ-algebra of subsets of X. That is, $\mathcal{E}$ is a collection of subsets of X satisfying

- $\mathcal{E}$ is non-empty so that there is at least one $A \subset X$ in $\mathcal{E}$
- $\mathcal{E}$ is closed under complementation: if $A \in \mathcal{E}$ then so too is $A^c = X \backslash A$
- $\mathcal{E}$ is closed under countable unions: if we have a countable collection $A_1, A_2, \cdots$ of subsets of X which are in $\mathcal{E}$, then their union $\bigcup_{n=1}^{\infty} A_n$ is also in $\mathcal{E}$.

Definition 2.4. *Let $(X, \mathcal{E})$ be a measure space and let $m \in \mathbb{N}$ with $m \geq 1$. A function $\mu : \mathcal{E} \to \mathbb{R}^m$ is called a measure if it satisfies the following properties*

- $\mu(\emptyset) = 0$
- *If $\{E_k\} \subset \mathcal{E}$ is a collection of pairwise disjoint sets, i.e. if $E_i \cap E_j = \emptyset$ for $i \neq j$, then $\mu\left(\bigcup_{k=0}^{\infty} E_k\right) = \sum_{k=0}^{\infty} \mu(E_k)$.*
- $\mu = [\mu_1, \cdots, \mu_m] \in \mathbb{R}^m$

If $m = 1$ we say that μ is a real measure and if $m > 1$ we say that μ is a vector-valued measure.

A set E is said to be measurable with respect to the measure μ if it belongs to the σ-algebra on which μ is defined.

Definition 2.5. *The total variation of a measure μ is given by*

$$|\mu|(E) = \sup\left\{\sum_{k=1}^{\infty} ||\mu(E_k)||\right\}$$

where $||\cdot||$ is the norm in $\mathbb{R}^m$ and the supremum is taken over all finite collections $\{E_k\}$ of pairwise disjoint sets in $\mathcal{E}$ such that $\bigcup_{k=1}^{\infty} E_k = E$.

In particular, as the indicated collection of sets, one can take the set E itself so that we obtain the inequality

$$||\mu(E)|| \leq |\mu|(E).$$

The smallest σ-algebra $\mathcal{B}$ that contains all open subsets of the space X is called the Borel algebra of X and the sets belonging to this algebra are called Borel sets. By virtue of the definition of a Borel set, all open sets and also all closed sets, being complements of open sets, are Borel sets. A measure μ defined on the measure space $(X, \mathcal{B})$ is called a Borel measure and any Borel measure which is finite on compact sets is called a Radon measure.

Let $\Omega \subset \mathbb{R}^n$, $n \geq 1$, $u \in L^1_{loc}(\Omega)$ and suppose that for all $i = 1, \cdots, n$ there exists a finite measure μ such that

$$\int_\Omega \frac{\partial v}{\partial x_i} u \, dx = -\int_\Omega v \, d\mu_i \quad \forall \; v \in C_0^1(\Omega).$$

Then we say that μ_i represents the generalised i-th first partial derivative of u so that

$$Du := (D_1 u, \cdots, D_n u) := (\mu_1, \cdots, \mu_n),$$

where $D_i u = \frac{\partial u}{\partial x_i}$ for $i = 1, \cdots, n$.

Definition 2.6. *A function $u \in BV(\Omega)$ if $u \in L^1(\Omega)$ and $\dfrac{\partial u}{\partial x_i}$ are Radon measures with finite total variation for all $i = 1, \cdots, n$ in the sense defined above.*

Thus $u \in BV(\Omega)$ if there exist Radon measures $\mu_1, \cdots, \mu_n$ such that $|\mu_i|(\Omega) < \infty$ $\forall i$ and

$$\int_\Omega \frac{\partial v}{\partial x_i} u \, dx = -\int_\Omega v \, d\mu_i \quad \forall \; v \in C_0^1(\Omega), \quad (i = 1, \cdots, n) \tag{2.32}$$

The variation $V(u, \Omega)$ of a function $u \in L^1_{\text{loc}}(\Omega)$ is defined by

$$V(u, \Omega) := \sup_{v \in C_0^1(\Omega)} \left\{ \int_\Omega u \, \text{div}\, v \, dx \;\; : \;\; ||v||_\infty \leq 1 \; \forall x \in \Omega, \; 1 \leq i \leq n \right\}, \tag{2.33}$$

as in [3, Definition 3.4] and it is shown in [3, Proposition 3.6] that $u \in BV(\Omega)$ if and only if $V(u,\Omega) < \infty$. It is also proven in [3, Proposition 3.6] that for any $u \in BV(\Omega)$, $V(u,\Omega)$ coincides with $|Du|(\Omega)$, the total variation of the measure Du. For $u \in BV(\Omega)$, we will denote $|Du|(\Omega) = V(u,\Omega)$ by $\int_\Omega |Du|$.

Suppose we take $\Omega \equiv (0,L) \subset \mathbb{R}$, $L > 0$ and consider the one-dimensional situation.

Definition 2.7. *For any function $u : \Omega \to \mathbb{R}$, the pointwise variation $pV(u,\Omega)$ of u in Ω is defined by*

$$pV(u,\Omega) = \sup\left\{\sum_{i=1}^{n-1} |u(x_{i+1}) - u(x_i)| \ : \ n \geq 2,\ 0 < x_1 < \cdots < x_n < L\right\},$$

so the above supremum is taken over all partitions of $[0,L]$.

Hence $pV(u,\Omega)$ is going to be sensitive to changes in the values of u even at a single point in Ω. Consequently, as in [3] we define the essential variation

$$eV(u,\Omega) := \inf\{pV(v,\Omega) \ : \ v = u \text{ a.e. in } \Omega\}, \tag{2.34}$$

and it is proven in [3, Theorem 3.27] and also in [27, Theorem 1, p.217] that for any $u \in L^1_{\text{loc}}(\Omega)$, the infimum in (2.34) is attained and coincides with the variation

$$\int_\Omega |u_x| = \sup\left\{\int_\Omega uv_x\,dx \ : \ v \in C^1_c(0,L),\ ||v||_\infty \leq 1\right\}, \tag{2.35}$$

as defined in (2.33) (except that $n = 1$ here).

With a view to Chapter 3, we will also need to define the functional

$$\int_\Omega \Psi(u_x),$$

for $u \in BV(\Omega)$ where Ψ is a convex function which has linear growth at infinity and whose argument is a measure. Following [23, Lemma 1.1], for $u \in BV(\Omega)$, we define

$$\int_\Omega \Psi(u_x) = \sup_{v \in \mathcal{D}_\Psi(C_0^\infty)} \left\{-\int_\Omega uv_x\,dx - \int_\Omega \Psi^*(v)\,dx\right\}, \tag{2.36}$$

where

$$\Psi^*(v) = \sup_{y\in\mathbb{R}}\{yv - \Psi(y)\} \tag{2.37}$$

is the conjugate or Legendre transform of Ψ and

$$\mathcal{D}_\Psi(C_0^\infty) = \{v \in C_0^\infty(\Omega) \ : \ \Psi^*(v) \in L^1(\Omega)\}.$$

Lemma 2.8. *Suppose $\Psi(s) = |s|$, then through the definition of $\int_\Omega \Psi(u_x)$ for $u \in BV(\Omega)$ in (2.36), we obtain*

$$\int_\Omega |u_x| = \sup_{v\in C_0^\infty}\left\{\int_\Omega uv_x\,dx \ : \ |v(x)| \le 1 \ \forall x \in \Omega\right\}, \tag{2.38}$$

as required by (2.35).

Proof. By definition,

$$\int_\Omega \Psi(u_x) = \int_\Omega |u_x| = \sup_{v\in\mathcal{D}_\Psi(C_0^\infty)}\left\{-\int_\Omega uv_x\,dx - \int_\Omega \Psi^*(v)\,dx\right\},$$

and so we need to find a formula for the Legendre transform of $\Psi(s) = |s|$ using (2.37). Suppose that $|v| > 1$ and consider first the case where $v > 1$ so that

$$yv - |y| > y - |y| = 0,$$

for all $y > 0$. Also, for such v,

$$yv - |y| = y(v + 1) < 0,$$

for all $y < 0$.

For $v < -1$ with $y > 0$ we have

$$yv - |y| = y(v - 1) < 0,$$

and for such v with $y = -x < 0$ where $x > 0$ we also have

$$yv - |y| = -xv - |x| > x - |x| = 0.$$

Therefore we have shown that for v such that $|v| > 1$,

$$\Psi^*(v) = \sup_{y\in\mathbb{R}}\{yv - |y|\} = +\infty.$$

Now we consider the case where $|v| \leq 1$. Then

$$yv - |y| = y(v-1) \leq 0,$$

for all $y \geq 0$ and

$$yv - |y| = y(v+1) \leq 0,$$

for all $y < 0$. Consequently, we have that for v such that $|v| \leq 1$,

$$\Psi^*(v) = \sup_{y\in\mathbb{R}}\{yv - |y|\} = 0.$$

Having exhausted all possibilities, we conclude that $v \in \mathcal{D}_\Psi(C_0^\infty(\Omega))$ only in the situation where $|v| \leq 1$ in which case $\Psi^*(v) = 0$. Therefore for $\Psi(s) = |s|$,

$$\mathcal{D}_\Psi(C_0^\infty) = \{v \in C_0^\infty(\Omega) \ : \ |v(x)| \leq 1 \ \forall x \in \Omega\},$$

and

$$\begin{aligned}\int_\Omega |u_x| &= \sup_{v\in C_0^\infty}\left\{-\int_\Omega uv_x\,dx \ : \ |v(x)| \leq 1 \ \forall x \in \Omega\right\} \\ &= \sup_{v\in C_0^\infty}\left\{\int_\Omega uv_x\,dx \ : \ |v(x)| \leq 1 \ \forall x \in \Omega\right\}.\end{aligned}$$

as in (2.38). □

Example 2.9. *Suppose we take* $\Omega = (0, L)$, $L > 0$ *and* $u(x) = H\left(x - \frac{L}{2}\right) \in BV(\Omega)$, *then*

$$\begin{aligned}\int_\Omega |u_x| &= \sup_{v\in C_0^\infty}\left\{-\int_\Omega uv_x\,dx \ : \ |v(x)| \leq 1 \ \forall x \in \Omega\right\} \\ &= \sup_{v\in C_0^\infty}\left\{-\int_0^L H\left(x - \frac{L}{2}\right)v_x\,dx \ : \ |v(x)| \leq 1 \ \forall x \in \Omega\right\} \\ &= \sup_{v\in C_0^\infty}\left\{-\int_{\frac{L}{2}}^L v_x\,dx \ : \ |v(x)| \leq 1 \ \forall x \in \Omega\right\} \\ &= \sup_{v\in C_0^\infty}\left\{v\left(\frac{L}{2}\right) \ : \ |v(x)| \leq 1 \ \forall x \in \Omega\right\} \\ &= 1.\end{aligned}$$

Lemma 2.10. *Suppose*

$$\Psi(s) = \sqrt{1+s^2} - 1,$$

then for $u \in BV(\Omega)$*,*

$$\int_\Omega \Psi(u_x) := \sup_{v \in C_0^\infty} \left\{ \int_\Omega u v_x \, dx + \int_\Omega \sqrt{1-v^2} - |\Omega| \ : \ |v(x)| \leq 1 \, \forall x \in \Omega \right\}. \quad (2.39)$$

Moreover, we have the following estimate

$$\int_\Omega |u_x| \, dx - |\Omega| \leq \int_\Omega \sqrt{1+u_x^2} - 1 \, dx \leq \int_\Omega |u_x| \, dx + |\Omega|, \quad (2.40)$$

for all $u \in BV(\Omega)$ *which we will make use of in Section 3.1.*

Proof. From (2.37)

$$\Psi^*(v) = \sup_{y \in \mathbb{R}} \{yv - \sqrt{1+y^2} + 1\}.$$

As in Lemma 2.8, we suppose that $|v| > 1$ and first consider the case where $v > 1$ for which

$$\begin{aligned} yv - \sqrt{1+y^2} + 1 &> y + 1 - \sqrt{1+y^2} \\ &> y + 1 - (1 + |y|) = 0, \end{aligned}$$

for all $y > 0$ where we have used the inequality

$$\begin{aligned} \sqrt{p+q} &< \sqrt{p + 2\sqrt{p}\sqrt{q} + q} \\ &= \sqrt{(\sqrt{p} + \sqrt{q})^2} = \sqrt{p} + \sqrt{q} \quad \forall p > 0, \ \forall q > 0. \end{aligned} \quad (2.41)$$

For such v, we also have

$$yv - \sqrt{1+y^2} + 1 < yv < 0,$$

for all $y < 0$.

Now suppose that $v < -1$ so that

$$\begin{aligned} yv - \sqrt{1+y^2} + 1 &< -y - \sqrt{1+y^2} + 1 \\ &< -y - 1 + 1 \\ &= -y < 0, \end{aligned}$$

for all $y > 0$.

Also, for such v we have, for $y = -x < 0$ with $x > 0$,

$$\begin{aligned} yv - \sqrt{1+y^2} + 1 &= -xv - \sqrt{1+x^2} + 1 \\ &> x - \sqrt{1+x^2} + 1 \\ &> x - (1 + |x|) + 1 \\ &= 0, \end{aligned}$$

using inequality (2.41) once again.

We have therefore proved that in the case where v is such that $|v| > 1$,

$$\Psi^*(v) = \sup_{y \in \mathbb{R}} \{yv - \sqrt{1+y^2} + 1\} = +\infty.$$

Consider the case of $|v| \leq 1$ with $v(x)$ fixed and define the function

$$g(y) = yv - \sqrt{1+y^2} + 1.$$

We want to determine the maximum of $g(y)$ with $v(x)$ fixed and such that $|v| \leq 1$ hence we consider

$$\begin{aligned} g'(y) = 0 \Rightarrow \frac{v\sqrt{1+y^2} - y}{\sqrt{1+y^2}} &= 0 \\ \Rightarrow v\sqrt{1+y^2} &= y \\ \Rightarrow y^2(1-v^2) &= v^2 \\ \Rightarrow y &= \frac{v}{\sqrt{1-v^2}} \end{aligned}$$

Hence

$$\begin{aligned} g\left(\frac{v}{\sqrt{1-v^2}}\right) &= \frac{v^2}{\sqrt{1-v^2}} - \frac{1}{\sqrt{1-v^2}} + 1 \\ &= -\sqrt{\frac{(1-v^2)^2}{1-v^2}} + 1 \\ &= -\sqrt{1-v^2} + 1 \end{aligned}$$

and

$$g''\left(\frac{v}{\sqrt{1-v^2}}\right) = (v^2-1)\sqrt{1-v^2} \leq 0,$$

so that $\max\limits_{y\in\mathbb{R}} g(y) = -\sqrt{1-v^2}+1$ for $|v| \leq 1$. Thus

$$\sup_{y\in\mathbb{R}}\{yv - \sqrt{1+y^2}+1\} = \begin{cases} +\infty & \text{if } |v|>1 \\ -\sqrt{1-v^2}+1 & \text{if } |v|\leq 1 \end{cases},$$

and we finally obtain

$$\begin{aligned} \int_\Omega \sqrt{1+u_x^2} - 1 &= \sup_{v\in C_0^\infty}\left\{-\int_\Omega uv_x\,dx + \int_\Omega \sqrt{1-v^2} - |\Omega| \ : \ |v(x)|\leq 1 \ \forall x\in\Omega\right\} \\ &= \sup_{v\in C_0^\infty}\left\{\int_\Omega uv_x\,dx + \int_\Omega \sqrt{1-v^2} - |\Omega| \ : \ |v(x)|\leq 1 \ \forall x\in\Omega\right\}, \end{aligned}$$

as required.

From the above calculation we also have

$$\begin{aligned} \int_\Omega \sqrt{1+u_x^2} - 1 &= \sup_{v\in C_0^\infty}\left\{\int_\Omega uv_x\,dx + \int_\Omega \sqrt{1-v^2}\,dx \ : \ |v(x)|\leq 1 \ \forall x\in\Omega\right\} - |\Omega| \\ &\geq \sup_{v\in C_0^\infty}\left\{\int_\Omega uv_x\,dx \ : \ |v(x)|\leq 1 \ \forall x\in\Omega\right\} - |\Omega| \\ &= \int_\Omega |u_x| - |\Omega| \end{aligned}$$

and

$$\begin{aligned}\int_\Omega \sqrt{1+u_x^2} - 1 &\leq \sup_{v\in C_0^\infty}\left\{\int_\Omega uv_x\,dx + \int_\Omega dx \;:\; |v(x)|\leq 1\ \forall x\in\Omega\right\} - |\Omega| \\ &= \int_\Omega |u_x| \\ &< \int_\Omega |u_x| + |\Omega|,\end{aligned}$$

so that we obtain (2.40), i.e.

$$\int_\Omega |u_x|\,dx - |\Omega| \leq \int_\Omega \sqrt{1+u_x^2} - 1 \leq \int_\Omega |u_x|\,dx + |\Omega|,$$

for all $u \in BV(\Omega)$ thus the lemma is proven. □

Example 2.11. *As in Example 2.9, we take* $\Omega = (0, L)$ *and* $u(x) = H\left(x - \frac{L}{2}\right)$ *so that we have*

$$\begin{aligned}\int_\Omega \sqrt{1+u_x^2} - 1 &= \sup_{v\in C_0^\infty}\left\{-\int_\Omega uv_x\,dx + \int_\Omega \sqrt{1-v^2}\,dx - |\Omega| \;:\; |v(x)|\leq 1\ \forall x\in\Omega\right\} \\ &= \sup_{v\in C_0^\infty}\left\{-\int_{\frac{L}{2}}^L v_x\,dx + \int_0^L \sqrt{1-v^2}\,dx \;:\; |v(x)|\leq 1\ \forall x\in\Omega\right\} - L \\ &= \sup_{v\in C_0^\infty}\left\{v\left(\frac{L}{2}\right) + \int_0^L \sqrt{1-v^2}\,dx \;:\; |v(x)|\leq 1\ \forall x\in\Omega\right\} - L,\end{aligned} \tag{2.42}$$

and since we are considering a supremum, we need to optimise both terms in (2.42).

To this end, consider the functions

$$w_\delta(x) = \begin{cases} \left(\frac{2x-L+2\delta}{2\delta}\right)_+, & 0\leq x < \frac{L}{2}, \\ \left(\frac{L-2x+2\delta}{2\delta}\right)_+, & \frac{L}{2} < x \leq L, \end{cases}$$

for some $0 < \delta < \frac{L}{2}$, *where* $(f(x))_+ = \max(0, f(x))$. *We have plotted the functions* $w_\delta(x)$ *for* $\delta = 0.1$, $\delta = 0.4$ *and* $\delta = 0.8$ *in Figure 2.11.*

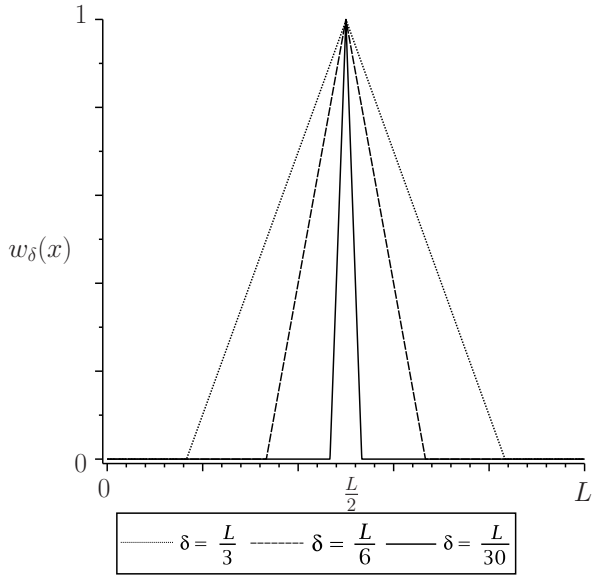

Figure 2.2: $w_\delta(x)$ for $\delta = \frac{L}{30}$, $\frac{L}{6}$ and $\frac{L}{3}$.

The function $v(x)$ that is the limit as δ tends to zero of $w_\delta(x)$, while not being a C_0^∞ function, will optimise both of the terms in (2.42). The first term, $v\left(\frac{L}{2}\right)$, when optimised is 1 *and the second term $\int_0^L \sqrt{1-v^2}\,dx$ when optimised is L. One could smooth out the edges of the sequence of functions $w_\delta(x)$ at each $x = \frac{L}{2} \pm \delta$ and at $x = \frac{L}{2}$ so that they will be $C_0^\infty(\Omega)$ and we therefore conclude that in the case where $u(x) = H\left(x - \frac{L}{2}\right)$ on $\Omega = (0, L)$,*

$$\int_\Omega \sqrt{1+u_x^2} - 1 = 1.$$

2.3 Liapunov-Schmidt reduction

In Chapter 4 and Chapter 5 we will study local bifurcation problems. Such problems may be formulated as an equation

$$\Theta(\lambda, u) = 0, \tag{2.43}$$

where the unknown u is the state variable and λ is the bifurcation parameter. We assume that $\Theta : \mathbb{R} \times X \to Y$ is a smooth mapping between Banach spaces X and

Y and such that

$$\Theta(\lambda, 0) = 0 \ \ \forall\ \lambda \in \mathbb{R}. \tag{2.44}$$

We will require that Θ satisfies the conditions of the Crandall-Rabinowitz Theorem which gives the solution set of (2.43) locally at a point $(\lambda, u) = (\lambda_k, 0)$ which will be a bifurcation point from the trivial solution to (2.43).

Theorem 2.12. *Let $\Theta : \mathbb{R} \times X \to Y$ satisfy (2.44) and suppose that the following conditions hold*

- $\mathrm{Ker}(\Theta_u(\lambda_k, 0))$ *is one-dimensional and spanned by v_k,*
- $\mathrm{codim}(\mathrm{Range}(\Theta_u(\lambda_k, 0))) = 1$,
- $\Theta_{\lambda u}(\lambda_k, 0)v_k \notin \mathrm{Range}(\Theta_u(\lambda_k, 0))$,

then there is a $\delta > 0$ and a non-trivial C^1-curve through $(\lambda_k, 0)$ given by

$$\{(\lambda(s), u(s)) \ : \ s \in (-\delta, \delta),\ (\lambda(0), u(0)) = (\lambda_k, 0)\},$$

and $\Theta(\lambda(s), u(s)) = 0$ for all $s \in (-\delta, \delta)$. Moreover, any solution of $\Theta(\lambda, u) = 0$ either lies on this curve or is of the form $(\lambda, 0)$.

Proof. See [56, Theorem 13.5]. □

Liapunov-Schmidt reduction is the process by which a problem such as (2.43) involving multiple solutions is reduced to a single equation $h(\lambda, y) = 0$ where $h : \mathbb{R} \times \mathbb{R} \to \mathbb{R}$ and whose solutions are locally in one-to-one correspondence with solutions of the original problem i.e. in a neighbourhood of a bifurcation point $(\lambda, u) = (\lambda_k, 0)$ from the trivial solution $u = 0$ to (2.43).

The linearisation of Θ applied to $v \in X$ is given by

$$d\Theta_{\lambda,u} \cdot v = \frac{d}{dh}\Theta(\lambda, u + hv)|_{h=0},$$

and we let S be $(d\Theta)_{\lambda_k,0} = \Theta_u(\lambda_k, 0)$ with $\ker(S)$ denoted by $\mathcal{K}$ and $\text{range}(S)$ denoted by $\mathcal{R}$. We assume that $S : X \to Y$ is a Fredholm operator of index zero meaning that $\dim \mathcal{K} < \infty$, $\mathcal{R}$ is closed and $\dim \mathcal{K} = \text{codim}\, \mathcal{R}$. The derivation of the reduced equation h can then be divided into the following five steps as in [34].

Step 1. Decompose the spaces X and Y into summands related to S as follows

$$X = \mathcal{K} \oplus \mathcal{K}^\perp, \qquad Y = \mathcal{R} \oplus \mathcal{R}^\perp.$$

Let $E : Y \to \mathcal{R}$ denote the projection of Y onto $\mathcal{R}$ so that $E(x) = x$ for $x \in \mathcal{R}$ ($ES = S$) and $E(x) = 0$ for $x \in \mathcal{R}^\perp$.

Step 2. Transfer the decomposition to the equation $\Theta(\lambda, u) = 0$. For this we note the relation

$$v = 0 \Leftrightarrow Ev = 0 \text{ and } (I - E)v = 0,$$

so that (2.43) can be written as the alternative pair of equations

$$E\Theta(\lambda, u) = 0, \tag{2.45a}$$

$$(I - E)\Theta(\lambda, u) = 0. \tag{2.45b}$$

Step 3. Decompose $u \in X$ as $u = v + w$ for $v \in \mathcal{K}$, $w \in \mathcal{K}^\perp$ and define a mapping $G : \mathbb{R} \times \mathcal{K} \times \mathcal{K}^\perp \to \mathcal{R}$ by

$$G(\lambda, v, w) = E\Theta(\lambda, v + w).$$

The derivative of G with respect to w at $(\lambda_k, 0)$ is $ES_{\mathcal{K}^\perp} = S_{\mathcal{K}^\perp}$ and since the operator $S_{\mathcal{K}^\perp}$ is Fredholm, $\mathcal{R}$ is closed and so

$$S_{\mathcal{K}^\perp} : \mathcal{K}^\perp \to \mathcal{R},$$

is non-singular so that (2.45a) is uniquely solvable near $(\lambda_k, 0)$ for w as a function of λ and v by the implicit function theorem. This leads to a function $W : \mathbb{R} \times \mathcal{K} \to \mathcal{K}^\perp$ such that

$$E\Theta(\lambda, v + W(\lambda, v)) = 0, \qquad W(\lambda_k, 0) = 0. \tag{2.46}$$

Step 4. Substitute the solution W of (2.45a) into (2.45b) to obtain the mapping $\phi : \mathbb{R} \times \mathcal{K} \to \mathcal{R}^{\perp}$ where

$$\phi(\lambda, v) = (I - E)\Theta(\lambda, v + W(\lambda, v)). \tag{2.47}$$

Step 5. Choose coordinates $v_k \in \mathcal{K}$ and $v_k^* \in \mathcal{R}^{\perp}$ so any $v \in \mathcal{K}$ can be written as $v = yv_k$ for $y \in \mathbb{R}$ and define $h : \mathbb{R} \times \mathbb{R} \to \mathbb{R}$ by

$$h(\lambda, y) = \langle v_k^*, \phi(\lambda, yv_k) \rangle , \tag{2.48}$$

where $\langle \cdot, \cdot \rangle$ denotes the inner product defined on Y. The definition of the reduced function h implies that the zeros of ϕ are in one-to-one correspondence with the zeros of h since $\phi(\lambda, yv_k) \in \mathcal{R}^{\perp}$ which implies that $\phi(\lambda, yv_k) \notin \mathcal{R}$ unless $\phi(\lambda, yv_k) = 0$ because of the way we have decomposed Y as a direct sum of $\mathcal{R}$ and $\mathcal{R}^{\perp}$, hence

$$\langle v_k^*, \phi(\lambda, yv_k) \rangle = 0 \Leftrightarrow \phi(\lambda, yv_k) = 0.$$

Note that if we substitute the definition of ϕ in (2.47) into (2.48) we obtain

$$h(\lambda, y) = \langle v_k^*, \Theta(\lambda, yv_k + W(\lambda, yv_k)) \rangle ,$$

where the projection E has dropped out since $v_k^* \in \mathcal{R}^{\perp}$ and for any $V \in Y$, $EV \in \mathcal{R}$.

While the bifurcation function h is not known explicitly, all its partial derivatives at a bifurcation point $(\lambda_k, 0)$ can be computed with the use of the following chain rule

$$\begin{aligned} &\frac{\partial}{\partial y} \left\{ (d^r \Theta)_{\lambda,u}(z_1, \ldots, z_r) \right\} \\ &\qquad = (d^{r+1}\Theta)_{\lambda,u} \left(\frac{\partial u}{\partial y}, z_1, \ldots, z_r \right) + \sum_{i=1}^{r} (d^r \Theta)_{\lambda,u} \left(z_1, \ldots, \frac{\partial z_i}{\partial y}, \ldots, z_r \right), \end{aligned} \tag{2.49}$$

where $r \in \mathbb{N}$ is fixed and $(d^r\Theta)_{\lambda,u}$ is a symmetric, multilinear function of r arguments given by

$$(d^r \Theta)_{\lambda,u}(z_1, \cdots, z_r) = \frac{\partial^r}{\partial t_1 \cdots \partial t_r} \Theta(\lambda, u + t_1 z_1 + \cdots + t_r z_r) \Big|_{t_1 = \cdots = t_r = 0}. \tag{2.50}$$

The derivatives of the reduced function

$$h(\lambda, y) = \langle v_k^*, \Theta(\lambda, yv_k + W(\lambda, yv_k))\rangle\,,$$

evaluated at $\lambda = \lambda_k$, $y = 0 \Rightarrow u = 0$ are given by

$$\begin{aligned} h_y &= \langle v_k^*, d\Theta(v_k)\rangle = 0 \\ h_{yy} &= \left\langle v_k^*, d^2\Theta(v_k, v_k)\right\rangle \\ h_{yyy} &= \left\langle v_k^*, d^3\Theta(v_k, v_k, v_k) - 3d^2\Theta(v_k, S^{-1}E[d^2\Theta(v_k, v_k)])\right\rangle \\ h_\lambda &= \langle v_k^*, \Theta_\lambda\rangle \\ h_{\lambda y} &= \left\langle v_k^*, d\Theta_\lambda(v_k) - d^2\Theta(v_k, S^{-1}E\Theta_\lambda)\right\rangle, \end{aligned} \tag{2.51}$$

and these are obtained by applying the chain rule in (2.49) to $\Theta(\lambda, yv_k + W(\lambda, yv_k))$ and then to the equation

$$E\Theta(\lambda, yv_k + W(\lambda, yv_k)) = 0,$$

in order to obtain formulae for $W_{yy}(\lambda_k, 0)$ and $W_\lambda(\lambda_k, 0)$ making use of the fact that $(d^r\Theta)_{\lambda,u}$ is a symmetric operator.

In Chapter 4 and Chapter 5 we will also require the following standard result from bifurcation theory.

Proposition 2.13. [34] *Let $h(\lambda, y) = 0$ be a bifurcation problem such that, when $(\lambda, y) = (\lambda_k, 0)$, we have*

$$h = h_y = h_{yy} = h_\lambda = 0 \quad \textit{and} \quad h_{yyy}h_{\lambda y} < 0; \tag{2.52}$$

then the number of solutions of $h(\lambda, y) = 0$ jumps from one to three as λ crosses λ_k and so a supercritical bifurcation occurs. If $h_{yyy}h_{\lambda y} > 0$ then the number of solutions jumps from three to one and a subcritical bifurcation occurs.

A proof of this result which requires only the use of the implicit function theorem can be found in [34].

2.4 Essential and natural boundary conditions

In Section 4.5 we will prove (Theorem 4.5) a result on the instability of classical solutions to a one-dimensional Neumann boundary value problem which requires the use of some calculus of variations since the problem has variational structure. This means that the solutions of the problem correspond to critical points of a (free energy) functional which is of the form

$$E(w) = \int_\Omega j(w, w')\, dx,$$

where we take $\Omega = (0, L) \subset \mathbb{R}$ for some $L > 0$ and

$$j(w, w') = W(w) + \epsilon\Psi(w'),$$

with $W(s) = \frac{s^4}{4} - \frac{s^2}{2}$ and $\Psi(s) = \sqrt{1+s^2} - 1$. Hence j has continuous partial derivatives with respect to w and w'. Thus we consider a variational problem of the form

$$E(w) = \int_\Omega j(w, w')\, dx \to \min, \tag{2.53}$$

on some space of functions $X(\Omega)$, say. In this section we distinguish between solving a problem such as (2.53) with **essential** boundary conditions and solving a problem such as (2.53) with **natural** boundary conditions.

A solution u to (2.53) will satisfy

$$\frac{d}{d\tau} E(u + \tau v)|_{\tau=0} = 0,$$

where v is from the set of admissible variations. Hence we consider

$$\begin{aligned}
\frac{d}{d\tau} E(u + \tau v)|_{\tau=0} &= \frac{d}{d\tau} \int_\Omega j(u + \tau v, u' + \tau v')\, dx\Big|_{\tau=0} \\
&= \int_\Omega j_u(u, u')v + j_{u'}(u, u')v'\, dx \\
&= \int_\Omega j_u(u, u')v\, dx + [j_{u'}(u, u')v]_0^L - \int_\Omega \frac{d}{dx} j_{u'}(u, u')v\, dx \\
&= \int_\Omega \left[j_u(u, u') - \frac{d}{dx} j_{u'}(u, u') \right] v\, dx + [j_{u'}(u, u')v]_0^L = 0.
\end{aligned} \tag{2.54}$$

Note that the boundary term $[j_{u'}(u,u')v]_0^L$ in (2.54) vanishes if $v(0) = v(L) = 0$ and these are known as **essential** boundary conditions in which case we are asking that the admissible variations v be in the function space

$$X_0(\Omega) = \{v \in X \ : \ v(0) = v(L) = 0\},$$

hence we minimise over a subspace X_0 of X and Dirichlet boundary conditions are built into the solution space.

The boundary term in (2.54) also vanishes for all v if

$$j_{u'}(u,u')(0) = j_{u'}(u,u')(L) = 0,$$

and these are the **natural** boundary conditions, they are a restriction on the assumed solution u to the variational problem rather than on the admissible variation v. It is the natural boundary conditions that we will consider in Section 4.5.

2.5 Uniqueness of solutions to an initial value problem

In the proof of Theorem 4.5 in Section 4.5 we also require the use of a result on the uniqueness of solutions to a certain initial value problem (see (4.34)). Consider the function

$$g(u,u') := \lambda f(u)(1 + (u')^2)^{\frac{3}{2}}, \tag{2.55}$$

where $\lambda = \frac{1}{\epsilon} \in (0,\infty)$, $f(u) = u - u^3$ and $u(x)$ is a (classical) solution of the problem

$$\begin{aligned} u'' &= -g(u,u'), \\ u'(0) &= u'(L) = 0, \end{aligned} \tag{2.56}$$

which is the Neumann stationary problem associated with (2.30) that we study in Chapter 4. If we set $u' = z$ and suppose that $u''(0) = z'(0) = 0$ then, using (2.56), the particular initial value problem which arises in Section 4.5 is given by

$$z'' + h_1(x)z'(x) + h_0(x)z(x) = 0, \quad z(0) = z'(0) = 0 \tag{2.57}$$

where $h_1(x) = \frac{\partial g}{\partial u'}$ and $h_0(x) = \frac{\partial g}{\partial u}$ with $g(u, u')$ given in (2.55).

Lemma 2.14. *Solutions of the initial value problem (2.57) are unique.*

Proof. Since $h_1(x)$ and $h_0(x)$ are continuous functions on some open interval J containing 0, they will both be bounded on any finite closed subinterval $[x_1, x_2]$ of J, i.e. there exists a constant $M(J) \equiv M$ such that

$$|h_0(x)| \leq M \text{ and } |h_1(x)| \leq M \text{ for all } x \in [x_1, x_2] \subset J.$$

We would like to show that (2.57) has a unique solution. Let $u(x)$ and $v(x)$ solve (2.57) and let $w(x) = u(x) - v(x)$ so that $w(0) = w'(0) = 0$. Choose $x_1, x_2 \in J$ such that $x_1 < 0 < x_2$. Let M be as above and let

$$p(x) = [w'(x)]^2 + [w(x)]^2,$$

so that $p(0) = 0$. For $x \in [x_1, x_2] \subset J$,

$$\begin{aligned} p'(x) &= 2w'(x)w''(x) + 2w(x)w'(x) \\ &= 2w'(x)[-h_1(x)w'(x) - h_0(x)w(x)] + 2w(x)w'(x) \\ &= -2h_1(x)[w'(x)]^2 - 2w'(x)h_0(x)w(x) + 2w(x)w'(x) \\ &= -2h_1(x)[w'(x)]^2 + 2w(x)w'(x)[1 - h_0(x)]. \end{aligned}$$

Hence

$$\begin{aligned} |p'(x)| &\leq 2|h_1(x)|[w'(x)]^2 + 2|w(x)||w'(x)||1 - h_0(x)| \\ &\leq 2|h_1(x)|[w'(x)]^2 + 2|w(x)||w'(x)|(1 + |h_0(x)|) \\ &\leq 2M[w'(x)]^2 + 2|w(x)||w'(x)|(1 + M) \\ &\leq 2M([w'(x)]^2 + [w(x)]^2) + 2|w(x)||w'(x)|(1 + M) \\ &\leq 2M([w'(x)]^2 + [w(x)]^2) + ([w(x)]^2 + [w'(x)]^2)(1 + M) \\ &= (1 + 3M)([w'(x)]^2 + [w(x)]^2) = (1 + 3M)p(x), \end{aligned}$$

and we have shown that

$$-Kp(x) \leq p'(x) \leq Kp(x), \quad x \in [x_1, x_2], \tag{2.58}$$

where $K = 1 + 3M$. In particular, from (2.58), we have

$$\begin{aligned} & e^{-Kx}p'(x) \leq e^{-Kx}Kp(x), \qquad x \in [0, x_2] \\ \Rightarrow \ & \frac{d}{dx}[e^{-Kx}p(x)] \leq 0, \qquad\qquad x \in [0, x_2], \end{aligned}$$

and so

$$e^{-Kx}p(x) \leq p(0) = 0 \Rightarrow p(x) \leq 0 \ \ \forall x \in [0, x_2].$$

But $p(x) \geq 0$ and so we have that $p(x) = 0$ for $x \in [0, x_2]$. Similarly, from (2.58),

$$\begin{aligned} & e^{Kx}p'(x) \geq -e^{Kx}Kp(x), \qquad x \in [x_1, 0] \\ \Rightarrow \ & \frac{d}{dx}[e^{Kx}p(x)] \geq 0, \qquad\qquad x \in [x_1, 0], \end{aligned}$$

and so

$$e^{Kx}p(x) \leq p(0) = 0 \Rightarrow p(x) \leq 0 \ \ \forall x \in [x_1, 0].$$

But $p(x) \geq 0$ hence $p(x) = 0$ for $x \in [x_1, 0]$. Hence we have shown that $p(x) \equiv 0$ on $[x_1, x_2]$ which implies that $w(x) = u(x) - v(x) = 0$ on $[x_1, x_2]$ and since x_1 and x_2 were arbitrary in J it follows that $u(x) \equiv v(x)$ for all $x \in J$ and so solutions of the initial value problem (2.57) are unique. □

Chapter 3

The Bistable Rosenau Equation: Well-posedness and Asymptotic Behaviour

In this chapter we study the following problem

$$\begin{aligned} u_t &= \epsilon(\psi(u_x))_x + f(u), \quad (x,t) \in Q_T \equiv \Omega \times (0,T), \\ \psi(u_x) &= 0, \quad (x,t) \in \partial\Omega \times (0,T), \\ u(x,0) &= u_0(x), \quad x \in \Omega, \end{aligned} \tag{3.1}$$

where $\Omega \subset \mathbb{R}$, $T > 0$, $\epsilon \in (0,\infty)$, $u(x,t)$ is the order parameter representing the state of the system at position x and time t, $f(u)$ is bistable and the flux function ψ is a monotone function of the gradient which saturates at a finite value as gradients become infinite. As discussed in Section 2.1.4, an appropriate choice for ψ in (3.1) is the mean curvature operator given by

$$\psi(s) = \frac{s}{\sqrt{1+s^2}},$$

so that $\psi(0) = 0$ and the boundary conditions in (3.1) can be written as

$$u_x = 0, \quad (x,t) \in \partial\Omega \times (0,T).$$

In Section 2.1.4, we noted that (3.1) is obtained as the L^2-gradient flow of the free energy functional in (2.25). In this chapter, using the methods of [22] we prove a well-posedness result for (3.1) and while this result can be shown to hold for any dimension n, we still we restrict ourselves to the one-dimensional case so that $\Omega \equiv (0, L)$, $L > 0$. In [22], similar results are proven for the case of a purely diffusive process so that $f(u) \equiv 0$ in (3.1) but here we prove a well-posedness result for the problem with a bistable kinetic nonlinearity $f(u)$ we take to be $u - u^3$. We keep the length L of the spatial domain Ω general since, as we will show in Chapter 4, the bifurcation structure for the stationary problem associated with (3.1) depends on the parameter ϵ as well as on the length L of the interval. We conclude this chapter with some numerical results in connection with the asymptotic behaviour of solutions to (3.1).

3.1 Well-posedness

The problem for which we prove a well-posedness result is given by

$$\begin{aligned} u_t &= \epsilon(\psi(u_x))_x + f(u), \quad (x,t) \in Q_T \equiv \Omega \times (0,T), \\ u_x &= 0, \quad (x,t) \in \partial\Omega \times (0,T), \\ u(x,0) &= u_0(x), \quad x \in \Omega, \end{aligned} \tag{3.2}$$

where $(0, T)$ is a finite time interval. Note that in what follows, the diffusion coefficient ϵ in (3.2) will be regarded as being fixed in $(0, \infty)$. In Section 2.1.4 we noted that discontinuous solutions to our problem may arise and in order to account for such solutions we will need to work in a space of functions in which discontinuous solutions are permissible. Hence we shall be working in BV, since in this space, functions are allowed to be discontinuous (see Section 2.2 for a discussion of BV). It is this space that we will use to define the notion of a variational inequality solution to (3.2) (see Definition 3.1) and it is the purpose of this section to prove a local existence and uniqueness result for a variational inequality solution to our problem.

We briefly note some properties of the function space $BV(\Omega)$ we will need in this section. For a further discussion of $BV(\Omega)$ see Section 2.2 where for example we show that a function of bounded variation is a function $u \in L^1(\Omega)$ whose partial derivatives in the sense of distributions are measures with finite total variation,

$$\int_\Omega |u_x|\,dx = \sup\left\{\int_\Omega u\,v_x\,dx \;:\; v \in C_0^\infty(\Omega),\ |v(x)| \le 1 \text{ for } x \in \Omega\right\}.$$

The space $BV(\Omega)$ endowed with the norm

$$||u||_{BV(\Omega)} = ||u||_{L^1(\Omega)} + \int_\Omega |u_x|\,dx,$$

is a Banach space but this norm-topology is too strong for many applications. For example, as noted in [3, p.121], continuously differentiable functions are not dense in $BV(\Omega)$ with respect to this topology. The topology on BV which we will require in this chapter is the BV-weak* topology defined by

$$u_j \xrightarrow{BV-w^*} u \Leftrightarrow u_j \to u \text{ in } L^1(\Omega) \text{ and } u_{jx} \rightharpoonup u_x \text{ in } M(\Omega),$$

where $M(\Omega)$ is the space of bounded measures on Ω and $u_{jx} \rightharpoonup u_x$ in $M(\Omega)$ means that

$$\int_\Omega u_{jx}\varphi\,dx \to \int_\Omega u_x\varphi\,dx,$$

for all $\varphi \in C_0^\infty(\Omega)$ (see [3, Definition 3.11]).

We also have the following compactness property [3, Proposition 3.13]: for every bounded sequence $\{u_j\} \subset BV(\Omega)$, there exists a subsequence $\{u_{j_k}\}$ and a function u in $BV(\Omega)$ such that $u_{j_k} \xrightarrow{BV-w^*} u$ as $k \to \infty$.

We need to define our notion of a variational inequality solution. To begin with, let us suppose that u is smooth enough so as to permit us to perform the calculations which follow. For smooth test functions $v \in C^\infty(Q_T)$, we multiply our equation

by $v-u$ and integrate by parts using the Neumann boundary conditions on u to obtain

$$\int_{Q_T}(u_t - f(u))(v-u)\,dx\,dt + \int_{Q_T}\epsilon\psi(u_x)(v_x-u_x)\,dx\,dt = 0.$$

Since $\Psi(s) = \sqrt{1+s^2}-1$ is convex, we have that $\Psi(v_x)-\Psi(u_x) \geq \Psi'(u_x)(v_x-u_x)$ and hence

$$\int_{Q_T}(u_t - f(u))(v-u)\,dx\,dt + \int_{Q_T}\epsilon(\Psi(v_x)-\Psi(u_x))\,dx\,dt \geq 0,$$

for smooth functions $v \in C^\infty(Q_T)$. This motivates the following definition of a variational inequality solution to our problem.

Definition 3.1. *Let $M(Q_T)$ denote the space of bounded measures on Q_T. A function $u \in L^\infty(Q_T) \cap L^\infty((0,T), BV(\Omega)) \cap \{u : u_x \in M(Q_T)\}$ is called a variational inequality solution of problem (3.2) if $u_t \in L^2(Q_T)$ and u satisfies the variational inequality*

$$\int_{Q_T}(u_t - f(u))(v-u)\,dx\,dt + \int_{Q_T}\epsilon(\Psi(v_x)-\Psi(u_x))\,dx\,dt \geq 0, \tag{3.3}$$

for all $v \in L^\infty(Q_T) \cap \{v : v_x \in M(Q_T)\}$.

Thus v_x, the distributional derivative of the function v, will be a measure with finite total variation. In Definition 3.1, the notation that $u \in L^\infty((0,T), BV(\Omega))$ means that the function $[0,T] \ni t \mapsto u(\cdot,t) \in BV(\Omega)$ belongs to $L^\infty(0,T)$ for almost every $t \in [0,T]$ i.e.

$$||u||_{L^\infty((0,T),BV(\Omega))} = \operatorname*{ess\,sup}_{0<t\leq T} ||u(\cdot,t)||_{BV(\Omega)} < \infty.$$

By the above discussion, classical solutions of (3.2) automatically satisfy variational inequality (3.3). To see that a smooth solution u of (3.3) also satisfies (3.2), choose as a test function $v = u + ch$ where $h \in C^\infty(Q_T)$, $c \in \mathbb{R}$, so that (3.3) becomes

$$\int_{Q_T}(u_t - f(u))(ch)\,dx\,dt + \int_{Q_T}\epsilon\Psi(u_x+ch_x)\,dx\,dt \geq \int_{Q_T}\epsilon\Psi(u_x)\,dx\,dt.$$

Hence from the Taylor series of $\Psi(u_x + ch_x)$ we have

$$c\int_{Q_T}(u_t - f(u))h\,dx\,dt + c\int_{Q_T}\epsilon\Psi'(u_x)h_x\,dx\,dt + \frac{c^2}{2}\int_{Q_T}\epsilon\Psi''(u_x)(h_x)^2\,dx\,dt + \ldots \geq 0.$$

Considering firstly, $c > 0$, then $c < 0$ and letting $c \to 0$ from above and below yields

$$\int_{Q_T}(u_t - f(u))h\,dx\,dt + \int_{Q_T}\epsilon\psi(u_x)h_x\,dx\,dt = 0 \ \ \forall\ h \in C^\infty(Q_T).$$

Integrating by parts and using the boundary conditions, we see that u classically satisfies (3.2).

We now formulate the main theorem of this section.

Theorem 3.2. *Problem (3.2) admits a unique variational inequality solution for all $T > 0$ for every $u_0(x) \in L^\infty(\Omega) \cap BV(\Omega)$.*

Proof. A standard method for proving existence results for this type of problem consists in replacing the original problem by a sequence of simpler problems for which one can show existence of a solution and for which the solutions of this sequence of problems converge in an appropriate topology to the solution of the original problem. Hence for $\gamma > 0$, consider the following regularised problem:

$$\begin{aligned} u_t &= \epsilon(\psi(u_x))_x + f(u), \quad (x,t) \in \Omega \times (0,T), \\ u_x &= 0, \quad (x,t) \in \partial\Omega \times (0,T), \\ u(x,0) &= u_0^\gamma(x), \quad x \in \Omega, \end{aligned} \tag{3.4}$$

where $u_0^\gamma(x)$ satisfies

$$u_0^\gamma \in C^\infty(\bar{\Omega}), \qquad u_{0x}^\gamma = 0 \ \text{ on } \ \partial\Omega,$$

$$||u_0^\gamma - u_0||_{L^\infty(\Omega)} \to 0 \ \text{ as } \ \gamma \to 0, \qquad ||u_0^\gamma||_{L^\infty(\Omega)} \leq ||u_0||_{L^\infty(\Omega)} + 1 = m_0,$$

and

$$\int_\Omega |u_{0x}^\gamma|\,dx \leq C(\Omega)\int_\Omega |u_{0x}|\,dx. \tag{3.5}$$

The existence of such a sequence of regularising initial data $u_0^\gamma \in C^\infty(\bar{\Omega})$ follows from the fact that the initial data $u_0 \in BV(\Omega)$ and because the space $C^\infty(\bar{\Omega})$ is dense in the space of functions of bounded variation with respect to the topology defined by the metric

$$d(u,v) = ||u-v||_{L^1(\Omega)} + \left| \int_\Omega |u_x| - \int_\Omega |v_x| \right|,$$

see for example [27, Section 5.2.2].

Let $u^\gamma(x,t)$ represent the unique classical solution to the regularised problem with the regular initial data $u_0^\gamma(x)$; these exist by standard parabolic theory, see for example Theorem 7.4, [43, Chapter V] which is proved for a more restricted type of quasilinear equation in divergence form but by the remark in [43, p.492], the proof survives without much change for problems of the type of (3.4). We want to show that there exists a function $u \in BV(Q_T)$ such that $u^\gamma \to u$ in $L^1(Q_T)$ as $\gamma \to 0$, which will be a variational inequality solution to our problem and that it does not depend on the choice of the sequence u^γ. As in [22], we will need to establish a series of convergence properties for, and a priori bounds on, the approximating solutions u^γ. Namely we show

Lemma 3.3.

A: the sequence $\{u^\gamma\}$ *is uniformly bounded in* $L^\infty(Q_T)$ *and the sequence* $\{u_t^\gamma\}$ *is uniformly bounded in* $L^2(Q_T)$,

B: the sequence $\{u^\gamma\}$ *is uniformly bounded in* $L^\infty((0,T), BV(\Omega))$ *and in* $BV(Q_T)$,

C: the sequence $\{u^\gamma\}$ *converges in the space* $L^\infty((0,T), L^2(\Omega))$ *and the sequence* $\{u^\gamma(\cdot,t)\}$ *converges in the space* $L^2(\Omega)$ *for all* $t \in [0,T]$.

Proof. [A]: In what follows, let Q_τ denote the space-time cylinder $\Omega \times (0,\tau)$ where τ is arbitrary in $[0,T]$. First of all, we have that

$$||u^\gamma||_{L^\infty(Q_T)} < m_0, \tag{3.6}$$

where $m_0 > 1$, by the parabolic maximum principle and properties of $f(\cdot)$. We show next that the sequence $\{u_t^\gamma\}$ is uniformly bounded in $L^2(Q_T)$. Multiply the regularised problem by u_t^γ and integrate over Q_τ:

$$\begin{aligned}\int_{Q_\tau} (u_t^\gamma)^2 \, dx \, dt &= -\int_{Q_\tau} \epsilon\psi(u_x^\gamma) u_{tx}^\gamma \, dx \, dt + \int_{Q_\tau} f(u^\gamma) u_t^\gamma \, dx \, dt \\ &= -\int_0^\tau \frac{d}{dt} \int_\Omega \epsilon\Psi(u_x^\gamma) \, dx \, dt + \int_0^\tau \frac{d}{dt} \int_\Omega F(u^\gamma) \, dx \, dt \\ &= -\int_\Omega (\epsilon\Psi(u_x^\gamma)|_{t=\tau} - \epsilon\Psi(u_0^\gamma)) \, dx + \int_\Omega (F(u^\gamma)|_{t=\tau} - F(u_0^\gamma)) \, dx,\end{aligned}$$

where $F(u) = \int_0^u f(s) \, ds$.

Hence

$$\begin{aligned}||u_t^\gamma||^2_{L^2(Q_\tau)} + \int_\Omega \epsilon\Psi(u_x^\gamma)|_{t=\tau} \, dx + \int_\Omega \left[\frac{(u^\gamma)^4}{4}\bigg|_{t=\tau} + \frac{(u_0^\gamma)^2}{2} \right] dx \\ \leq \int_\Omega \epsilon\Psi(u_{0x}^\gamma) \, dx + \left(\frac{m_0^4}{4} + \frac{m_0^2}{2} \right) |\Omega|, \qquad (3.7)\end{aligned}$$

from the bounds we have on u_0^γ and on u^γ. Hence using the bound on $\int_\Omega \Psi(u_x) \, dx$ in (2.40) and subsequently the bound in (3.5), it follows from (3.7) taking $\tau = T$, that

$$\begin{aligned}||u_t^\gamma||^2_{L^2(Q_T)} &\leq \int_\Omega \epsilon\Psi(u_{0x}^\gamma) \, dx + \left(\frac{m_0^4}{4} + \frac{m_0^2}{2} \right) |\Omega| \\ &\leq \int_\Omega \epsilon |u_{0x}^\gamma| \, dx + \left(\frac{m_0^4}{4} + \frac{m_0^2}{2} + \epsilon \right) |\Omega| \\ &\leq C(\Omega) \int_\Omega \epsilon |u_{0x}| \, dx + C_1(\epsilon) < \infty, \qquad (3.8)\end{aligned}$$

since $u_0 \in BV(\Omega)$ and where $C_1(\epsilon) = \left(\frac{m_0^4}{4} + \frac{m_0^2}{2} + \epsilon \right) |\Omega|$. Thus we have that the sequence $\{u_t^\gamma\}$ is uniformly bounded in $L^2(Q_T)$ and therefore also in $L^1(Q_T)$.

[B]: We also need to show that the sequence $\{u^\gamma\}$ is uniformly bounded in the space $L^\infty((0,T), BV(\Omega))$ and also that $\{u^\gamma\}$ is uniformly bounded in $BV(Q_T)$. To see the former, first note that (3.7) also implies that

$$\int_\Omega \epsilon\Psi(u_x^\gamma)|_{t=\tau} \, dx \leq C(\Omega) \int_\Omega \epsilon |u_{0x}| \, dx + C_1(\epsilon),$$

but since τ was arbitrary in $[0,T]$ we have, using (2.40) once again, that for all $t \in [0,T]$

$$C(\Omega)\int_\Omega \epsilon|u_{0x}|\,dx + C_1(\epsilon) \geq \int_\Omega \epsilon\Psi(u_x^\gamma)\,dx \geq \int_\Omega \epsilon|u_x^\gamma|\,dx - \epsilon|\Omega|,$$

$$\Rightarrow \int_\Omega |u_x^\gamma|\,dx \leq C(\Omega)\int_\Omega |u_{0x}|\,dx + C_2(\epsilon) + |\Omega| = C_3 < \infty, \tag{3.9}$$

where $C_2(\epsilon) = \frac{1}{\epsilon}C_1(\epsilon)$. This, together with the fact that $u^\gamma(\cdot,t) \in L^1(\Omega)$ for all $t \in [0,T]$ implies that

$$||u^\gamma(\cdot,t)||_{BV(\Omega)} < C_4 \quad \forall\ t \in [0,T],$$

with C_4 independent of γ and of t and so $\sup\limits_{0<t\leq T} ||u^\gamma(\cdot,t)||_{BV(\Omega)} < C_4$. Hence we have that the sequence $\{u^\gamma\}$ is indeed uniformly bounded in $L^\infty((0,T),BV(\Omega))$.

Since $u^\gamma(\cdot,t) \in L^1(\Omega)\ \forall\ t \in [0,T]$, we infer that $u^\gamma \in L^1(Q_T)$ and since (3.9) implies that

$$\int_0^T \int_\Omega |u_x^\gamma|\,dx\,dt \leq C_3 T,$$

we have that

$$||u^\gamma||_{BV(Q_T)} < C_5,$$

for C_5 independent of γ and so u^γ is also uniformly bounded in $BV(Q_T)$.

[C]: We now establish that the sequence $\{u^\gamma(\cdot,t)\}$ converges in the space $L^2(\Omega)$ as $\gamma \to 0$ for all $t \in [0,T]$ and that the sequence $\{u^\gamma\}$ converges in the space $L^\infty((0,T),L^2(\Omega))$ as $\gamma \to 0$. To this end, consider u^{γ_m} and u^{γ_n} both satisfying the regularised problem, multiply the difference of the two equations by the difference $u^{\gamma_m} - u^{\gamma_n}$, then integrate over Q_τ to obtain

$$\frac{1}{2}\int_{Q_\tau} \frac{\partial}{\partial t}(u^{\gamma_m} - u^{\gamma_n})^2\,dx\,dt = -\int_{Q_\tau} \epsilon(\psi(u_x^{\gamma_m}) - \psi(u_x^{\gamma_n}))(u_x^{\gamma_m} - u_x^{\gamma_n})\,dx\,dt$$
$$+ \int_{Q_\tau} (f(u^{\gamma_m}) - f(u^{\gamma_n}))(u^{\gamma_m} - u^{\gamma_n})\,dx\,dt. \tag{3.10}$$

Since the function $\psi(s)$ is monotonic, the first term on the right-hand side of (3.10) is non-positive and so (3.10) becomes

$$\begin{aligned}\int_0^\tau \frac{d}{dt}\left(\int_\Omega (u^{\gamma_m}-u^{\gamma_n})^2\,dx\right)dt &\le 2\int_{Q_\tau}(f(u^{\gamma_m})-f(u^{\gamma_n}))(u^{\gamma_m}-u^{\gamma_n})\,dx\,dt\\ &= 2\int_{Q_\tau}\left[(u^{\gamma_m}-u^{\gamma_n})-\{(u^{\gamma_m})^3-(u^{\gamma_n})^3\}\right](u^{\gamma_m}-u^{\gamma_n})\,dx\,dt\\ &= 2\int_{Q_\tau}\left[1-\{(u^{\gamma_m})^2+u^{\gamma_m}u^{\gamma_n}+(u^{\gamma_n})^2\}\right](u^{\gamma_m}-u^{\gamma_n})^2\,dx\,dt\\ &\le 2\int_{Q_\tau}|\{(u^{\gamma_m})^2+u^{\gamma_m}u^{\gamma_n}+(u^{\gamma_n})^2\}-1||u^{\gamma_m}-u^{\gamma_n}|^2\,dx\,dt\\ &\le 2|3m_0^2-1|\int_{Q_\tau}|u^{\gamma_m}-u^{\gamma_n}|^2\,dx\,dt\\ &= \int_0^\tau |6m_0^2-2|\left(\int_\Omega (u^{\gamma_m}-u^{\gamma_n})^2\,dx\right)dt. \qquad (3.11)\end{aligned}$$

Thus if we define $C(m_0)=|6m_0^2-2|$ then we have, since τ is arbitrary in $[0,T]$

$$\frac{d}{dt}\int_\Omega (u^{\gamma_m}-u^{\gamma_n})^2\,dx \le C(m_0)\int_\Omega (u^{\gamma_m}-u^{\gamma_n})^2\,dx.$$

Hence Gronwall's inequality implies that

$$\int_\Omega (u^{\gamma_m}-u^{\gamma_n})^2\,dx \le e^{C(m_0)\tau}\int_\Omega (u_0^{\gamma_m}-u_0^{\gamma_n})^2\,dx,$$

so that from (3.11)

$$\begin{aligned}\int_\Omega (u^{\gamma_m}-u^{\gamma_n})^2|_{t=\tau}\,dx &\le \int_0^\tau C(m_0)\left(\int_\Omega (u^{\gamma_m}-u^{\gamma_n})^2\,dx\right)dt+\int_\Omega (u_0^{\gamma_m}-u_0^{\gamma_n})^2\,dx\\ &\le (C(m_0)\tau\, e^{C(m_0)\tau}+1)\int_\Omega (u_0^{\gamma_m}-u_0^{\gamma_n})^2\,dx,\end{aligned}$$

but since τ was arbitrary in $[0,T]$ and u^{γ_m} and u^{γ_n} both satisfy the regularised problem, we have

$$||u^{\gamma_m}(\cdot,t)-u^{\gamma_n}(\cdot,t)||_{L^2(\Omega)}\to 0 \ \text{ as } \ \gamma_m,\gamma_n\to 0 \ \text{ for all } t\in[0,T].$$

So $u^{\gamma_n}(\cdot,t)$ is Cauchy in $L^2(\Omega)$ for all $t\in[0,T]$ hence the sequence $u^{\gamma_n}(\cdot,t)$ converges in $L^2(\Omega)$ for all $t\in[0,T]$ and from this it follows that u^γ converges in $L^\infty((0,T),L^2(\Omega))$. Thus Lemma 3.3 is established. □

We now pass to the limit as $\gamma \to 0$ making use of the above properties of the sequence u^γ. We have shown that there exists a unique $u \in L^\infty((0,T), L^2(\Omega))$ such that

$$||u^\gamma(\cdot,t) - u(\cdot,t)||_{L^2(\Omega)} \to 0 \text{ as } \gamma \to 0 \;\; \forall t \in [0,T],$$

and

$$||u^\gamma - u||_{L^2(Q_T)} \to 0 \text{ as } \gamma \to 0,$$

but then this implies convergence in L^1 so that we have

$$||u^\gamma(\cdot,t) - u(\cdot,t)||_{L^1(\Omega)} \to 0 \text{ as } \gamma \to 0 \;\; \forall t \in [0,T],$$

and

$$||u^\gamma - u||_{L^1(Q_T)} \to 0 \text{ as } \gamma \to 0, \tag{3.12}$$

using the Cauchy-Schwarz inequality.

We have also shown uniform boundedness of u_t^γ in $L^2(Q_T)$, hence $||u_t^\gamma||_{L_2(Q_T)} \leq C$ and so by weak compactness in $L^2(Q_T)$, we can extract a subsequence that we still denote as $\{u_t^\gamma\}$ which is such that

$$u_t^\gamma \rightharpoonup u_t \text{ in } L^2(Q_T) \text{ with } u_t \in L^2(Q_T).$$

This implies that given $\varphi \in L^2(\Omega)$ we have

$$\int_0^t \langle u_t^\gamma(x,s), \varphi \rangle_{L^2(\Omega)} \, ds = \langle u^\gamma(x,t), \varphi \rangle_{L^2(\Omega)} - \langle u_0^\gamma(x), \varphi \rangle_{L^2(\Omega)},$$

and letting $\gamma \to 0$ gives

$$\int_0^t \langle u_t(x,s), \varphi \rangle_{L^2(\Omega)} \, ds = \langle u(x,t), \varphi \rangle_{L^2(\Omega)} - \langle u_0(x), \varphi \rangle_{L^2(\Omega)},$$

from which it follows that the limit function $u(x,t)$ satisfies the initial condition, $u(x,0) = u_0(x)$, and following the same reasoning as for (3.6), the limit function u is also uniformly bounded in $L^\infty(Q_T)$.

We now prove that the limit function u is in $BV(Q_T)$. We have shown that the sequence $\{u^\gamma\}$ is uniformly bounded in $BV(Q_T)$. Hence we can extract a subsequence denoted $\{u^{\gamma_i}\}$ that converges weakly to some BV function η. That is to say, $u^{\gamma_i}(x,t) \rightharpoonup \eta(x,t)$ in $BV(Q_T)$-weak* with $\eta \in BV(Q_T)$, but this means that $u^{\gamma_i} \to \eta$ in $L^1(Q_T)$, so from (3.12), by the uniqueness of the limit, we must have

$$u = \eta \in BV(Q_T). \tag{3.13}$$

Hence by definition of BV functions on Q_T, we conclude from (3.13) that the weak first derivative in space of u is a bounded measure on Q_T.

We can now show that the limit function u is such that $u(\cdot,t) \in BV(\Omega)$ for every $t \in [0,T]$. That the sequence $\{u^\gamma\}$ is uniformly bounded in $L^\infty((0,T), BV(\Omega))$ means that

$$||u^{\gamma_i}(\cdot,t)||_{BV(\Omega)} < C_6, \quad \text{for almost every } t \in [0,T].$$

Fix an arbitrary t_0 in $[0,T]$. We can extract a subsequence $\{u^{\gamma_j}\}$ of $\{u^{\gamma_i}\}$ such that $u^{\gamma_j}(\cdot,t_0) \rightharpoonup U(\cdot,t_0)$ weak* in $BV(\Omega)$ with $U(\cdot,t_0) \in BV(\Omega)$. But this means that $u^{\gamma_j}(\cdot,t_0) \to U(\cdot,t_0)$ in $L^1(\Omega)$ and so we have once again from (3.12) that $u(\cdot,t) = U(\cdot,t) \in BV(\Omega)$ for all $t \in [0,T]$ since t_0 was arbitrary in $[0,T]$.

In [22] it is shown that for $u \in BV(\Omega)$ and Ψ convex, the functional $\int_\Omega \Psi(u_x)\,dx$ is lower semi-continuous with respect to L^1-convergence. Hence, since $u(\cdot,t) \in BV(\Omega)$ for all $t \in [0,T]$ and since $||u^\gamma(\cdot,t) - u(\cdot,t)||_{L^1(\Omega)} \to 0$ as $\gamma \to 0$ for all $t \in [0,T]$, we must have that

$$\int_\Omega \Psi(u_x)\,dx \le \liminf_{\gamma \to 0} \int_\Omega \Psi(u_x^\gamma)\,dx \ \text{ for all } t \in [0,T]. \tag{3.14}$$

We noted earlier that from (3.7), it follows that

$$\int_\Omega \Psi(u_x^\gamma)\,dx \le C(\Omega) \int_\Omega |u_{0x}| + C_2(\epsilon) \quad \forall t \in [0,T]. \tag{3.15}$$

Hence taking the limit inferior of (3.15) as $\gamma \to 0$, we see that by (2.40)

$$\int_\Omega |u_x|\,dx - |\Omega| \leq \int_\Omega \Psi(u_x)\,dx$$
$$\leq \liminf_{\gamma\to 0} \int_\Omega \Psi(u_x^\gamma)\,dx \leq C(\Omega)\int_\Omega |u_{0x}|\,dx + C_2(\epsilon) \quad \forall t \in [0,T].$$

Thus we are lead to conclude that $||u(\cdot,t)||_{BV(\Omega)} < \infty$ for all $t \in [0,T]$ and consequently

$$u \in L^\infty((0,T), BV(\Omega)).$$

For later, note that one may integrate (3.14) with respect to t on $[0,T]$ and obtain

$$\liminf_{\gamma\to 0} \int_{Q_T} \Psi(u_x^\gamma)\,dx\,dt \geq \int_{Q_T} \Psi(u_x)\,dx\,dt.$$

An additional result that we will need when passing to the limit as $\gamma \to 0$ is that $||u^\gamma - u||_{L^1(Q_T)} \to 0$ as $\gamma \to 0$ implies that $||f(u) - f(u^\gamma)||_{L_1(Q_T)} \to 0$. This follows easily when one considers

$$\int_0^T \int_\Omega |f(u) - f(u^\gamma)|\,dx\,dt = \int_0^T \int_\Omega |u - u^3 - (u^\gamma - (u^\gamma)^3)|\,dx\,dt$$
$$\leq \int_0^T \int_\Omega |u - u^\gamma|\,dx\,dt + \int_0^T \int_\Omega |u - u^\gamma||u^2 + uu^\gamma + (u^\gamma)^2|\,dx\,dt$$
$$\leq \int_0^T \int_\Omega |u - u^\gamma|\,dx\,dt + 3m_0^2 \int_0^T \int_\Omega |u - u^\gamma|\,dx\,dt \ \to 0 \text{ as } \gamma \to 0.$$

So far we have shown that the limit function u is such that

$$u \in L^\infty(Q_T) \cap L^\infty((0,T), BV(\Omega)) \cap \{u : u_x \in M(Q_T)\},$$

so that all that remains is to be proven is that the limit function u satisfies the variational inequality (3.3). Note that the variational inequality holds for the solutions u^γ of the regularised problems with test functions taken from the smooth sequence $\{v^n\}_{n\in\mathbb{N}} \subset C^\infty(Q_T)$ i.e.

$$\int_{Q_T} (u_t^\gamma - f(u^\gamma))(v^n - u^\gamma)\,dx\,dt + \int_{Q_T} \epsilon(\Psi(v_x^n) - \Psi(u_x^\gamma))\,dx\,dt \geq 0, \tag{3.16}$$

for $n = 1, 2, \cdots$. It is shown in [23, Thm 2.2] that the space $C^\infty(Q_T)$ is dense in $BV(Q_T)$ equipped with the topology defined by the distance

$$d(u,w) = ||u - w||_{L^1(Q_T)} + \left|\int_{Q_T} |u_x| - \int_{Q_T} |w_x|\right| + \left|\int_{Q_T} \Psi(u_x) - \int_{Q_T} \Psi(w_x)\right|,$$

which means in particular that one can approximate $BV(Q_T)$ functions by a sequence of $C^\infty(Q_T)$ functions, i.e. for $v \in BV(Q_T)$, there exists a sequence $\{v^n\} \in C^\infty(Q_T)$ such that

$$\int_{Q_T} \Psi(v_x^n)\,dx\,dt \to \int_{Q_T} \Psi(v_x) \text{ as } n \to \infty,$$

and

$$\int |v^n - v|\,dx\,dt \to 0 \text{ as } n \to \infty.$$

This combined with all the properties established in Lemma 3.3 for solutions u^γ to the regularised problem, means that one may pass to the limit as $n \to \infty$ and subsequently as $\gamma \to 0$ in inequality (3.16) to obtain the result.

As usual, in order to prove uniqueness of a variational inequality solution to our problem we suppose non-uniqueness and derive a contradiction. Hence suppose there are two variational inequality solutions u_1 and u_2 satisfying problem (3.2) and therefore the variational inequality (3.3) with

$$u_1(x,0) = u_2(x,0) = u_0(x). \tag{3.17}$$

Take the variational inequality first with $u = u_1$, $v = u_2$ and then with $u = u_2$, $v = u_1$ so that

$$\int_{Q_\tau} \left(\frac{\partial u_1}{\partial t} - f(u_1)\right)(u_2 - u_1)\,dx\,dt + \int_{Q_\tau} \epsilon[\Psi((u_2)_x) - \Psi((u_1)_x))]\,dx\,dt \geq 0,$$

and

$$\int_{Q_\tau} \left(\frac{\partial u_2}{\partial t} - f(u_2)\right)(u_1 - u_2)\,dx\,dt + \int_{Q_\tau} \epsilon[\Psi((u_1)_x) - \Psi((u_2)_x)]\,dx\,dt \geq 0.$$

Adding these two inequalities gives

$$\int_{Q_\tau} \frac{\partial(u_1 - u_2)}{\partial t}(u_1 - u_2)\,dx\,dt \leq \int_{Q_\tau} (f(u_1) - f(u_2))(u_1 - u_2)\,dx\,dt.$$

As before

$$\int_\Omega (u_1-u_2)^2\,dx|_{t=\tau} \le \int_0^\tau C(m_0)\left(\int_\Omega (u_1-u_2)^2\,dx\right)dt + \int_\Omega (u_1(x,0)-u_2(x,0))^2\,dx$$
$$\le (C(m_0)\tau\, e^{C(m_0)T}+1)\int_\Omega (u_1(x,0)-u_2(x,0))^2\,dx,$$

using again the Gronwall inequality. Thus it follows from (3.17) that

$$||u_1(\cdot,\tau)-u_2(\cdot,\tau)||_{L^2(\Omega)}=0,$$

and uniqueness follows from τ being arbitrary in $[0,T]$. □

3.2 Numerical analysis

In this section we present some numerical simulations in connection with the asymptotic behaviour of solutions to the bistable Rosenau equation

$$\begin{aligned} u_t &= \epsilon(\psi(u_x))_x + f(u), \quad (x,t)\in Q_T \equiv \Omega\times(0,T), \\ u_x &= 0, \quad (x,t)\in \partial\Omega\times(0,T), \\ u(x,0) &= u_0(x), \quad x\in\Omega, \end{aligned} \tag{3.18}$$

for $\Omega = (0,L)\subset\mathbb{R}$, $L>0$. In the experiments which follow, in order to solve (3.18) numerically, we have used the built-in MATLAB partial differential equation (PDE) solver pdepe which can be used to solve initial-boundary value problems for systems of parabolic and elliptic PDEs in one space variable x and time t. We note that pdepe is not specifically designed to deal with degenerate parabolic problems and so we cannot guarantee how well it will handle discontinuities; nevertheless, we will see that its handling does appear to agree empirically with that implied in the analysis of Section 3.1 and also with the analysis in Chapter 4. Pdepe uses an ODE solver in t and finite differences in x. Hence it works on a discrete spatial grid consisting of, say, $N+1$ mesh points $x_1, x_2, \cdots, x_{N+1}$ where $N\in\mathbb{N}$ and so we need to consider how we would regard a particular numerical solution to (3.18) found using pdepe as being discontinuous. Hence for $N=N_1$ and particular initial data $u_0(x)$, suppose we obtain a numerical solution $u(x,t)$

to (3.18) at a particular time $t \in (0, T]$ and that there exists an $x_0 \in \Omega$ such that for some fixed $1 < i < N_1 + 1$ we have $x_i = x_0$ and

$$|u(x_{i+1}, t) - u(x_i, t)| = \delta_{N_1},$$

for some $\delta_{N_1} > 0$. Now suppose N is increased to $N_k = kN_1$, $k \in \mathbb{N}$, so that we will have $x_0 = x_{k(i-1)+1} = x_j$ for $1 < j < N_k + 1$ and suppose that

$$|u(x_{j+1}, t) - u(x_j, t)| = \delta_{N_k},$$

for $\delta_{N_k} > 0$. If the decreasing sequence $\delta_{N_1} > \delta_{N_2} > \cdots$ is such that $\delta_{N_k} \nrightarrow 0$ as $k \to \infty$ then we regard the numerical solution $u(x, t)$ to (3.18) as having a discontinuity at $x = x_0 \in \Omega$.

Experiment 3.4. We consider solving (3.18) with the following piecewise constant initial data

$$u_0(x) = \left\{ \frac{(-1)^n}{2^n},\ x \in \left[\frac{L}{2^n}, \frac{L}{2^{n-1}} \right],\ n = 1, 2, \cdots \right\}, \tag{3.19}$$

as plotted in Figure 3.1 where we have taken $L = 2.5$. We note that this particular initial data (3.19) was suggested by Professor Vivian Hutson of The University of Sheffield in order to establish conditions in [36] on the initial data under which the non-coarsening theorem of [25] discussed in Section 2.1.3 for solutions to the integro-differential equation (2.20) holds. For details see [36, Theorem 3.3].

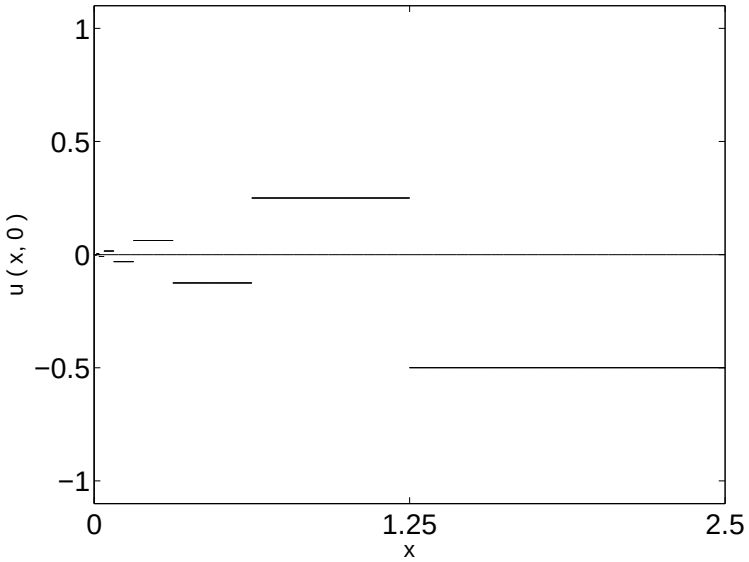

Figure 3.1: Initial data $u_0(x)$ from (3.19).

As discussed in Section 2.2, in the one-dimensional setting, the BV norm of a function u is its pointwise total variation $pV(u, \Omega)$ defined in Definition 2.7. The pointwise total variation of a piecewise constant function is simply the sum of the absolute value of the jumps it undergoes, therefore

$$\begin{aligned} pV(u_0(x), \Omega) &= \sum_{k=1}^{\infty} \left| \frac{(-1)^k}{2^k} - \frac{(-1)^{k+1}}{2^{k+1}} \right| \\ &= \sum_{k=1}^{\infty} \frac{3}{2^{k+1}} \\ &= \frac{3}{2} < \infty. \end{aligned}$$

If $\epsilon = 0$ in (3.18) so that we are solving the kinetic equation $u_t = f(u)$, then any part of $u_0(x)$ which is positive will tend to $+1$ as $t \to \infty$ and any part of $u_0(x)$ which is negative will tend to -1 as $t \to \infty$. Hence $u_0(x) \to u(x)$ as $t \to \infty$ as in Figure 3.2 but we note that since we will have finitely many space mesh points, neither the initial data $u_0(x)$ in (3.19) nor the solution $u(x)$ to which $u_0(x)$ converges can entirely be realised numerically.

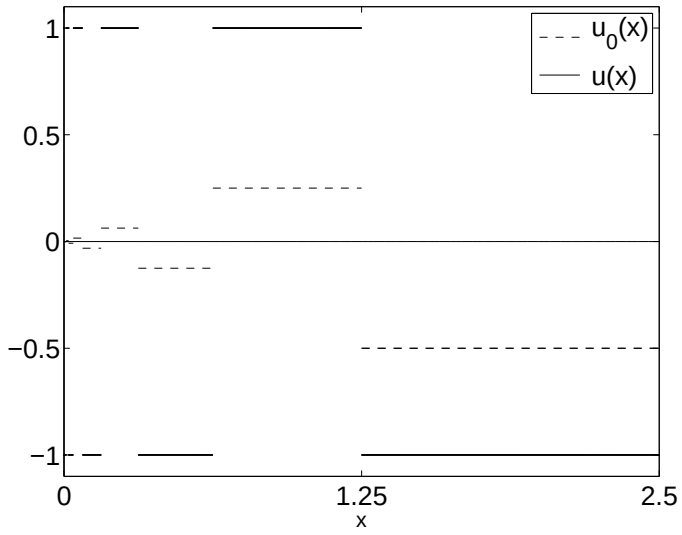

Figure 3.2: Solution to (3.18), (3.19) with $\epsilon = 0$, $L = 2.5$.

In order to account for domains $x \in \left[\frac{L}{2^n}, \frac{L}{2^{n-1}}\right]$ which get smaller and smaller as $n \to \infty$ we need to take the space mesh to be finer at values of $x \in [0, L]$ closer to zero. Specifically, for $N = 15000$, we define our space mesh in MATLAB as

follows

$$x = \left[0 : \frac{L}{100N} : \frac{L}{1024}, \frac{L}{1024} + \frac{L}{100N} : \frac{L}{N} : L\right], \tag{3.20}$$

so that for $x \in \left[0, \frac{L}{1024}\right]$, $\Delta x = \frac{L}{100N}$ and for $x \in \left[\frac{L}{1024} + \frac{L}{100N}, L\right]$, $\Delta x = \frac{L}{N}$. Since there will be infinitely many contributions to the pointwise total variation of the solution $u(x)$ to (3.18), (3.19) for $\epsilon = 0$, the BV norm of $u(x)$ is infinite. In fact,

$$pV(u(x), \Omega) = \sum_{k=1}^{\infty} \left|(-1)^k - (-1)^{k+1}\right| = \infty.$$

and so for $\epsilon = 0$ we have initial data (3.19) with finite BV norm converging to the solution in (3.2) which has infinite BV norm.

Suppose we now take $\epsilon > 0$ but small and solve (3.18) with the initial data $u_0(x)$ as in (3.19). We take $\epsilon = 0.00001$, $L = 2.5$ and the space mesh in (3.20) with $N = 15000$ and the solution converged to the solution u in Figure 3.3 which is approximately piecewise constant. For a brief discussion of how we measure the numerical convergence for large time of solutions to (3.18) in this and subsequent experiments in the thesis, see the remark at the end of this section.

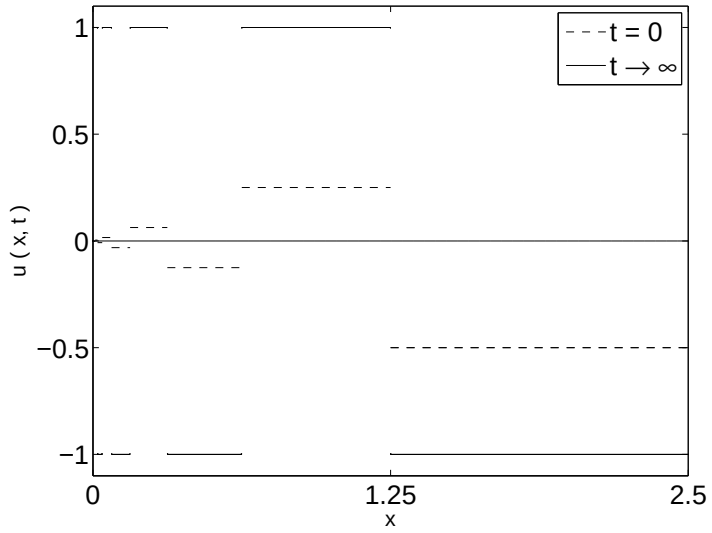

Figure 3.3: Solution to (3.18), (3.19) with $\epsilon = 0.00001$, $L = 2.5$.

This solution at first sight looks very similar to the one obtained in Figure 3.2 for $\epsilon = 0$ however, we calculated the pointwise variation $pV(u, \Omega)$ of the solution in Figure 3.3 to be approximately equal to 13.99989 for this particular space mesh. In Figure 3.4, we examine the difference between the solutions corresponding to $\epsilon = 0$ (left) and $\epsilon = 0.00001$ (right) for smaller values of x, namely for $x \in \left[0, \frac{L}{10}\right]$.

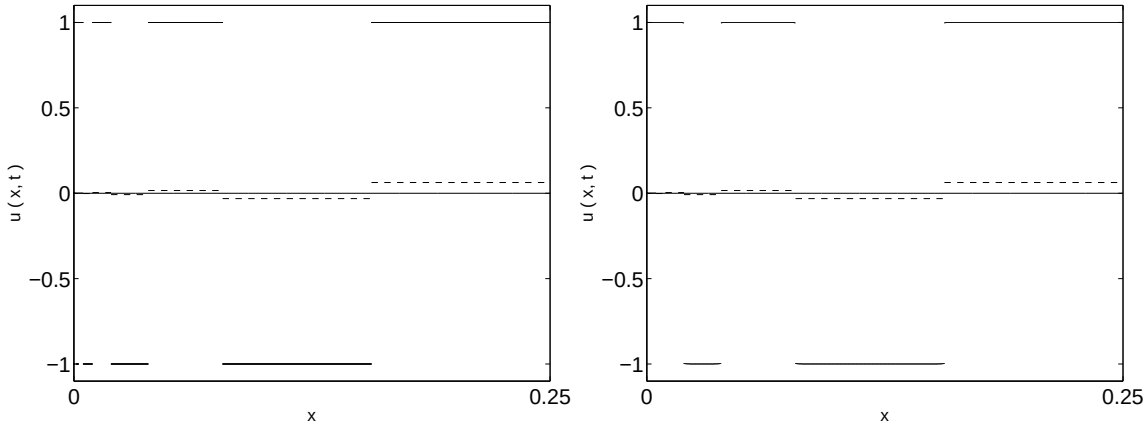

Figure 3.4: Solution to (3.18), (3.19) with $\epsilon = 0$ (left) and $\epsilon = 0.00001$ (right) for x small $\left(0 \leq x \leq \frac{L}{10}\right)$, $L = 2.5$.

When $\epsilon = 0$ there are an infinite number of regions in $[0, L]$ in which the solution either equals $+1$ or -1 and for $\epsilon = 0.00001$, there is a finite number (7, in this case) of regions in $[0, L]$ in which the solution is approximately equal to either $+1$ or -1 and the solution has finite BV norm. Hence we have initial data (3.19) with a finite BV norm converging to a solution with infinite BV norm for $\epsilon = 0$ and to a solution with finite BV norm for $\epsilon > 0$. To test whether the value ($\simeq 13.99989$) obtained above for $pV(u, \Omega)$ for the solution u to (3.18), (3.19) in the case $\epsilon = 0.00001$ can be regarded as mesh-independent we also present a plot of $pV(u, \Omega)$ against N from (3.20) for solutions to (3.18), (3.19) for various values of ϵ in Figure 3.5.

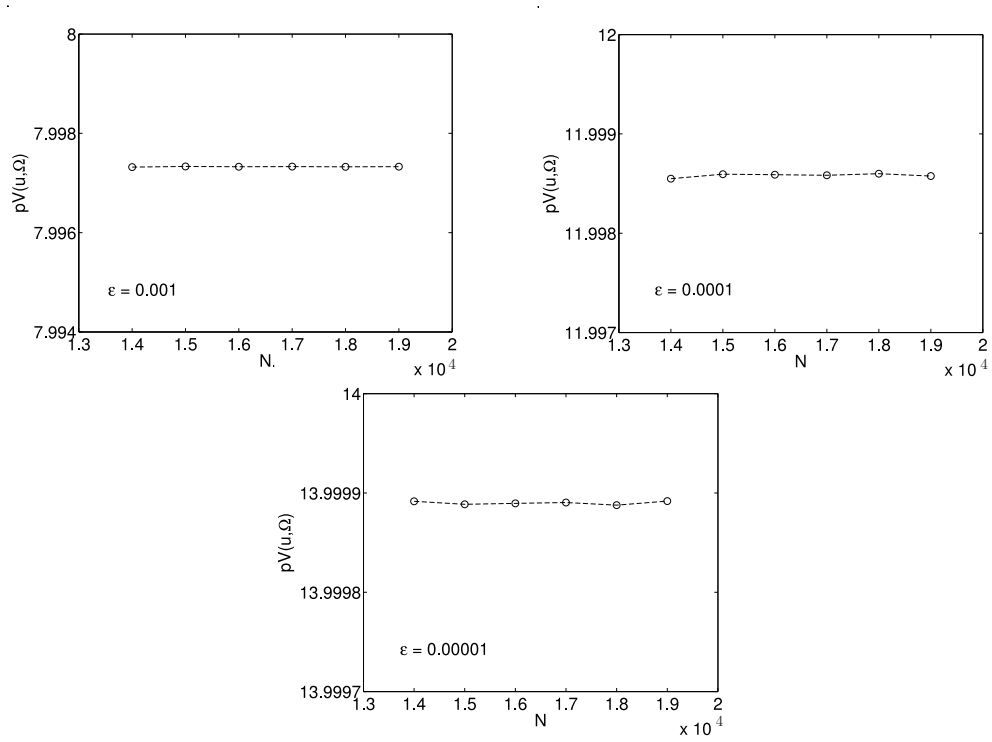

Figure 3.5: Plot of $pV(u, \Omega)$ versus N for solutions to (3.18), (3.19) with (3.20) in the cases $\epsilon = 0.001$, $\epsilon = 0.0001$ and $\epsilon = 0.00001$.

Experiment 3.5. Experiment 3.4 leads on naturally to a discussion of **coarsening** (or non-coarsening) of solutions for (3.18), a notion which was described in Section 2.1.3. Suppose we take

$$u_0(x) = \frac{4x(L-x)}{L^2} \sin\left(\frac{10\pi x^2}{L^2}\right), \tag{3.21}$$

as sign-changing initial data for (3.18). We aim to see whether or not solutions to (3.18), (3.21) will coarsen to ± 1 for sufficiently small $\epsilon > 0$. This time we partition the space interval $[0, L]$ by the $N + 1$ evenly spaced points

$$0 = x_1 < x_2 < \ldots < x_{N+1} = L, \tag{3.22}$$

so that $\Delta x = \frac{L}{N}$. We fix $N = 10000$ and present the time evolutions of the initial data (3.21) to equilibrium for $\epsilon = 0.05$ and $\epsilon = 0.001$ in Figures 3.6 and 3.7 respectively. As shown in Figure 3.6, with $\epsilon = 0.05$, only partial coarsening can be observed while in Figure 3.7, for $\epsilon = 0.001$, the solution of (3.18) through u_0 in (3.21) does not coarsen at all.

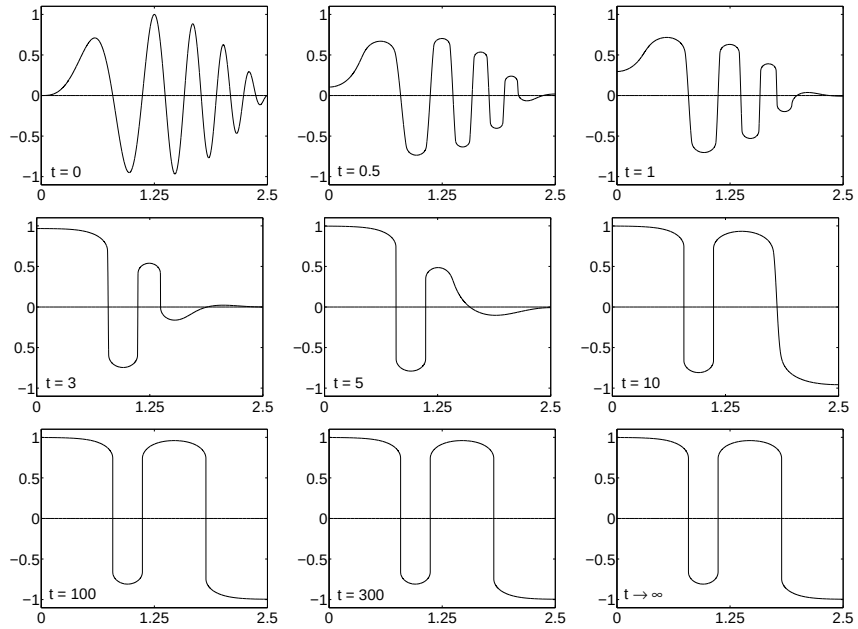

Figure 3.6: Time evolution of the solution of (3.18), (3.21) with $\epsilon = 0.05$.

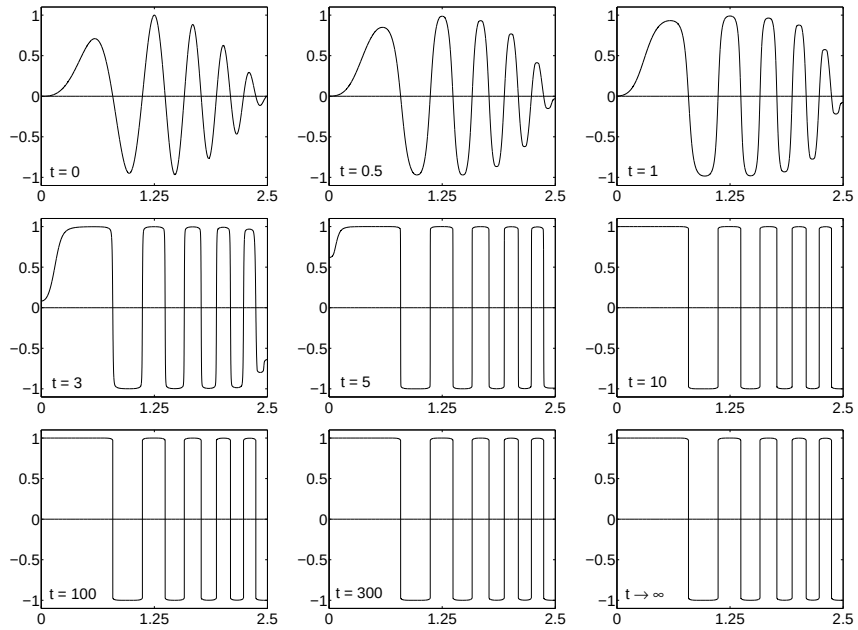

Figure 3.7: Time evolution of the solution of (3.18), (3.21) with $\epsilon = 0.001$.

Experiment 3.6. The partial coarsening of solutions to (3.18), (3.21) observed in Experiment 3.5 for larger ϵ, suggests that a Conway-Hoff-Smoller type result may hold for (3.18). That is, it may be that for large enough ϵ, the *only* stable equilibria for (3.18) are the constant equilibria ± 1 of the kinetic equation (2.22). This would mean that for a sufficiently large diffusion coefficient, solutions to the bistable Rosenau equation are asymptotic to solutions of the kinetic equation $u_t = f(u)$. The result is proven in [56, Chapter 14] and in [21] for the case of the Allen-Cahn equation (2.7) and in [36] for the non-local Allen-Cahn equation (2.20) under the assumption that the kernel $J(\cdot)$ in (2.20) is non-negative. We partition the space interval as in (3.22) taking $N = 10000$.

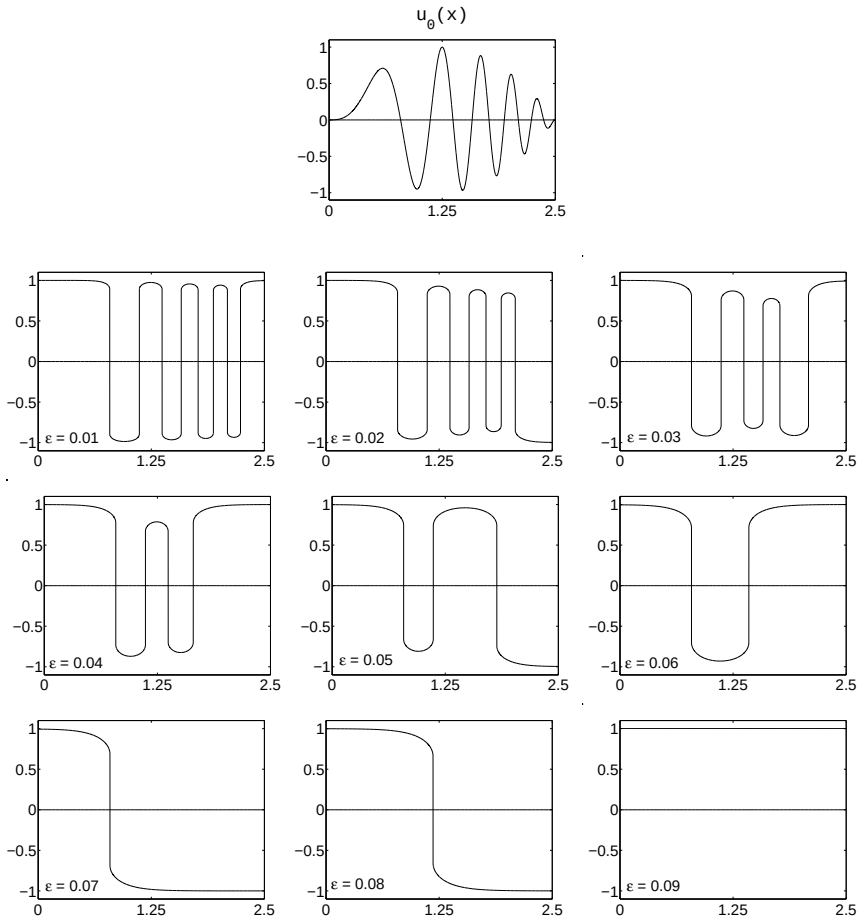

Figure 3.8: Equilibrium solutions to (3.18), (3.19) with $L = 2.5$ for various values of ϵ.

In Figure 3.8 we have plotted the initial data in (3.21) together with the equilibrium solutions of (3.18) to which the solution converged for various values of ϵ increased from $\epsilon = 0.01$ to $\epsilon = 0.09$ in increments of 0.01. Hence in this instance, for ϵ large enough, the solution converges to a constant solution (namely $u = +1$) of the kinetic equation $u_t = f(u)$.

Remark: We note that the convergence of numerical solutions of (3.18) to equilibrium states in the above experiments was assessed in general by numerically solving (3.18) for particular initial data firstly up to some time $T = T_1$ and then again up to a larger time $T = kT_1$, $k \in \mathbb{N}$ and then comparing the two solutions to see whether

$$||u(x, kT_1) - u(x, T_1)||_1 = \sum_{j=1}^{N} |u(x_j, kT_1) - u(x_j, T_1)| < \text{tol},$$

for some tolerance tol we took to be 10^{-8} and where $(x_1, x_2, \cdots, x_{N+1})$ denotes the particular chosen space mesh.

3.3 Conclusions

We have presented a quasilinear reaction-diffusion equation (3.2) with a bistable kinetic nonlinearity $f(u)$ and Neumann boundary conditions as a model for solid-solid phase transitions in the case of large gradients and we have defined solutions to (3.2) via a variational inequality. This allowed us to obtain a well-posedness result for the problem in the space of functions of bounded variation. We also carried out some numerical experiments pertaining to the asymptotic behaviour of solutions to (3.2). We are not aware of any analytical results for the asymptotic behaviour of solutions to this problem. One would like to be able to prove rigorously a result on convergence to equilibria for (3.2). The main technique used to prove convergence to equilibria is usually the Simon-Łojasiewicz inequality [19] but we do not have sufficient knowledge of the free energy functional to be able

to apply such a result in our case. One would need to prove that the free energy functional (2.28) associated with (3.2) is analytic, i.e. that it can be written locally as a convergent power series.

The bistable Rosenau equation (3.1) is a singular perturbation of the kinetic equation

$$u_t = f(u), \quad x \in \Omega \tag{3.23}$$

since (3.1) is not well-posed backwards in time. However, (3.23) has an uncountable number of stationary solutions and the results of Experiment 3.5 suggest that there is still an uncountable number of stationary solutions to (3.1) for $\epsilon > 0$ small enough since solutions do not coarsen for small ϵ. The results of Experiment 3.4 suggest that if we are working in the space of functions of bounded variation then there cannot be a one-to-one correspondence between solutions of (3.23) and (3.1) since we found an example of initial data (3.19) with a finite BV norm which converged to a solution with infinite BV norm in the case that $\epsilon = 0$ and to a solution with finite BV norm when $\epsilon > 0$. Proving a Conway-Hoff-Smoller type result such as the one suggested by Experiment 3.6 for (3.18) usually requires having access to the spectrum of the diffusion operator (or, as in [39], a representation of the semigroup via the variation of constants formula) but it is not clear how one even defines the spectrum of the diffusion operator in (3.18). Proving such a result for (3.18) remains an open problem.

Chapter 4

The Stationary Problem for the Bistable Rosenau Equation

We devote this chapter to the study of the following bistable quasilinear equation with saturating flux

$$\begin{aligned} (\psi(u'))' + \lambda f(u) = 0, \quad x \in \Omega, \\ \psi(u') = 0, \quad x \in \partial\Omega, \end{aligned} \tag{4.1}$$

where $\Omega \equiv (0, L) \subset \mathbb{R}$, $L > 0$ and $\lambda \in (0, \infty)$. We noted in Section 2.1.4 that a particular suitable choice of saturating flux function is

$$\psi(s) = \frac{s}{\sqrt{1+s^2}}, \tag{4.2}$$

and we take $f(u)$ to be the usual bistable nonlinearity $u - u^3$. With these choices for $\psi(u_x)$ and $f(u)$, equation (4.1) is the stationary problem associated with (3.18) with $\lambda = \frac{1}{\epsilon}$ and we may write (4.1) as

$$\begin{aligned} -\left(\frac{u'}{\sqrt{1+(u')^2}}\right)' = \lambda f(u), \quad x \in (0, L), \\ u'(0) = u'(L) = 0, \end{aligned} \tag{4.3}$$

which is the one-dimensional prescribed mean curvature equation with a bistable right hand side and Neumann boundary conditions. Solutions to (4.3) are defined

in the following way.

Definition 4.1. *We define a BV solution of (4.3) to be a function $u \in BV(\Omega)$ satisfying the variational inequality*

$$-\lambda \int_\Omega f(u)(v-u)\,dx + \int_\Omega \Psi(v_x) - \Psi(u_x)\,dx \geq 0 \ \ \forall v \in BV(\Omega), \tag{4.4}$$

where $\Psi'(s) = \psi(s)$.

Note that the variational inequality in (4.4) is obtained from the variational inequality (3.3) associated with (3.18) by taking u to be independent of time t in (3.3). As in the discussion before Definition 3.1 about variational inequality solutions to the time dependent problem (3.18), we note that classical i.e. $C^2((0,L)) \cap C^1([0,L])$ solutions of (4.3) will automatically satisfy variational inequality (4.4).

We find the first integral $J(u,u')$ for (4.1) by multiplying (4.1) by u'

$$\begin{aligned}(\psi(u'))'u' + \lambda f(u)u' &= \psi'(u')u''u' + \lambda f(u)u' \\ &= \psi'(u')u''u' + \psi(u')u'' - \psi(u')u'' + \lambda f(u)u' \\ &= \frac{d}{dx}\left[\psi(u')u' - \Psi(u') + \lambda F(u)\right] = 0,\end{aligned}$$

where $F'(u) = f(u)$. Hence the quantity

$$J(u,u') = \psi(u')u' - \Psi(u') + \lambda F(u), \tag{4.5}$$

is constant on the classical orbits of (4.1).

The boundary value problem in (4.3) for different choices of the nonlinearity $f(u)$ and boundary conditions has received attention from a variety of authors including Pan [47, 48, 49], Bonheure *et al.* [9], Obersnel [46] and Habets and Omari [37]. In [37], Habets and Omari study (4.3) with Dirichlet boundary conditions, taking $f(u) = u^p$ for $p > 0$, and they investigate the influence the concavity of this choice

of $f(u)$ has on the multiplicity of positive solutions to the problem. Note that they can consider (4.3) on only the unit interval $[0,1]$ since u^p is homogeneous of degree p and so it is possible to scale the fixed parameter L out of the space domain as follows: set $y = x/L$ and $v = u/L$, and then $v(y)$ satisfies

$$-\frac{\ddot{v}}{(1+(\dot{v})^2)^{\frac{3}{2}}} = \mu f(v), \quad y \in (0,1),$$

where $\mu = \lambda L^{p+1}$, and the overdot denotes differentiation with respect to y. Thus, in the case of [37] it is possible to incorporate the length L of the space interval in the parameter μ, and hence in this case the associated bifurcation diagram cannot change as L is changed. Note that the same is true also of the semilinear case $\psi(s) = s$ which gives the Allen-Cahn equation (2.7). Pan [47, 48, 49] however has studied a variant of the Liouville, Bratu-Gelfand problem, taking an exponential nonlinearity, $f(u) = e^u$, and both in his case and our case of $f(u) = u - u^3$, the nonlinearities are non-homogeneous, so that different bifurcation behaviours in λ are in principle possible for different values of L. This is indeed the case as we shall demonstrate in Section 4.2.

4.1 Phase plane analysis

We rewrite (4.3) as a first order system

$$\begin{cases} u' = v, \\ v' = -\lambda(1+v^2)^{\frac{3}{2}} f(u), \end{cases} \tag{4.6}$$

and analyse the classical solutions of (4.6) by phase plane methods. This system has the first integral given by (4.5) but if we set $H = 1 - J$, an alternative form of a first integral is

$$H(u,u') = \frac{1}{\sqrt{1+(u')^2}} - \lambda F(u), \tag{4.7}$$

and for classical solutions to (4.3), the level curves of $H(u, u')$ determine the global structure of the phase portrait for (4.6) since each phase curve lies entirely in one energy level set $H = \text{const}$.

In Figure 4.1, we show the phase portraits for $\lambda = 3$, 4 and 5 and from these portraits one can see the effect that increasing λ has on the qualitative structure of the phase portrait. For example, in the case where $\lambda = 3$, the saddle points $(1, 0)$ and $(-1, 0)$ are connected by a heteroclinic orbit. This is not the case for $\lambda \geq 4$. Instead, the trajectories have vertical asymptotes at $u = \pm\sqrt{1 - \frac{2}{\sqrt{\lambda}}}$ which is seen by solving $H(\pm 1, 0) = H(u, -\infty)$ for $u \in (-1, 1)$ with $\lambda \geq 4$. We shall consider this point in more detail in Proposition 4.2.

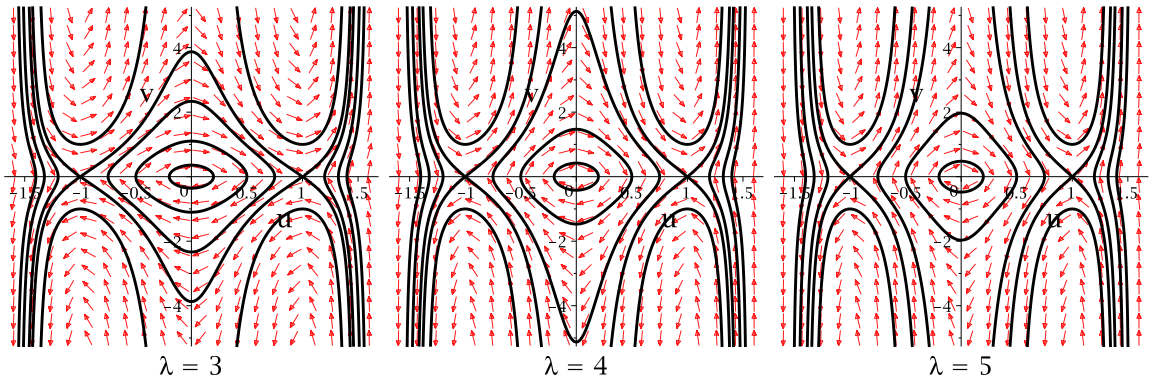

Figure 4.1: Phase portraits with $\lambda = 3$, $\lambda = 4$ and $\lambda = 5$.

4.1.1 The semilinear case

Consider the semilinear case,

$$u'' + \lambda f(u) = 0, \tag{4.8}$$
$$u'(0) = u'(L) = 0,$$

where $f(u) = u - u^3$ and $\lambda \in (0, \infty)$ as above. Problem (4.8) is the stationary problem for the Allen-Cahn equation (2.7) in one dimension and we note that (4.8)

can be converted to the first order system

$$\begin{cases} u' = v, \\ v' = -\lambda f(u), \end{cases} \tag{4.9}$$

where, unlike the situation in the quasilinear case (4.3), the saddle points $(\pm 1, 0)$ can always be connected by a heteroclinic solution for any value of λ. Hence since Neumann solutions to (4.8) are contained within the heteroclinic loop for all λ, all steady state solutions to the Allen-Cahn equation with Neumann boundary conditions are smooth. We will show in Section 4.6 that this is not true of the Neumann problem in (4.3).

Chafee [17] proved that in this one-dimensional situation where the domain Ω is an interval, the only stable solutions to (4.8) are the constant solutions $u = \pm 1$. Casten and Holland [16] and Matano [45] obtained the same conclusion for arbitrary dimension $n \in \mathbb{N}$ and Ω convex. In Section 4.5 we obtain a similar result for *classical* solutions to (4.3) in the one-dimensional case.

We note that any solution to (4.8) can always be identified with one of the monotone-decreasing solutions: if $(\lambda_1, u_m(x))$ represents a monotonic decreasing solution to (4.8) (with period $2L$) then (u_m, u_m') is the lower half of a periodic orbit in the phase plane of (4.9) with $\lambda = \lambda_1$. But then for any $k \in \mathbb{N}$, $(k^2\lambda_1, u_m(kx))$ also satisfies (4.8) and this solution can be viewed as part of the same periodic orbit as above only we are wrapping around $\frac{k}{2}$ of a period in "less time" so that the solution $(k^2\lambda_1, u_m(kx))$ has period $\frac{2L}{k}$. In fact, by phase plane arguments it can be shown that any non-monotone solution to (4.8) is merely the periodic extension of a monotone solution. Also, any monotone-increasing solution $w(x)$ to (4.8) can be written as $w(x) = u_m(L - x)$ hence *any* solution to (4.8) can be determined from the monotone-decreasing solutions to (4.8). We will see that there is no corresponding statement like this in the case of the quasilinear problem (4.3).

4.1.2 The quasilinear case

As in the semilinear case, a classical solution of the Neumann problem for (4.3) is part of a trajectory starting on the u-axis in the phase plane for (4.6), which encircles the origin in a clockwise direction and ends on the u-axis taking a "time" L in which to do this. For example, monotone-decreasing solutions start on the positive u-axis and end on the negative u-axis as shown in Figure 4.2. From now on we will concentrate on multiplicity questions for monotone-decreasing solutions of the Neumann problem for (4.3).

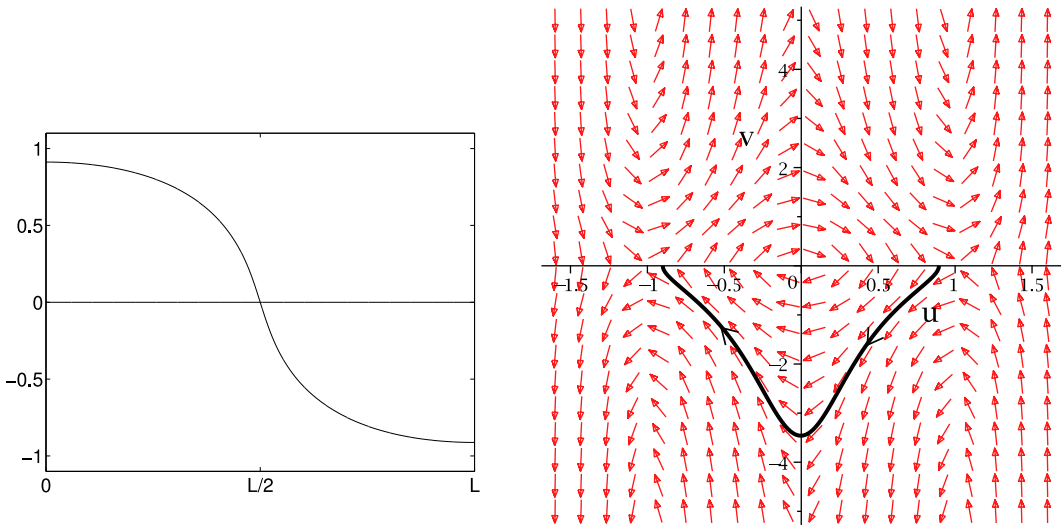

Figure 4.2: A classical solution to (4.3) and its corresponding phase curve for $L = 2.5$, $\lambda = 3$.

We have noted that for $\lambda \geq 4$ there are no heteroclinic solutions connecting the saddle points at $(\pm 1, 0)$. Let us consider this point in more detail.

Proposition 4.2. *For each $\lambda \geq 4$ there exists a value $r_\lambda \in (0, 1]$ (see Figure 4.3) such that:*

1. *The orbit passing through the point $(r_\lambda, 0)$ on the positive u-axis in the phase plane satisfies $u' \to -\infty$ as $u \to 0$.*

2. *Orbits passing through points* $(r,0)$, $r_\lambda < r \leq 1$ *are such that* $u' \to -\infty$ *as* u *tends to some value* $\bar{u}_\lambda(r) > 0$.

3. *Orbits passing through points* $(r,0)$, $0 < r < r_\lambda$ *are such that* $|u'| < \infty$ *as* $u \to 0$.

Proof. This is a simple computation using the function $H(u,v)$ of (4.7). For the value $r_\lambda \in (0,1]$ to exist, we must have $H(r_\lambda,0) = H(0,-\infty)$. This is equivalent to requiring that $\lambda F(r_\lambda) = 1$ for some $r_\lambda \in (0,1]$, so that

$$r_\lambda = \sqrt{1-\sqrt{1-\frac{4}{\lambda}}}, \tag{4.10}$$

and it is now clear that such a r_λ would only exist for $\lambda \geq 4$. Note that $r_\lambda = 1$ when $\lambda = 4$ and that $r_\lambda \to 0$ as $\lambda \to \infty$.

To find the vertical asymptotes $\bar{u}_\lambda(r)$ of orbits passing through $(r,0)$, $r \geq r_\lambda$ for $\lambda \geq 4$, we solve the equation $H(r,0) = H(\bar{u}_\lambda(r),-\infty)$, obtaining

$$\bar{u}_\lambda(r) = \sqrt{1-\sqrt{1+\frac{4}{\lambda}-2r^2+r^4}}. \tag{4.11}$$

Of course $\bar{u}_\lambda(r_\lambda) = 0$. □

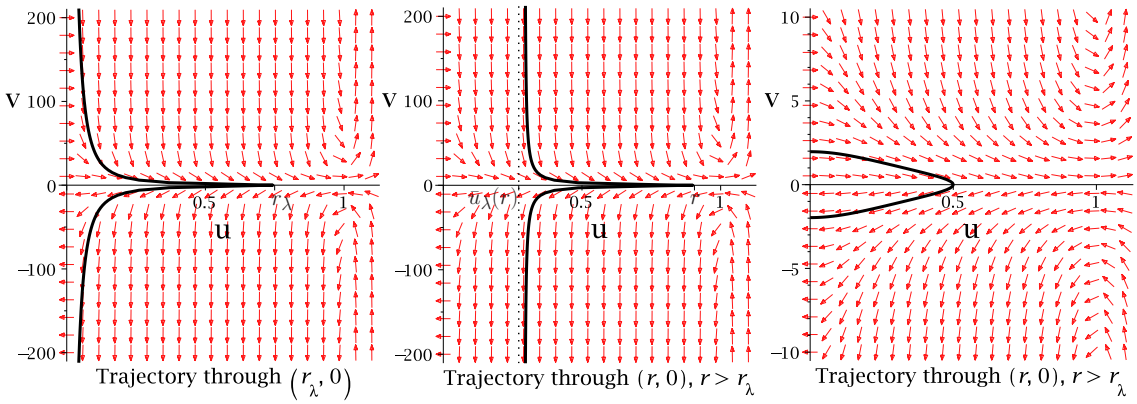

Figure 4.3: Trajectories through points on the u-axis with $\lambda \geq 4$, ($\lambda = 5$, $r_\lambda \simeq 0.7435$).

Note that for $\lambda > 4$ we can formally construct a non-classical (continuous) solution of the Neumann problem that conserves $H(u, v)$ as follows: start on the u-axis at $(r_\lambda, 0)$ in the phase plane and end on the negative u-axis at $(-r_\lambda, 0)$ and take a "time" L in which to do this. We will call such a solution the **critical solution** for (4.3) so that for a given $\lambda > 4$, there is a particular L for which this so-called critical solution $u(x)$ is possible, and this value of L is defined to be such that $u'\left(\frac{L}{2}\right) = -\infty$. We give an illustration of the form of the critical solution for a particular L and λ in Figure 4.4.

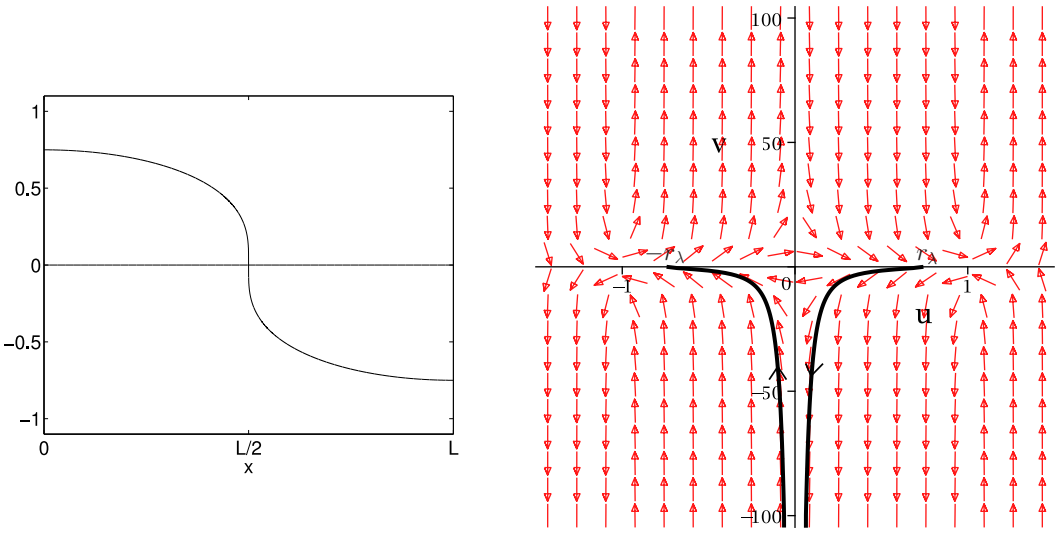

Figure 4.4: Critical solution of (4.3) in the case $\lambda = 5$, $L = 1.140420442$.

For the moment, we are interested in characterising the exact number of (monotone-decreasing) classical solutions of the Neumann problem for (4.3) not only as the parameter λ varies but also as the interval length L is changed since as we have suggested, changing the length parameter L can have an effect on the exact number of classical solutions of (4.3). As a starting point we note that due to the $\mathbb{Z}_2$-symmetry of the problem, we can expect bifurcation from the trivial solution $u = 0$ to be pitchforks. Moreover, we show that we can apply the bifurcation from a simple eigenvalue result due to Crandall and Rabinowitz (see Theorem 2.12)

which states that a branch of nontrivial solutions emanates from the trivial solution at each eigenvalue λ_k of the linearised problem about the trivial solution. This will give us the solution set of (4.3) locally at $(\lambda_k, 0)$ where λ_k is the k-th eigenvalue of equation (4.3) linearised about the trivial solution $u = 0$.

Let us define a mapping

$$\Theta : \mathbb{R} \times X \to C((0, L)), \tag{4.12}$$

where

$$X = \{u \in C^2((0, L)) : u'(0) = u'(L) = 0\}, \tag{4.13}$$

and

$$\Theta(\lambda, u) = \frac{u''}{(1 + (u')^2)^{\frac{3}{2}}} + \lambda f(u),$$

for $\lambda > 0$. Hence problem (4.3) can be written as

$$\Theta(\lambda, u) = 0, \qquad \lambda > 0,\ u \in X,$$

with $\Theta(\lambda, 0) = 0$ and we note that the linearisation of the operator Θ is

$$d\Theta_{\lambda,u} \cdot v = \frac{d}{dh}\Theta(\lambda, u + hv)|_{h=0} = \frac{v''}{(1 + (u')^2)^{\frac{3}{2}}} - \frac{3u''u'v'}{(1 + (u')^2)^{\frac{5}{2}}} + \lambda f'(u)v.$$

Thus equation (4.3) linearised about the trivial solution $u = 0$ is given by

$$d\Theta_{\lambda,0} \cdot v = v'' + \lambda v. \tag{4.14}$$

The null space $\ker(d\Theta_{\lambda,0})$ is one-dimensional when $\lambda = \lambda_k = \frac{k^2\pi^2}{L^2}$ and spanned by $v_k(x) = \cos\left(\frac{k\pi x}{L}\right)$. Denoting $d\Theta_{\lambda_k,0}$ by S, we have that the range of S

$$\begin{aligned} R(S) &= \left\{ w \in C((0, L)) : \int_0^L w(x) \cos\left(\frac{k\pi x}{L}\right) dx = 0 \right\} \\ &= [\ker(S)]^{\perp}, \end{aligned} \tag{4.15}$$

which has codimension 1. To see why the range space of S is as in (4.15), set $v_k(x) = \cos\left(\frac{k\pi x}{L}\right)$ and suppose

$$Sz = z'' + \lambda_k z = w,$$

so that w is a member of the range of the operator S and $z(x)$ is in the domain of the operator S. Consider

$$\begin{aligned}
\int_0^L w(x)v_k(x)\,dx &= \int_0^L (z''(x) + \lambda_k z(x))v_k(x)\,dx \\
&= [z'(x)v_k(x)]_0^L - \int_0^L z'(x)v_k'(x)\,dx + \lambda_k \int_0^L z(x)v_k(x)\,dx \\
&= -[z(x)v_k'(x)]_0^L + \int_0^L z(x)v_k''(x)\,dx + \lambda_k \int_0^L z(x)v_k(x)\,dx \\
&= 0, \quad \left(\text{since } v_k''(x) = -\frac{k^2\pi^2}{L^2}\cos\left(\frac{k\pi x}{L}\right) = -\lambda_k v_k(x)\right)
\end{aligned}$$

as required. Finally, $\Theta_{u\lambda}(\lambda_k, 0)\cdot v_k(x) = f'(0)v_k(x) \notin R(S)$, since for all $k \in \mathbb{N}$

$$\int_0^L f'(0)v_k(x)v_k(x)\,dx = f'(0)\int_0^L \cos^2\left(\frac{k\pi x}{L}\right)\,dx = f'(0)\frac{L}{2} \neq 0.$$

Hence from Theorem 2.12, the conditions of the Crandall and Rabinowitz theorem are satisfied and so the solution set of (4.3) near $(\lambda, u) = (\lambda_k, 0)$ consists of two parts; the line of trivial solutions $\{(\lambda, 0)\}$ and a curve $\{(\lambda(s), u(s, x))\}$, $|s - s_0| \leq \delta$ (for $\delta > 0$), with $(\lambda(s_0), u(s_0, x)) = (\lambda_k, 0)$ and $u_s(s_0, x) = v_k(x)$. We will return to the map (4.12) in Section 4.3.

4.2 The time map

To get more information about multiplicity of solutions as we change λ and L, we now define and analyse the time map for classical solutions. This is a well-known technique in the analysis of boundary value problems, see for example Schaaf [55] and Smoller and Wasserman [57]. Note that in this section, we will use a mixture of analytical results and numerics.

Definition 4.3. *We define the (classical part of the)* **time map** $T_\lambda(r)$ *to be the "time" it takes for solutions starting at* $u(0) = r$, $u'(0) = 0$ *to reach* $u = 0$.

From this definition, given that the points $(\pm 1, 0)$ are saddles we have that the domain of the classical part of the time map, $D(T_\lambda)$, is given by

$$D(T_\lambda) = \begin{cases} (0,1) & \text{if } \lambda \leq 4, \\ (0, r_\lambda] & \text{if } \lambda > 4. \end{cases}$$

Hence the classical part of the time map $T = T_\lambda(r)$ is such that the problem

$$-\left(\frac{u'}{\sqrt{1+(u')^2}}\right)' = \lambda f(u) := f_\lambda(u), \quad u(0) = r, \ u'(0) = 0, \tag{4.16}$$

has a solution $u \in C^2((0,L)) \cap C^1([0,L])$ with $u(t) > 0$ in $[0,T)$ and $u(T) = 0$.

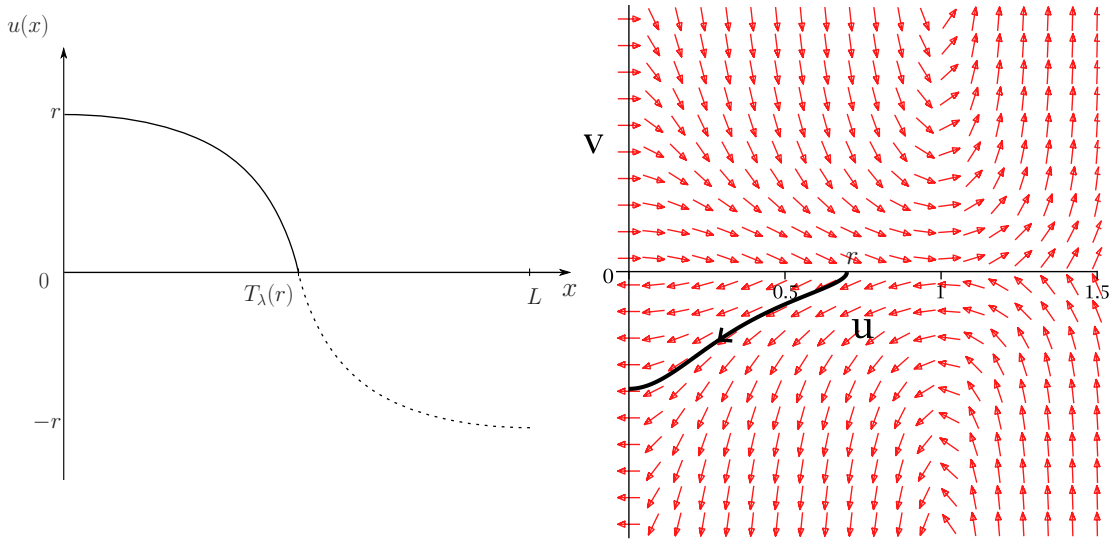

Figure 4.5: Time map $T_\lambda(r)$ for $\lambda = 4$, $L = 1.440087338$ with $r = u(0) = 0.7$.

Hence from the way we have defined the classical part of the time map $T_\lambda(r)$ in Definition 4.3 and with the aid of the diagram in Figure 4.5, it is easy to see that, given L, for a particular value of λ, a monotone-decreasing classical solution to

the Neumann problem (4.3) exists iff we can find $r \in D(T_\lambda)$ such that

$$T_\lambda(r) = \frac{L}{2}. \tag{4.17}$$

and in such case $r = u(0)$.

Note that, more generally, given L, for a particular value of λ, there exists a classical solution to the Neumann problem with k zeros in $[0, L]$ for $k \in \mathbb{N}$ iff we can find $r \in D(T_\lambda)$ such that

$$T_\lambda(r) = \frac{L}{2k}. \tag{4.18}$$

Since the number of (monotone) classical solutions of the stationary problem (4.3) coincides with the number of positive solutions of (4.17), it will be useful to compute an explicit formula for the classical part of the time map $T_\lambda(r)$ and to study its properties as we vary λ.

Let $F_\lambda(u) = \lambda F(u)$. To satisfy Neumann boundary conditions in (4.3), we must have that $H(u, u') = H(r, 0) = 1 - F_\lambda(r)$, i.e.

$$1 - \frac{1}{\sqrt{1 + (u')^2}} = F_\lambda(r) - F_\lambda(u).$$

Solving this equality for u' and setting $\chi(t) = \dfrac{1-t}{\sqrt{2-t}}$ as in [37], gives

$$u' = -\frac{\sqrt{F_\lambda(r) - F_\lambda(u)}}{\chi(F_\lambda(r) - F_\lambda(u))},$$

where we have taken the negative square root since we are dealing with monotone-decreasing solutions. Thus an explicit formula for $T_\lambda(r)$ is

$$T_\lambda(r) = \int_0^{T_\lambda(r)} dx = \int_0^r \frac{\chi(F_\lambda(r) - F_\lambda(u))}{\sqrt{F_\lambda(r) - F_\lambda(u)}}\, du, \tag{4.19}$$

which becomes

$$T_\lambda(r) = \int_0^r \frac{4 - 2\lambda r^2 + \lambda r^4 + 2\lambda u^2 - \lambda u^4}{\sqrt{8 - 2\lambda r^2 + \lambda r^4 + 2\lambda u^2 - \lambda u^4}\sqrt{\lambda(2r^2 - r^4 - 2u^2 + u^4)}}\, du,$$

for $f_\lambda(u) = \lambda(u - u^3)$. Note that $T_\lambda(r)$ is well-defined and continuous on $D(T_\lambda)$ since

$$f_\lambda(u) > 0 \Rightarrow F'_\lambda(u) > 0 \Rightarrow F_\lambda(r) - F_\lambda(u) > 0,$$

because $u \in (0, r)$. Also, for $\lambda < 4$,

$$\lambda[F(r) - F(u)] < \lambda[F(1) - F(0)] = \frac{\lambda}{4} < 2,$$

and for $\lambda \geq 4$,

$$\lambda[F(r) - F(u)] < \lambda[F(r_\lambda) - F(0)] = 1 < 2.$$

Hence for all λ, $2 - \lambda[F(r) - F(u)] > 0$.

Let us substitute $u = rs$ in (4.19) so that

$$T_\lambda(r) = r \int_0^1 \frac{\chi(F_\lambda(r) - F_\lambda(rs))}{\sqrt{F_\lambda(r) - F_\lambda(rs)}}\, ds := r \int_0^1 G(r, s)\, ds.$$

Computing the Taylor expansion of the function $rG(r, s)$ about the point $r = 0$ and integrating in s, we have

$$T_\lambda(r) = \frac{\pi}{2\sqrt{\lambda}} + \frac{3}{32}\frac{\pi(2-\lambda)}{\sqrt{\lambda}} r^2 - \frac{3}{2048}\frac{\pi(5\lambda^2 - 20\lambda - 76)}{\sqrt{\lambda}} r^4 + O(r^6). \tag{4.20}$$

From (4.20) we can derive a number of conclusions. First of all we have

$$\lim_{r \to 0} T_\lambda(r) = \frac{\pi}{2\sqrt{\lambda}}. \tag{4.21}$$

Secondly, the coefficient of the r^2 term

$$\frac{3\pi(2-\lambda)}{32\sqrt{\lambda}},$$

changes sign from positive to negative when $\lambda = 2$. Thus for $\lambda < 2$, $T_\lambda(r)$ is initially monotone-increasing, while for $\lambda > 2$ it is initially monotone-decreasing. Furthermore, by (4.10) we have that $r_\lambda = O(\lambda^{-\frac{1}{2}})$ for λ large. Therefore since $D(T_\lambda) \to 0$ as $\lambda \to \infty$ and since the remainder term in the Taylor series (4.20) with $r = r_\lambda$ is $O(\lambda^{-\frac{1}{2}})$, we conclude that for λ large enough, $T_\lambda(r)$ is always decreasing on $D(T_\lambda)$. Also observe that for $\lambda \leq 4$, since $(u, u') = (\pm 1, 0)$ are saddle points,

$$\lim_{r \to 1} T_\lambda(r) = \infty. \tag{4.22}$$

This means that we have (at least) three different types of behaviour of the classical part of the time map, depending on the values of λ; these are indicated in Figure 4.6 generated using MAPLE (note the differences in vertical scale).

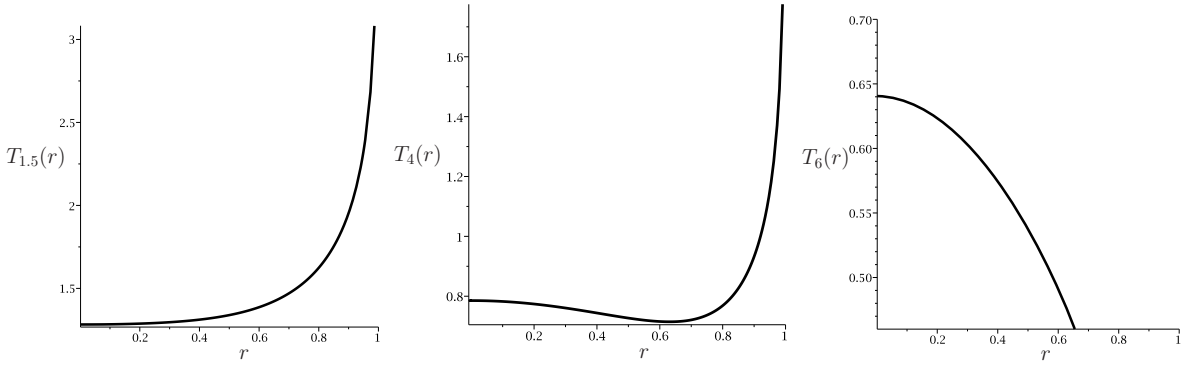

Figure 4.6: Time maps $T_\lambda(r)$ for $\lambda = 1.5$, $\lambda = 4$ and $\lambda = 6$.

From Figure 4.6, the time map corresponding to $\lambda = 1.5$ is monotonically increasing in its domain, the time map corresponding to $\lambda = 4$ has a turning point in its domain and the time map corresponding to $\lambda = 6$ is monotonically decreasing in its domain. A study of such diagrams shows that for $\lambda > 2$, the classical part of the time map $T_\lambda(r)$ may have a turning point in its domain (at some $r_t(\lambda) \in D(T_\lambda)$, say) provided λ is not too large as is the case for $\lambda = 6$ wherein the turning point occurs outside the domain of the classical part of the time map and within the domain of the non-classical part of the time map $S_\lambda(r)$ which we define in Section 4.6.

Remark: We have not proved that the turning point which must exist for $T_\lambda(r)$ for intermediate values of λ by the above calculation (as seen in Figure 4.6 for $\lambda = 4$) is unique and rely for that on numerical evidence.

We can show that, for small enough λ, the classical part of the time map $T_\lambda(r)$ will always be monotonic increasing by taking the series expansion of $rG(r,s)$ in λ at $\lambda = 0$, found using MAPLE, with the leading term in the expansion given by

$$\frac{1}{\sqrt{\lambda}} \frac{\sqrt{2}r}{\sqrt{2r^2 - r^4 - 2r^2s^2 + r^4s^4}} = \frac{1}{\sqrt{\lambda}} P(r,s).$$

The integral of this function $P(r,s)$ in s from 0 to 1 is given by

$$\int_0^1 P(r,s)\, ds = \frac{\sqrt{2}}{\sqrt{2-r^2}} \,\text{EllipticK}\left(\frac{r}{\sqrt{2-r^2}}\right) = Q(r), \tag{4.23}$$

where EllipticK(k) is the *complete* elliptic integral of the first kind,

$$\text{EllipticK}(k) = \int_0^{\frac{\pi}{2}} \frac{d\theta}{\sqrt{1-k^2\sin^2\theta}} = \int_0^1 \frac{dt}{\sqrt{1-t^2}\sqrt{1-k^2t^2}}, \quad (t = \sin\theta),$$

(elliptic integrals are termed *complete* when the amplitude is equal to $\frac{\pi}{2}$ as is the case above).

So (4.23) explicitly gives us the leading term of $T_\lambda(r)$ as $\lambda \to 0$ and by the nature of elliptic functions we have that it is indeed monotonic increasing for λ small enough and, as we would expect from (4.22), for such λ

$$\lim_{r\to 1} T_\lambda(r) = \infty,$$

since $\lim_{k\to 1} \text{EllipticK(k)} = \infty$.

In Figure 4.7 we see that $\frac{1}{\sqrt{\lambda}}Q(r)$, the leading term of $T_\lambda(r)$ as $\lambda \to 0$ with $Q(r)$ given in (4.23), captures the behaviour of $T_\lambda(r)$ for small λ with λ in this case taken to be $\lambda = 0.05$.

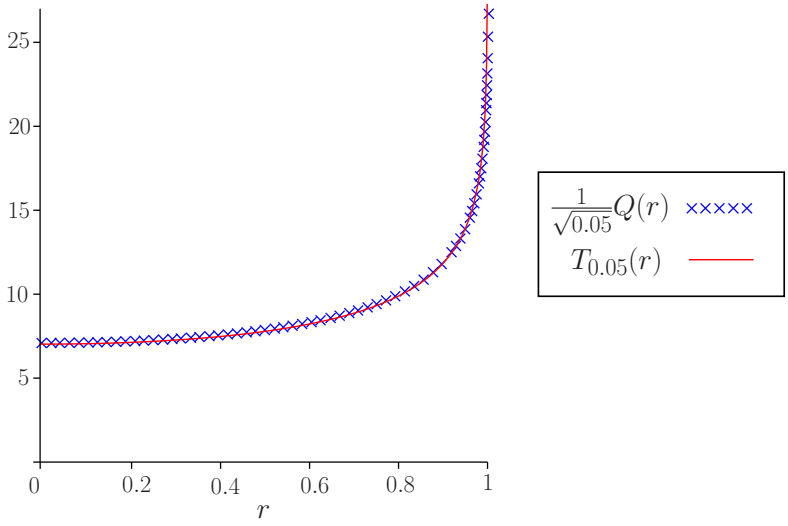

Figure 4.7: Comparison of the numerical plot of the time map $T_\lambda(r)$ for $\lambda = 0.05$ with the leading term of $T_\lambda(r)$ for small λ.

4.3 Liapunov-Schmidt reduction

We would like to determine the dependence of the direction of the pitchfork on the parameter L. The easiest way of doing this is to use the Liapunov-Schmidt reduction which was described in Section 2.3. Let us first show that our bifurcation problem is amenable to a Liapunov-Schmidt reduction.

Recall the one-dimensional prescribed mean curvature equation with a bistable

nonlinearity and Neumann boundary conditions

$$(\psi(u'))' + \lambda f(u) = 0, \tag{4.24}$$
$$u'(0) = u'(L) = 0,$$

where $\lambda = \frac{1}{\epsilon}$ is our bifurcation parameter, $\psi(s) = \frac{s}{\sqrt{1+s^2}}$ and $f(u) = u - u^3$. In order to set up the Liapunov-Schmidt reduction for (4.24), we return to the mapping Θ from Section 4.1 and defined in (4.12). We hence rewrite (4.24) as

$$\Theta(\lambda, u) = 0, \qquad \lambda > 0,\ u \in X, \tag{4.25}$$

with X as in (4.13) and we observe that $\Theta(\lambda, 0) = 0$ for all $\lambda \in \mathbb{R}$.

In order to investigate possible multiplicity of solutions to (4.24), we study the linearisation $d\Theta_{\lambda,u}$ of Θ. From (4.14), the linearisation of Θ at the trivial solution $u = 0$ for a given value of λ is given by

$$d\Theta_{\lambda,0} \cdot v = v'' + \lambda v.$$

As discussed in Section 4.1, the values $\lambda_k = \frac{k^2\pi^2}{L^2}$ are points of bifurcation from the trivial solution, which by the $\mathbb{Z}_2$-symmetry of the problem must be pitchforks. Hence as noted at the end of Section 4.1, $\ker(d\Theta_{\lambda,0})$ is one-dimensional when $\lambda = \lambda_k = \frac{k^2\pi^2}{L^2}$ for $k = 1, 2, \ldots$ and is spanned by $v_k = \cos\left(\frac{k\pi x}{L}\right)$.

We aim to show that in a neighbourhood of a bifurcation point, solutions of $\Theta(\lambda, u) = 0$ on X are in one-to-one correspondence with solutions of the reduced equation $h(\lambda, y) = 0$, $y \in \mathbb{R}$. Let $S = (d\Theta)_{\lambda_k,0}$ and denote the null-space and range of S by $\mathcal{K}$ and $\mathcal{R}$ respectively. Since S is a second order elliptic differential operator, we know from [34, Appendix 4, p332] that it is Fredholm of index zero and so the reduction outlined in Section 2.3 is applicable to (4.24).

In accordance with Section 2.3, we split X by writing

$$X = \mathcal{K} \oplus \mathcal{K}^{\perp},$$

where

$$\mathcal{K}^{\perp} = \left\{ u \in X : \int_0^L u(x) \cos\left(\frac{k\pi x}{L}\right) \, dx = 0 \right\},$$

is the orthogonal complement of $\mathcal{K}$ in X with respect to the inner product

$$\langle u, v \rangle = \int_0^L u(x)v(x) \, dx.$$

Similarly, we split the range space Y into its active and passive subspaces so that

$$Y = \mathcal{R} \oplus \mathcal{R}^{\perp}.$$

However, we have from (4.15) that

$$\mathcal{R} = \mathcal{K}^{\perp}, \tag{4.26}$$

and by the Fredholm Alternative,

$$\mathcal{R}^{\perp} = \ker(S^*),$$

where S^* denotes the adjoint of S. However, we also have that S is self-adjoint since

$$\begin{aligned}
\langle Su, v \rangle &= \langle u'' + \lambda_k u, v \rangle \\
&= \int_0^L u''(x)v(x) + \lambda_k u(x)v(x) \, dx \\
&= [u'(x)v(x)]_0^L - \int_0^L u'(x)v'(x) \, dx + \int_0^L \lambda_k u(x)v(x) \, dx \\
&= -[u(x)v'(x)]_0^L + \int_0^L u(x)v''(x) \, dx + \int_0^L \lambda_k u(x)v(x) \, dx \\
&= \int_0^L u(x)[v''(x) + \lambda_k v(x)] \, dx. \\
&= \langle u, Sv \rangle \qquad \forall u, v \in D(S) = X,
\end{aligned}$$

and so

$$\mathcal{R}^{\perp} = \ker(S^*) = \mathcal{K}.$$

Therefore, both X and Y have the same decompositions and so the simplest choice of coordinates in the Liapunov-Schmidt reduction is to set

$$v_k = v_k^* = \cos\left(\frac{k\pi x}{L}\right).$$

As discussed in Section 2.3, it is rarely possible to obtain an explicit formula for the reduced function $h(\lambda, y)$. Instead we calculate the derivatives of the reduced function at the bifurcation point $\lambda = \lambda_k$, $y = 0$ using the derivatives of the original function $\Theta(\lambda, u)$ so as to determine locally the form of the bifurcation. Since our original function Θ in (4.25) is odd, i.e.

$$\Theta(\lambda, -u) = -\Theta(\lambda, u), \tag{4.27}$$

the formulae in (2.51) are simplified considerably since, when $u = 0$, we have

$$(d^2\Theta)_{\lambda_k,0} = 0, \quad \Theta_\lambda = 0;$$

so terms involving S^{-1} in (2.51) will vanish. Thus at the bifurcating point $y = 0$, $\lambda = \lambda_k$ we have

$$\begin{aligned} h = h_y = h_{yy} = h_\lambda = 0,& \\ h_{yyy} &= \left\langle \cos, d^3\Theta(\cos, \cos, \cos)\right\rangle, \\ h_{\lambda y} &= \left\langle \cos, d\Theta_\lambda \cdot \cos\right\rangle. \end{aligned}$$

Now, at $\lambda = \lambda_k$, $u = 0$

$$\begin{aligned} (d^3\Theta)(v_1, v_2, v_3) &= \frac{\partial^3}{\partial t_1 \partial t_2 \partial t_3}\Theta(\lambda_k, t_1v_1 + t_2v_2 + t_3v_3)|_{t_1=t_2=t_3=0} \\ &= -3(2\lambda_k v_1v_2v_3 + v_1''v_3'v_2' + v_2''v_3'v_1' + v_3''v_2'v_1'). \end{aligned} \tag{4.28}$$

so that

$$\begin{aligned} h_{yyy} &= \left\langle \cos, \frac{9\pi^4}{L^4}\cos\sin^2 - 6\frac{k^2\pi^2}{L^2}\cos^3\right\rangle \\ &= 3\int_0^L \left\{\frac{3\pi^4}{L^4}\cos^2\left(\frac{k\pi x}{L}\right)\sin^2\left(\frac{k\pi x}{L}\right) - 2\frac{k^2\pi^2}{L^2}\cos^4\left(\frac{k\pi x}{L}\right)\right\} dx \\ &= \frac{9}{8}\frac{k^2\pi^2(k^2\pi^2 - 2L^2)}{L^3}. \end{aligned} \tag{4.29}$$

Similarly $\Theta_\lambda(u) = f(u)$, so that $(d\Theta_\lambda)_{\lambda_k,0} \cdot v = v$; thus

$$h_{\lambda y} = \langle \cos, \cos \rangle = \frac{L}{2} > 0. \tag{4.30}$$

We are finally in a position to determine the value of L for which there is a transition between a supercritical and a subcritical bifurcation. Using Proposition 2.13, (4.29) and (4.30) we have proved

Proposition 4.4. *The k-th bifurcation from the trivial solution is a supercritical pitchfork if $L > k\pi/\sqrt{2}$ and a subcritical pitchfork if the inequality is reversed.*

We relate this to the study of the time map (4.19) in Section 4.2 by noting that $\lim_{r\to 0} T_\lambda(r) = \frac{\pi}{2\sqrt{\lambda}}$ from (4.21) and if we set

$$\frac{\pi}{2\sqrt{\lambda}} = \frac{L}{2},$$

then for monotone classical solutions to (4.24), the critical value of $L = \frac{\pi}{\sqrt{2}}$ found by Liapunov-Schmidt reduction in the case $k = 1$, corresponds to when $\lambda = 2$ which represents the value of λ for which the time map $T_\lambda(r)$ changes from being initially monotone-increasing to being initially monotone-decreasing in $D(T_\lambda)$.

4.4 Bifurcation diagrams

Recall from Proposition 4.2 that for $\lambda > 4$, the equation

$$r = \sqrt{1 - \sqrt{1 - \frac{4}{\lambda}}},$$

gives the value of the right end-point of the domain of the classical part of the time map $T_\lambda(r)$ which we defined in Definition 4.3. Solving this equation instead for λ we obtain the inverse of r_λ considered as a function of r,

$$\lambda = \Lambda(r) = \frac{4}{1-(1-r^2)^2}.$$

Hence we can define a function

$$g(r) = T_{\Lambda(r)}(r), \tag{4.31}$$

which will give the values of the classical parts of time maps evaluated at the right end-points of their domains; this will be useful in the discussion which follows on the bifurcation diagrams corresponding to different values of L. From the foregoing analysis we see that $g(r)$ is a monotone-increasing function satisfying

$$g(0) = 0, \ \lim_{r\to 1} g(r) = \infty.$$

Let us use the results obtained in Section 4.2 and Section 4.3 to discuss the various (minimal) possibilities for bifurcation of monotone solutions to the Neumann problem (4.24) by referring to Figures 4.8, 4.9, and 4.10 below. There we have plotted some of the classical parts of the time maps $T_\lambda(r)$ for values of λ increasing down the vertical axis and we have fixed L firstly to be sufficiently large, say L_1 (Figure 4.8), then intermediate, say L_2 (Figure 4.9) and finally sufficiently small, say L_3 (Figure 4.10). In the left-hand sides of these figures we analyse how many intersections there are between $T_\lambda(r)$ (for varying values of λ) and the values of $\frac{L_i}{2}$, $i = 1, 2, 3$ and in the right-hand sides, we plot the resulting bifurcation diagrams corresponding to each value of L_i. The curve $g(r)$ as defined in (4.31), represents the values of the time maps evaluated at the right end-points of their domains.

Starting with $L = L_1$ as in Figure 4.8, the first intersection occurs for $T_{\lambda_*}(r)$, where $\lambda_* = \pi^2/L_1^2$ and for L_1 sufficiently large, λ_* will be a supercritical pitchfork

bifurcation point.

There continues to be a single intersection between $T_\lambda(r)$ and $\frac{L_1}{2}$ for values of λ up to and including λ^* for which the intersection occurs at the value of the corresponding classical part of the time map evaluated at the right end-point of its domain (i.e. we have that $T_{\lambda^*}(r_{\lambda^*}) = \frac{L_1}{2}$). For all subsequent λ there are no intersections between $T_\lambda(r)$ and $\frac{L_1}{2}$ and hence no further classical solutions to the Neumann problem. Note that the solution we obtain for the value λ^* is the critical solution discussed in Figure 4.4.

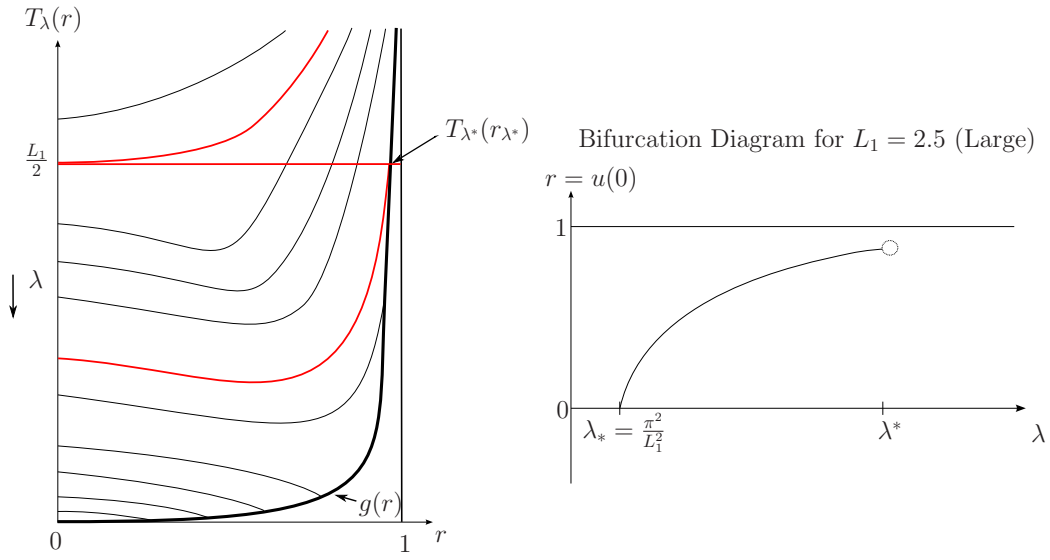

Figure 4.8: Plots of time maps $T_\lambda(r)$ intersecting with $\frac{L_1}{2}$ (left) and the corresponding bifurcation diagram (right).

The intermediate values of L are such that the first time map to solve the equation $T_\lambda(r) = L/2$ has a turning point. In this case the bifurcation point is a subcritical pitchfork and the diagram will exhibit a saddle-node at some value λ_*; see Figure 4.9. Again, there is a value λ^* beyond which no classical solutions exist.

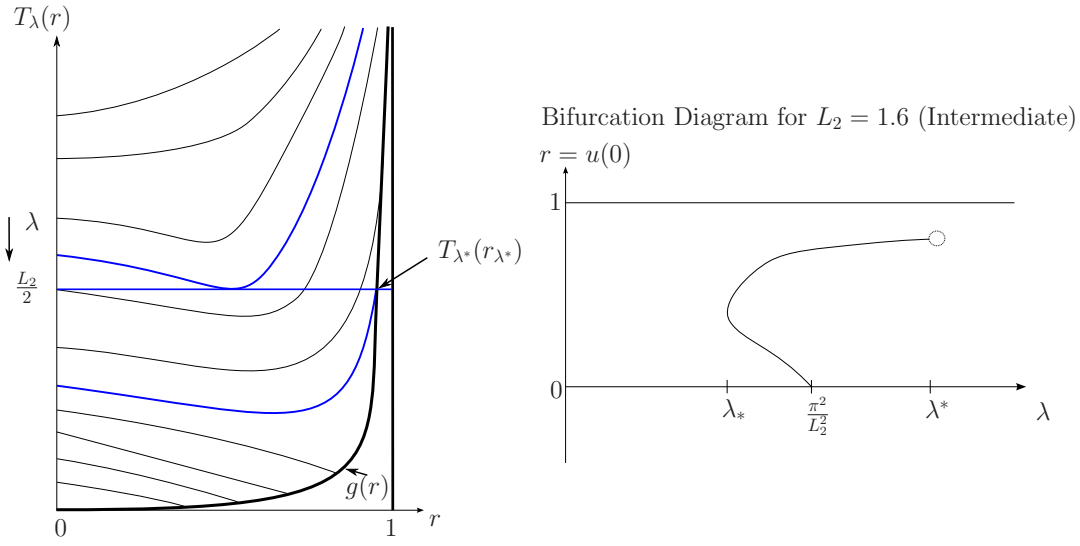

Figure 4.9: Plots of time maps $T_\lambda(r)$ intersecting with $\frac{L_2}{2}$ (left) and the corresponding bifurcation diagram (right).

Finally we consider $L = L_3$, the situation where the first intersection is with a monotone-decreasing time map. Here the bifurcation is again a subcritical pitchfork, but the classical solutions stop existing before we reach a saddle-node; see Figure 4.10

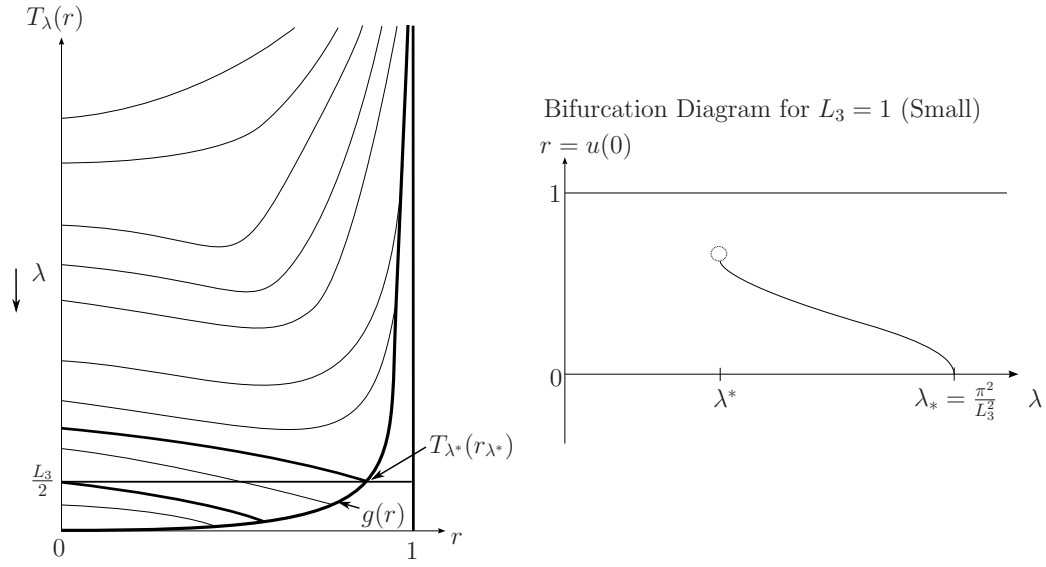

Figure 4.10: Plots of time maps $T_\lambda(r)$ intersecting with $\frac{L_3}{2}$ (left) and the corresponding bifurcation diagram (right).

To summarise, for a given L, there exists a value of $\lambda = \lambda^*(L)$ beyond which there are no further intersections between $T_\lambda(r)$ and $\frac{L}{2}$. That is, $\lambda^*(L)$ is such that

$$T_{\lambda^*}(r_{\lambda^*}) = \frac{L}{2},$$

then, in the case of a large or intermediate value of L,

$$\text{for } \lambda > \lambda^*, \ T_\lambda(r) < \frac{L}{2} \ \ \forall\ r \in D(T_\lambda),$$

and, in the case of a small value of L,

$$\text{for } \lambda < \lambda^*, \ T_\lambda(r) > \frac{L}{2} \ \ \forall\ r \in D(T_\lambda).$$

In all cases, for a given value of L, there comes a value $\lambda^*(L)$ at which the bifurcation diagrams for monotone classical solutions to the Neumann problem (4.24) stop and the stationary solutions develop infinite gradient. Note that for L sufficiently large, $\lambda^*(L) \simeq 4$ since $r_\lambda \to 1$ as $\lambda \to 4$, $\lim_{r\to 1} T_\lambda(r)$ is infinite for all $\lambda \leq 4$ and $T_\lambda(r_\lambda) < \infty$ for all $\lambda > 4$.

Remark: We note that similar analyses can be done for non-monotone solutions to (4.24) via Proposition 4.4 and (4.18), but unlike the semilinear case, there is no easy way to infer the behaviour of all branches from that of the monotone one.

4.5 Instability of non-trivial classical solutions to the Neumann problem

In this Section we prove that the non-constant classical solutions to (4.24) discussed above are unstable. This result is comparable with the result obtained in [17] for the semilinear problem (4.8) which shows that the only stable solutions to (4.8) are the constant solutions $u = \pm 1$. Solutions to the Neumann problem in (4.24) arise as critical points of the free energy functional introduced in Section 2.1.4

$$E[u] = \int_0^L \Psi(u') - \lambda F(u)\, dx, \tag{4.32}$$

where $\Psi'(s) = \psi(s)$ and $F'(s) = f(s)$. This is because the first variation of $E[u]$ is determined from

$$\frac{d}{dh}E[u+hv]|_{h=0} = \langle -\left[(\psi(u'))' + \lambda f(u)\right], v\rangle_{L^2(\Omega)} \qquad \forall\ v \in L^2(\Omega),$$

and so $u \in C^2((0,L)) \cap C^1([0,L])$ that is a solution to the Neumann problem (4.24) is such that $\frac{d}{dh}E[u+hv]|_{h=0} = 0$ for all $v \in L^2((0,L))$ and (4.24) has variational structure.

Theorem 4.5. *Non-constant classical solutions to (4.24) are unstable.*

Proof. We show that a non-constant solution $u \in C^2((0,L)) \cap C^1([0,L])$ to (4.24) is unstable in the sense that there exists some path v along which the second variation of the free energy functional is strictly negative. This will mean that there are no non-constant $C^2((0,L)) \cap C^1([0,L])$ local minimisers of the free energy functional (4.32).

Indeed, for $u \in C^2((0,L)) \cap C^1([0,L])$ and $v \in L^2((0,L))$ consider $\varphi(h) = E[u+hv]$. If $\frac{d}{dh}E[u+hv]|_{h=0} = 0$ and $\frac{d^2}{dh^2}E[u+hv]|_{h=0} < 0$, i.e. if $\varphi'(0) = 0$ and $\varphi''(0) < 0$, then φ has a strict relative maximum at $h = 0$ so that $E[u+hv] < E[u]$ for all sufficiently small $h \neq 0$.

Hence we consider the second variation of the free energy functional

$$\begin{aligned}\frac{d^2}{dh^2}E[u+hv]|_{h=0} &= \int_0^L \Psi''(u')(v')^2 - \lambda F''(u)v^2\,dx. \\ &= \int_0^L \psi'(u')(v')^2 - \lambda f'(u)v^2\,dx,\end{aligned}$$

and we take a classical solution u to the stationary problem and show that $\frac{d^2}{dh^2}E[u+hv]|_{h=0}$ can be non-positive for at least one sensible choice of path/direction v. Note that since we consider Neumann (natural) boundary conditions, there are no restrictions that one needs to place on boundary values of the variations v as explained in Section 2.4.

Following the approach of Carr, Gurtin and Slemrod in [15] which is concerned with the minimisation problem for a one-dimensional elastic bar placed in a soft loading device, for a non-constant solution $u(x) \in C^2((0,L)) \cap C^1([0,L])$ to the Neumann problem (4.24) we choose

$$v(x) = u'(x) + \delta\beta(x) \in C^1((0,L)),$$

where $\beta(x) = \frac{L-x}{L}$ and δ is some arbitrary constant. For such v, we have

$$\begin{aligned}
&\frac{d^2}{dh^2}E[u+hv]|_{h=0} \\
&= \int_0^L \left\{\psi'(u')[(u'')^2 + 2\delta\beta' u'' + \delta^2(\beta')^2] - \lambda f'(u)\left[(u')^2 + 2\delta u'\beta + \delta^2\beta^2\right]\right\} dx
\end{aligned}$$

$$= \frac{d^2}{dh^2}E[u+hu']|_{h=0} + 2\delta\int_0^L \left[\psi'(u')\beta' u'' - \lambda f'(u)u'\beta\right] dx + \delta^2\frac{d^2}{dh^2}E[u+h\beta]|_{h=0}. \tag{4.33}$$

From (4.24)

$$-\lambda f(u) = \psi'(u')u'' \Rightarrow -\lambda f'(u)u' = \psi''(u')(u'')^2 + \psi'(u')u''',$$

and so

$$\begin{aligned}
\frac{d^2}{dh^2}E[u+hu']|_{h=0} &= \int_0^L \left\{\psi'(u')(u'')^2 - \lambda f'(u)(u')^2\right\} dx \\
&= \int_0^L \left\{\psi'(u')(u'')^2 + \psi''(u')(u'')^2u' + \psi'(u')u'''u'\right\} dx \\
&= \int_0^L \left\{\psi'(u')[(u'')^2 + u'''u'] + \psi''(u')(u'')^2u'\right\} dx \\
&= \int_0^L \left\{\psi'(u')[(u''u')'] + \psi''(u')(u'')^2u'\right\} dx \\
&= [\psi'(u')u''u']_0^L - \int_0^L \psi''(u')(u'')^2u'\,dx + \int_0^L \psi''(u')(u'')^2u'\,dx \\
&= 0,
\end{aligned}$$

because of the Neumann boundary conditions on u. Also,

$$\begin{aligned}
&\int_0^L \{\psi'(u')\beta' u'' - \lambda f'(u)u'\beta\}\, dx \\
&= \int_0^L \left\{\psi'(u')\beta' u'' + \psi''(u')(u'')^2\beta + \psi'(u')u'''\beta\right\} dx \\
&= \int_0^L \left\{\psi'(u')\left[\beta' u'' + u'''\beta\right] + \psi''(u')(u'')^2\beta\right\} dx \\
&= \int_0^L \left\{\psi'(u')\left[(\beta u'')'\right] + \psi''(u')(u'')^2\beta\right\} dx \\
&= [\psi'(u')\beta u'']_0^L - \int_0^L \psi''(u')(u'')^2\beta\, dx + \int_0^L \psi''(u')(u'')^2\beta\, dx \\
&= -u''(0),
\end{aligned}$$

and we establish that $u''(0) \neq 0$ by considering the equation for $u' = z$ in which case

$$z' = u'' = -\lambda f(u)(1 + (u')^2)^{\frac{3}{2}} := -g(u, u'),$$

and

$$z'' = -\frac{\partial g}{\partial u} z - \frac{\partial g}{\partial u'} z'. \tag{4.34}$$

Suppose that $u''(0) = 0$ and treat (4.34) as an initial value problem with $z(0) = z'(0) = 0$. By inspection, $z \equiv 0$ is a solution to problem (4.34) and by uniqueness of solutions to such initial value problems (see Lemma 2.14) we must have that $z \equiv 0$ is the only solution to the problem which would imply that $u(x)$ is constant and this contradiction means that $u''(0) \neq 0$.

Thus (4.33) becomes

$$\frac{d^2}{dh^2} E[u + hv]|_{h=0} = -2\delta u''(0) + \delta^2 \frac{d^2}{dh^2} E[u + h\beta]|_{h=0},$$

and whatever the situation that arises in the two terms above, we will always able to choose some δ with $|\delta|$ small enough in such a way that $\frac{d^2}{dh^2} E[u + hv]|_{h=0} < 0$. Hence Theorem 4.5 is proven.

□

Remark: The key to this kind of argument lies in the choice of path v. Chmaj and Ren [20] studied stationary solutions to the non-local Allen-Cahn equation (2.20) in one dimension and proved that the van der Waals functional (2.19) does not admit non-constant C^1 local minimisers. They could choose $v = u'$ as an admissible path since there are no boundary conditions to their problem (since there are no derivative terms) and so they had more freedom over which paths they could choose. We could not have chosen $v = u'$ to establish Theorem 4.5 since we require that the minimiser u satisfies the Neumann boundary conditions and have no such restrictions on the choice of path v. However choosing $v = u'$ would mean that we would require $v(0) = v(L) = 0$ as if we were minimising over some subspace of the whole space with Dirichlet boundary conditions which we are not.

4.6 Non-classical solutions to the Neumann problem

Non-classical solutions for problems related to the prescribed mean curvature equation have been considered, to some extent, in [9]. However, in that paper the non-classical solutions are $C^\infty((0, L))$. In [46] and [49], existence and multiplicity of sign-changing solutions that are possibly discontinuous at points at which the solutions attain the value zero are discussed. Below we show a construction for $\lambda > \lambda^*$ of solutions (in the BV sense) that are discontinuous *in the interior of the interval*. Moreover, we show numerically that this construction delivers an uncountable number of solutions, and that, surprisingly, the set of solutions is dynamically stable.

We will again focus on monotone-decreasing solutions to (4.24). For definiteness, take L to be large enough so that we are discussing the supercritical case, i.e. take $L > \frac{\pi}{\sqrt{2}}$ by Proposition 4.4. For $\lambda > 4$ let us define a mapping $S_\lambda(r)$ as the time taken for solutions starting at $u(0) = r$, $u'(0) = 0$ (for some $r \geq r_\lambda$) to reach

$u = \bar{u}_\lambda(r)$, where $\bar{u}_\lambda(r)$ is given by (4.11). An explicit form for $S_\lambda(r)$ is

$$S_\lambda(r) = \int_{\bar{u}_\lambda(r)}^{r} \frac{\chi(F_\lambda(r) - F_\lambda(u))}{\sqrt{F_\lambda(r) - F_\lambda(u)}}\, du,$$

where now the domain of $S_\lambda(r)$, $D(S_\lambda) = [r_\lambda, 1)$. Note that at the value r_λ from Proposition 4.2, the classical and non-classical parts of the time map coincide, i.e. we have $T_\lambda(r_\lambda) = S_\lambda(r_\lambda)$.

Proposition 4.6. *For a particular value of $\lambda > 4$, there exists a non-classical monotone-decreasing solution to the Neumann problem (4.24) if we can find $r_1, r_2 \in [r_\lambda, 1)$ (where without loss of generality, $r_1 \geq r_2$) such that $S_\lambda(r_1) + S_\lambda(r_2) = L$.*

So for example, if we set $r_1 = r_2 = r^* \geq r_\lambda$ with $S_\lambda(r^*) = \frac{L}{2}$, we can construct a (so far formal) non-classical solution to (4.24) by starting on the positive u-axis in the phase plane at $u = r^*$ and ending on the negative u-axis at $u = -r^*$ as depicted in Figure 4.11. There will need to be a jump connecting the two trajectories from the "point" $(\bar{u}_\lambda(r^*), -\infty)$ to the "point" $(-\bar{u}_\lambda(r^*), -\infty)$ and in this way, we would have constructed a non-classical solution to (4.24) which has zero mean and obviously $S_\lambda(r^*) + S_\lambda(r^*) = L$.

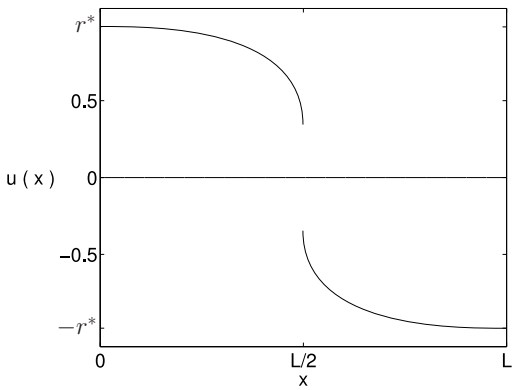

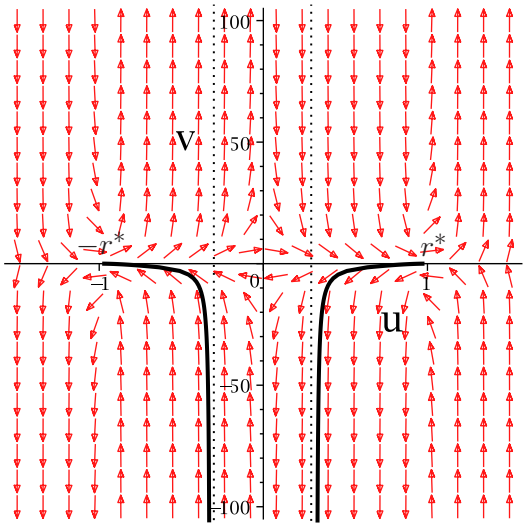

Figure 4.11: Non-classical solution with zero mean for $\lambda = 5$, $L = 2.5$ and $r^* \simeq 0.9818$.

We can also construct non-classical solutions to (4.24) for a particular value of λ that do not have zero mean: we could start on the positive u-axis in the phase plane at $u = r_1 > r_\lambda$ and end on the negative u-axis at $u = -r_2 < -r_\lambda$ with $r_1 > r_2$. Again, there will have to be a jump to connect the two trajectories from the "point" $(\bar{u}_\lambda(r_1), -\infty)$ to the "point" $(-\bar{u}_\lambda(r_2), -\infty)$, and to satisfy the boundary conditions we must have $S_\lambda(r_1) + S_\lambda(r_2) = L$. Figure 4.12 (left) gives an indication of how one can construct such a non-classical solution with positive mean: we have a value of $\frac{L}{2}$ and, for a particular value of λ, we have merged the classical (red) and non-classical (blue) time maps, T_λ and S_λ with an intersection between $S_\lambda(r)$ and $\frac{L}{2}$ at the value of this non-classical part of the time map evaluated at $r = r^*$, which corresponds to the non-classical solution with zero mean constructed in Figure 4.11. If we move up in the diagram from $\frac{L}{2}$ by a certain amount δ with $S_\lambda(r_1) = \frac{L}{2} + \delta$ and move down by the same amount δ with $S_\lambda(r_2) = \frac{L}{2} - \delta$ then we will indeed have constructed a non-classical stationary solution to the problem satisfying $S_\lambda(r_1) + S_\lambda(r_2) = L$ as required. The diagram in Figure 4.13 shows such a non-classical solution that does not have zero mean.

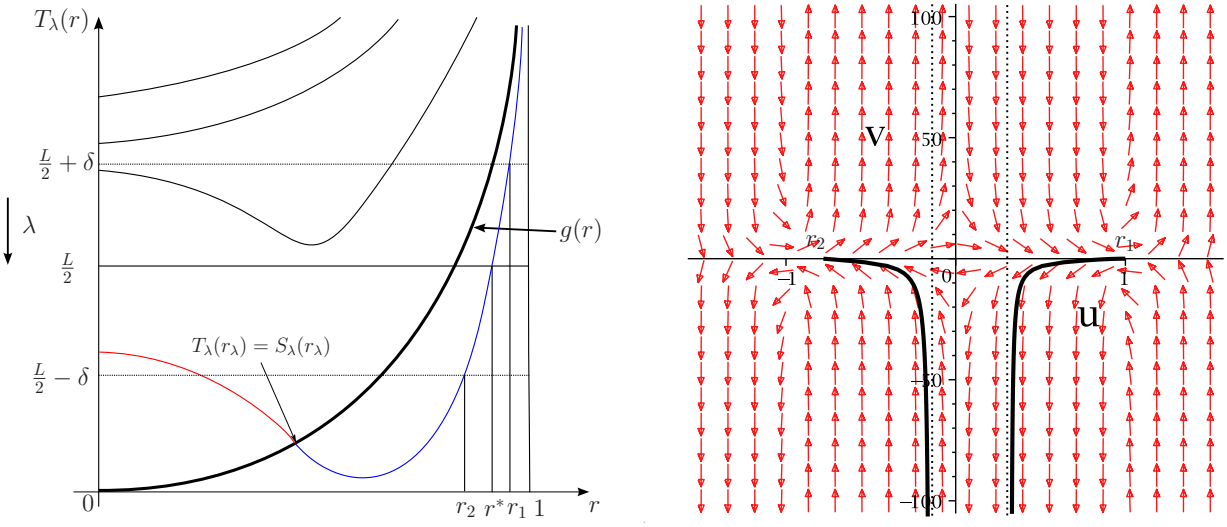

Figure 4.12: Construction of a non-classical solution.

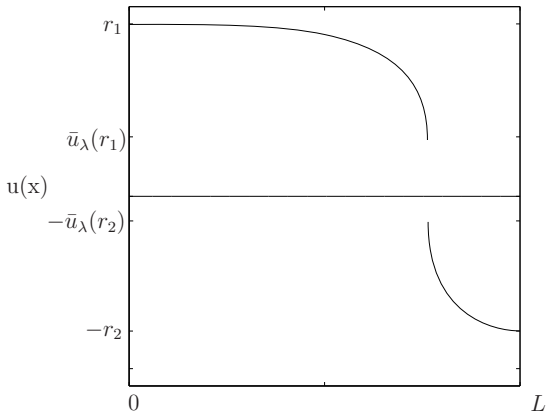

Figure 4.13: A Non-classical solution of (4.24) with positive mean for $\lambda = 5$, $L = 2.5$, $r_1 \simeq 0.9978$, $r_2 \simeq 0.7795$.

The above constructions are formal but we can show that they define BV solutions to the Neumann problem (4.24) i.e. they satisfy the variational inequality (4.4). We have the following theorem:

Theorem 4.7. *Suppose there exists $x_0 \in (0, L)$ such that*

- *for $x \in [0, x_0)$ and for $x \in (x_0, L]$, $u(x)$ resides in level curves of the Hamiltonian $H(u, u_x)$,*
- *$S_\lambda(u(0)) + S_\lambda(u(L)) = L$ where $S_\lambda(u(0)) = x_0$ and $S_\lambda(u(L)) = L - x_0$,*
- *$u_x(x) \to -\infty$ as $x \to x_0^{\pm}$.*

Then $u(x)$ is a BV solution of (4.24).

Proof. Consider $v \in BV(\Omega)$ and the $C^\infty(\Omega)$ sequence $v_n = v * \varphi_n$ for all n where φ_n is the standard mollifier so that $v_n \to v$ with respect to the topology in $BV(\Omega)$ defined by the metric

$$d(u, v) = ||u - v||_{L^1(\Omega)} + \left| \int_\Omega |u_x| - \int_\Omega |v_x| \right|, \tag{4.35}$$

see for example [27, p172]. Note that (4.35) does not assert that $\int_\Omega |u_x - v_x| \to 0$. Since the functional $\int_\Omega \Psi(v_x)$ is convex, by [23, Lemma 2.2] we have that

$$
\begin{aligned}
&-\lambda \int_\Omega f(u)(v-u)\,dx + \int_\Omega (\Psi(v_x) - \Psi(u_x))\,dx \\
&\qquad = \lim_{n\to\infty} \left\{ -\lambda \int_\Omega f(u)(v_n - u)\,dx + \int_\Omega (\Psi(v_{nx}) - \Psi(u_x))\,dx \right\}.
\end{aligned}
$$

Hence

$$
\begin{aligned}
&-\lambda \int_\Omega f(u)(v-u)\,dx + \int_\Omega (\Psi(v_x) - \Psi(u_x))\,dx \\
&= \lim_{n\to\infty} \left\{ -\lambda \int_\Omega f(u)(v_n - u)\,dx + \int_\Omega (\Psi(v_{nx}) - \Psi(u_x))\,dx \right\} \\
&= \lim_{n\to\infty} \left\{ -\lambda \int_0^L f(u)(v_n - u)\,dx + \int_0^{x_0} (\Psi(v_{nx}) - \Psi(u_x))\,dx + \int_{x_0}^L (\Psi(v_{nx}) - \Psi(u_x))\,dx \right\} \\
&\geq \lim_{n\to\infty} \left\{ -\lambda \int_0^L f(u)(v_n - u)\,dx + \int_0^{x_0} \Psi'(u_x)(v_{nx} - u_x)\,dx + \int_{x_0}^L \Psi'(u_x)(v_{nx} - u_x)\,dx \right\} \\
&= \lim_{n\to\infty} \left\{ -\lambda \int_0^L f(u)(v_n - u)\,dx + [\Psi'(u_x)(v_n - u)]_0^{x_0} - \int_0^{x_0} \frac{d}{dx}\Psi'(u_x)(v_n - u)\,dx \right. \\
&\qquad\qquad \left. + [\Psi'(u_x)(v_n - u)]_{x_0}^L - \int_{x_0}^L \frac{d}{dx}\Psi'(u_x)(v_n - u)\,dx \right\} \\
&= \lim_{n\to\infty} \left\{ -\int_0^{x_0} \left[\lambda f(u) + \frac{d}{dx}\psi(u_x)\right](v_n - u)\,dx - \int_{x_0}^L \left[\lambda f(u) + \frac{d}{dx}\psi(u_x)\right](v_n - u)\,dx \right. \\
&\qquad\qquad \left. + \lim_{x\to x_0^-} \psi(u_x)(v_n - u) - \lim_{x\to x_0^+} \psi(u_x)(v_n - u) \right\} \\
&= \lim_{n\to\infty} \left\{ -\int_0^{x_0} \left[\lambda f(u) + \frac{d}{dx}\psi(u_x)\right](v_n - u)\,dx - \int_{x_0}^L \left[\lambda f(u) + \frac{d}{dx}\psi(u_x)\right](v_n - u)\,dx \right. \\
&\qquad\qquad \left. - v_n(x_0) + u(x_0^-) + v_n(x_0) - u(x_0^+) \right\} \\
&> \lim_{n\to\infty} \left\{ -\int_0^{x_0} \left[\lambda f(u) + \frac{d}{dx}\psi(u_x)\right](v_n - u)\,dx - \int_{x_0}^L \left[\lambda f(u) + \frac{d}{dx}\psi(u_x)\right](v_n - u)\,dx \right\} \\
&= 0,
\end{aligned}
$$

because $u(x)$ must satisfy the Euler-Lagrange equation (4.24) in regions for which

$u(x)$ is classical. Thus we obtain

$$-\lambda \int_\Omega f(u)(v-u)\,dx + \int_\Omega (\Psi(v_x) - \Psi(u_x))\,dx \geq 0 \quad \forall v \in BV(\Omega).$$

□

Remark: We note that while Theorem 4.7 is only proven for monotone non-classical solutions to (4.24), it can be extended to non-monotone non-classical solutions $u(x)$ which have $k \in \mathbb{N}$ discontinuities at $x_i \in (0, L)$, $i = 1, \cdots, k$ with $x_1 < \cdots < x_k$ where we would require that

$$kS_\lambda(u(0)) + kS_\lambda(u(L)) = L.$$

4.6.1 The existence of uncountably many solutions

Suppose we fix a supercritical L, then for each $\lambda > \lambda^*(L)$ (with $\lambda^*(L)$ as defined in Section 4.4), there will be a range, depending on λ, in which the position $x_0 \in (0, L)$ of the interface in the non-classical solution $u(x)$ to (4.24) can appear. Since we must have that

$$S_\lambda(u(0)) + S_\lambda(u(L)) = L,$$

it is easy to see using Figure 4.14 that for each $\lambda > \lambda^*(L)$

$$x_0 \in \left[\min_{r \in [r_\lambda, 1)} S_\lambda(r), L - \min_{r \in [r_\lambda, 1)} S_\lambda(r) \right], \tag{4.36}$$

where

$$\min_{r \in [r_\lambda, 1)} S_\lambda(r) = \begin{cases} S_\lambda(r_\lambda) & \text{if } r_t \in D(T_\lambda), \\ S_\lambda(r_t) & \text{if } r_t \in D(S_\lambda)\ . \end{cases}$$

So suppose we have some $\lambda_1 > \lambda^*(L)$ and that $S_{\lambda_1}(r)$ has a turning point at some $r_t \in D(T_{\lambda_1})$ as in Figure 4.14 (left). Then for this value of λ there will be "outer" solutions $u_1(x)$ and $u_2(x)$ to (4.24), where $u_1(0) = r_{\lambda_1}$ and $u_1(L) = -r_1$ with $S_{\lambda_1}(r_1) = L - S_{\lambda_1}(r_{\lambda_1})$ and $u_2(x) = -u_1(L - x)$ as depicted in Figure 4.15 (left).

Now suppose we have $\lambda_2 > \lambda^*(L)$ with $\lambda_2 > \lambda_1$ and that $S_{\lambda_2}(r)$ has a turning point at an $r_t \in D(S_{\lambda_2})$ in Figure 4.14 (right). Then for this value of λ there will

be "outer" solutions $u_1(x)$ and $u_2(x)$ to (4.24), where $u_1(0) = r_t$, $u_1(L) = -r_1$ and again $u_2(x) = -u_1(L - x)$ as depicted in Figure 4.15 (right).

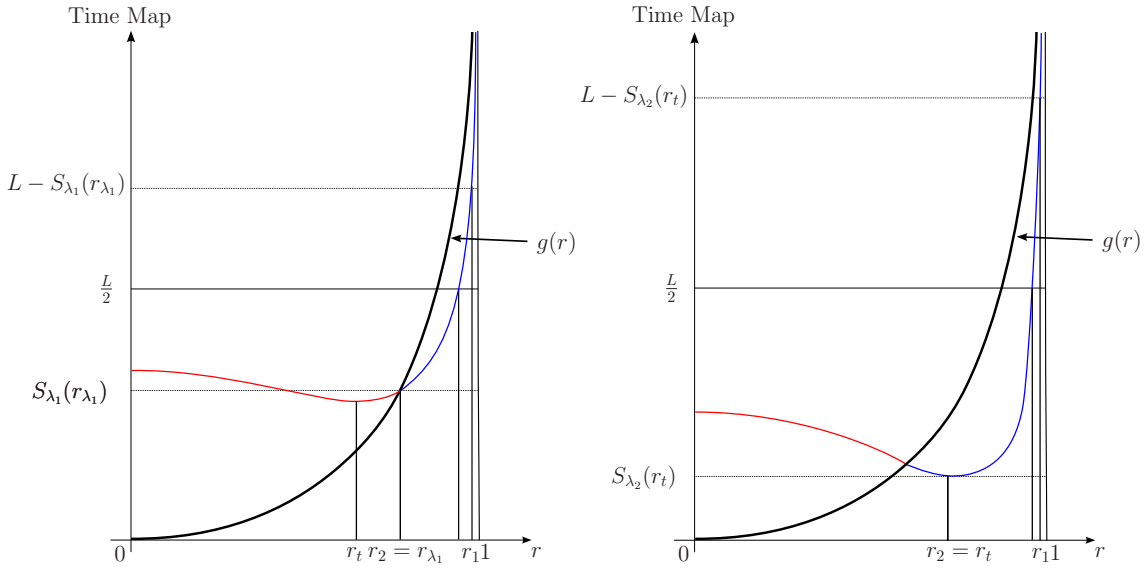

Figure 4.14: Construction of the non-classical "outer" solutions for $\lambda = \lambda_1$ [$r_t \in D(T_{\lambda_1})$] (left) and $\lambda = \lambda_2$ [$r_t \in D(S_{\lambda_2})$] (right) with $\lambda_1 < \lambda_2$, ($L = 2.5$, $\lambda_1 = 4.5$, $\lambda_2 = 8$ with $\min_{r\in[r_\lambda,1)} S_\lambda(r) \simeq 0.6854$ for $\lambda = 4.5$ and $\min_{r\in[r_\lambda,1)} S_\lambda(r) \simeq 0.3332$ for $\lambda = 8$ - see (4.36)).

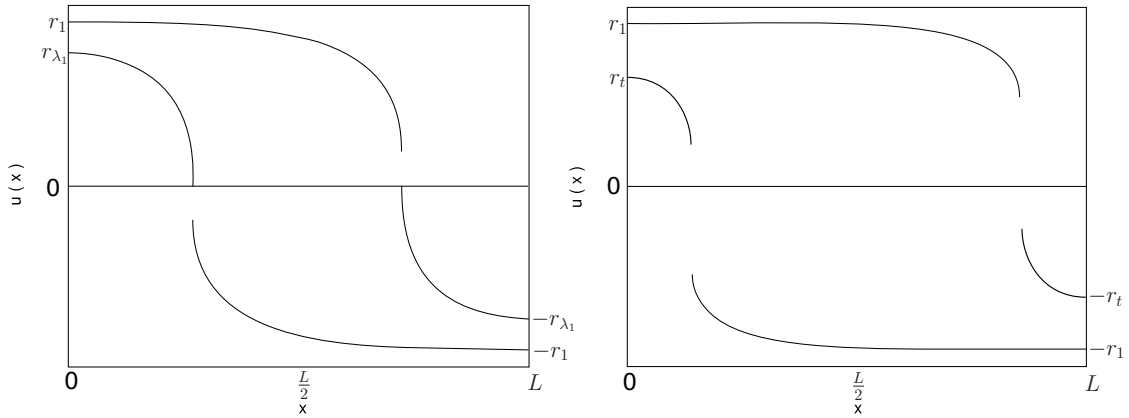

Figure 4.15: The non-classical "outer" solutions for $\lambda = \lambda_1$ [$r_t \in D(T_{\lambda_1})$] (left) and $\lambda = \lambda_2$ [$r_t \in D(S_{\lambda_2})$] (right) with $\lambda_1 < \lambda_2$, ($L = 2.5$, $\lambda_1 = 4.5$, $\lambda_2 = 8$ with $r_1 \simeq 0.9955$, $r_2 = r_\lambda \simeq 0.8165$ for $\lambda = 4.5$ and $r_1 \simeq 0.9998$, $r_2 = r_t \simeq 0.6498$ for $\lambda = 8$.

As we show below, the set of BV solutions constructed above has dynamical stability properties: we can generate quite easily initial conditions for which the dynamic problem (3.18) converges as $t \to \infty$ to a discontinuous solution such as in Figure 4.11 or Figure 4.13 and certainly *not* to a spatially homogeneous solution. To be more specific, we take

$$u_0(x) = -\alpha \tanh\left(\beta\left(\frac{x}{L} - \delta\right)\right), \tag{4.37}$$

which serves as an approximation to the discontinuous steady state with discontinuity at some $x_0 = \delta L$ for $\delta \in (0,1)$. Note that in (4.37),

$$u_0(0) = -u_0(L) = \alpha \in (0,1),$$

and β is large and such that $u_0'(x_0) = -\frac{\alpha\beta}{L}$. As usual we partition the space interval $[0, L]$ by $N+1$ equally spaced grid points

$$0 = x_1 < x_2 < \ldots < x_j < \ldots < x_{N+1} = L, \tag{4.38}$$

where $x_j = (j-1)\Delta x$ and $\Delta x = \frac{L}{N} = x_{j+1} - x_j$. Throughout the numerical experiments which follow, we fix $N = 10000$. For $L = 2.5$ (supercritical) with $\lambda = 5 > \lambda^*(2.5) \simeq 4.019534$, we solve (3.18) using the built-in MATLAB PDE solver pdepe we used for the numerical simulations of Section 3.2 and we present the time evolution of the initial function

$$u_0(x) = -0.9 \tanh\left[500\left(\frac{x}{L} - 0.965\right)\right],$$

in Figure 4.16.

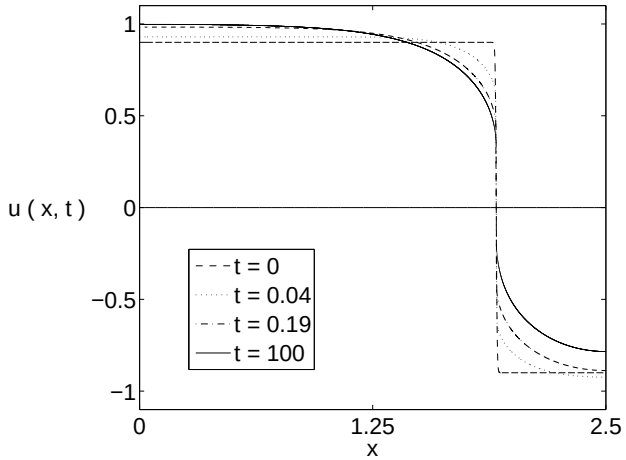

Figure 4.16: Time evolution of the initial data $u_0(x)$ in (4.37) for $\lambda = 5$, $L = 2.5$ with $\alpha = 0.9$, $\beta = 500$ and $\gamma = 0.765$.

Hence we have numerical evidence suggesting that the discontinuous equilibria for (3.18) constructed above are **normally** stable in $BV(\Omega)$ in the sense of [51]. Note that if $\mathcal{E}$ denotes the set of equilibria for the problem, then $u_* \in \mathcal{E}$ is said to be normally stable in $BV(\Omega)$ if solutions starting near $u_* \in \mathcal{E}$ exist globally and converge in BV to some (other) point on $\mathcal{E}$. We expect that the generalised principle of linearised stability developed in [51] should be applicable in this situation.

4.6.2 The free energy of solutions

Since we have a continuum of solutions to (4.24) for $\lambda > \lambda^*(L)$ with interfaces positioned at some

$$x_0 \in \left[\min_{r\in[r_\lambda,1)} S_\lambda(r), L - \min_{r\in[r_\lambda,1)} S_\lambda(r)\right],$$

it is interesting to know which has the lowest energy. In Figure 4.17, we fix $L = 2.5$ (supercritical), and $\lambda = 5 > \lambda^*(L) \approx 4.019534$ and solve the dynamic problem (3.18), (4.37) with $\alpha = 0.9$, $\beta = 500$ and $\delta = 0.5, 0.7, 0.73$ and 0.765 respectively and each solution converges to a discontinuous steady state. We treat $E[u](t)$, the free energy for the solution $u(x,t)$ to (3.18), (4.37), as an integral with respect to x and apply the trapezoidal rule at each time step. Then for a particular stationary solution $u(x)$ to the bistable Rosenau equation in (3.18)

$$\begin{aligned} E[u(x)](t=T) &= \int_0^L \sqrt{1+(u'(x))^2} - 1 - \lambda F(u(x))\,dx \\ &= \int_0^L \mathcal{E}(x)\,dx \\ &\simeq \frac{\Delta x}{2}[\mathcal{E}(0) + 2\mathcal{E}(x_2) + 2\mathcal{E}(x_3) + \ldots + 2\mathcal{E}(x_N) + \mathcal{E}(L)], \end{aligned}$$

using the discretisation of the space interval $[0, L]$ in (4.38). Hence we have also plotted in Figure (4.17) the time evolution of the free energy for each of the

stationary solutions obtained above with a given interface at some $x_0 \in (0, L)$.

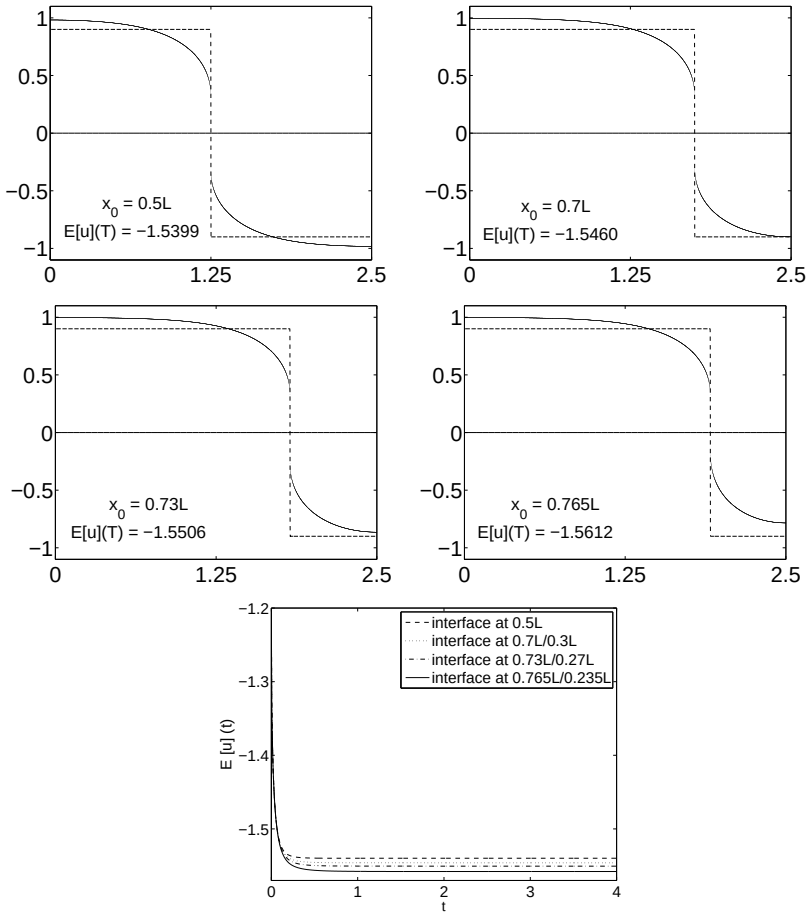

Figure 4.17: Time evolution of the free energy for the stationary solutions to (3.18), (4.37) with interface at $x_0 = 1.25$, 1.75, 1.825 and 1.9125.

Since $E[u] = E[-u]$ for any solution $u(x)$ to (4.24), a given monotone non-classical solution $u(x)$ with interface positioned at $x_0 = S_\lambda(u(0))$ will have the same free energy as the corresponding monotone non-classical solution $v(x) = -u(L - x)$ with interface positioned at $x_0 = L - S_\lambda(u(0))$. To see this, consider

$$\begin{aligned} E[v] &= \int_0^L \sqrt{1 + [v'(x)]^2} - 1 - \lambda F(v(x))\, dx \\ &= \int_0^L \sqrt{1 + [u'(L-x)]^2} - 1 - \lambda F(u(L-x))\, dx \\ &= \int_0^L \sqrt{1 + [u'(x)]^2} - 1 - \lambda F(u(x))\, dx = E[u]. \end{aligned}$$

Hence we have Figure 4.18 in which the plot of the position of the interface x_0 against energy $E[u]$ for a particular value of L and $\lambda > \lambda^*(L)$ is shown where the outer values x_1 and x_2 represent $\min_{r\in[r_\lambda,1)} S_\lambda(r)$ and $L - \min_{r\in[r_\lambda,1)} S_\lambda(r)$ respectively. Note in the case of $\lambda = 5$, $\min_{r\in[r_\lambda,1)} S_\lambda(r) = S_\lambda(r_\lambda)$.

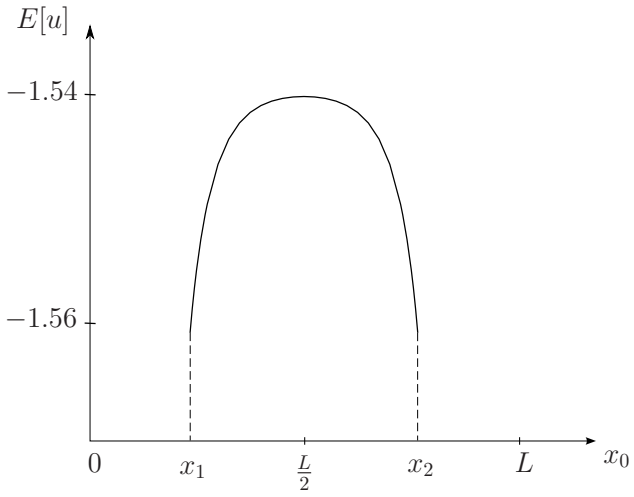

Figure 4.18: Plot of position of interface x_0 against energy $E[u]$ of stationary solutions to (4.24) corresponding to $L = 2.5$ and $\lambda = 5$.

4.6.3 Propagation of discontinuities

Finally for a fixed supercritical L, we take initial data with a jump discontinuity in $(0, L)$ and solve the full evolution problem (3.18) for λ large enough so that there can exist discontinuous equilibria to (3.18), i.e. for $\lambda > \lambda^*(L)$. We take $L = 2.5$, $\lambda = 5 > \lambda^*(L) \simeq 4.019534$ and the following piecewise constant initial data

$$u_0(x) = \begin{cases} 0.7 & 0 \le x \le \frac{L}{2} \\ -0.2 & \frac{L}{2} < x \le L. \end{cases} \tag{4.39}$$

The solution to (3.18), (4.39) at various times is presented in Figure 4.19.

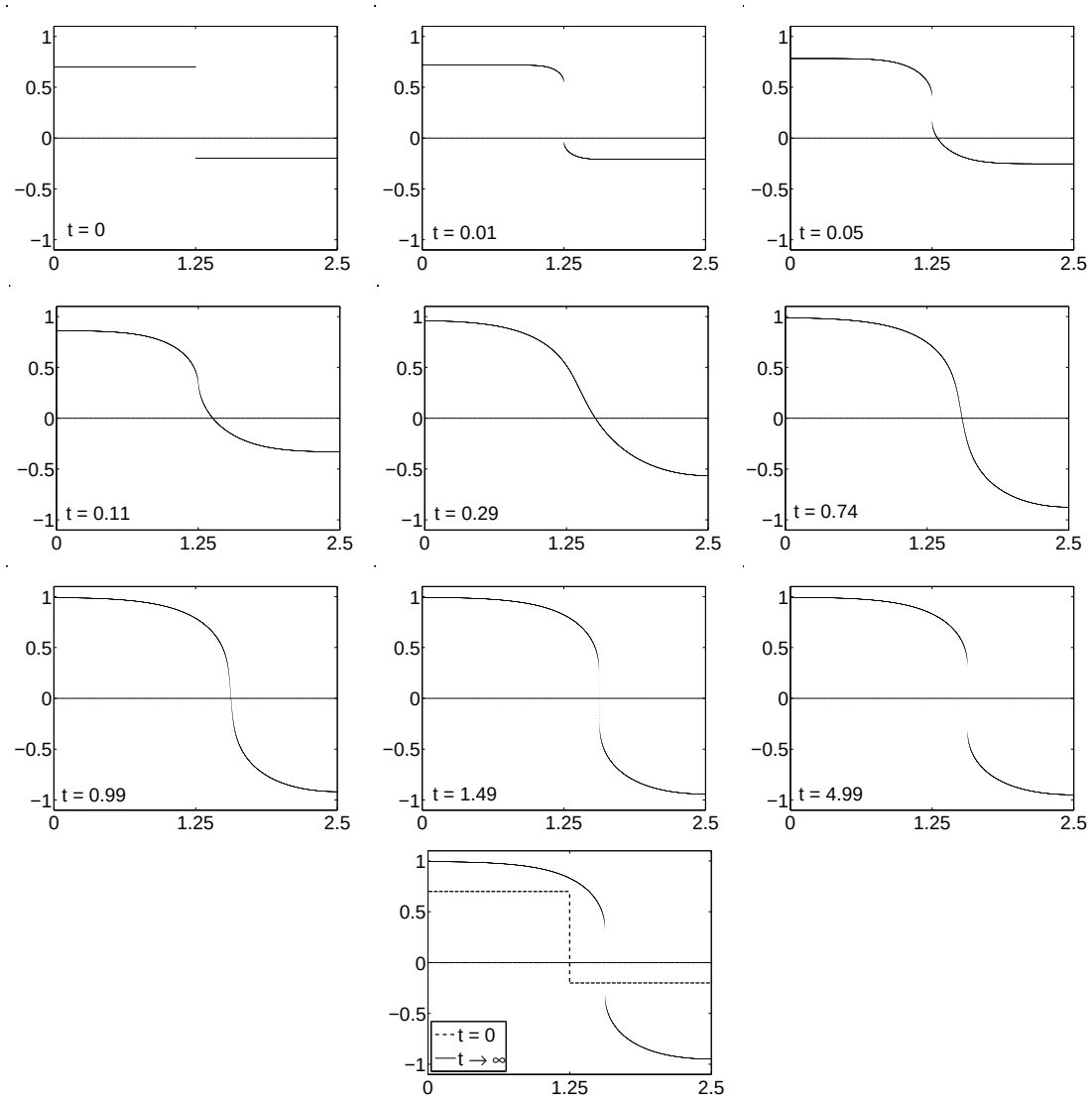

Figure 4.19: Solution to (3.18), (4.39) with $L = 2.5$ and $\lambda = 5$ at various times.

This numerical experiment suggests that if we take initial data endowed with a discontinuity in $(0, L)$ then, if the discontinuity is to move, the solution to (3.18) must become continuous first. This is also true of the integro-differential equation in (2.20) since that equation generates a semigroup in L^∞ in which the propagation of discontinuities is impossible.

4.7 Conclusions

We undertook the investigation of a boundary value problem (4.1) associated with a quasilinear reaction-diffusion equation (3.18) with a bistable kinetic nonlinearity $f(u)$ and Neumann boundary conditions. The results we have obtained are surprising. Firstly, the bifurcation structure depends not only on the diffusion coefficient ϵ but also on the length L of the space interval, which is not the case for the corresponding semilinear equation (for which $\psi(s) = s$ in (4.1)), for equations with diffusion governed by, say, the p-Laplacian operator

$$\psi(s) = \psi_p(s) = |s|^{p-2}s, \quad p > 1,$$

or indeed for equations with diffusion governed by the prescribed mean curvature operator (4.2), with a homogeneous kinetic nonlinearity. A physical interpretation of this dependence of the bifurcation diagrams on the length L is required.

Secondly, we have shown that as the bifurcation parameter $\lambda = \frac{1}{\epsilon}$ is increased, solutions to (4.24) develop infinite gradient and that for λ large enough, classical solutions to the problem cease to exist. We note that this cessation of classical solutions to a boundary value problem as a parameter passes through a critical threshold has recently been observed in models for microelectromechanical systems [10]. We also proved that the non-constant classical solutions to problem (4.24) are unstable since the free energy functional does not admit non-constant classical local minimisers. We have also presented a construction for non-classical solutions to (4.24) which are discontinuous in $(0, L)$ and shown that this construction satisfies our definition of a BV solution to the problem. Furthermore, there is numerical evidence (see Figure 4.17 and also Figure 4.19) to suggest that the problem possesses a wealth of apparently stable discontinuous stationary solutions, which is reminiscent of the situation in the integro-differential analogue of the Allen-Cahn equation (2.20), [25, 30]. Hence the loss in continuity of solutions to (4.1) appears to coincide with a gain in stability. The elucidation of the mechanism by which

stability is generated is an interesting open question. We note that this interplay of continuity and stability of stationary solutions as the bifurcation parameter is varied is observed in the case of the integro-differential equation (2.20) in [7]. For comparison with the semilinear situation, it is well-known that the classical Allen-Cahn equation with Neumann boundary conditions has no stable non-constant solutions on any convex domain.

Chapter 5

Non-local Mass Conserving Bistable Rosenau Equation

It is not hard to show that the bistable Rosenau equation discussed in the previous two chapters does not preserve the average value of the order parameter. This is not a drawback if we are modelling phase transitions in a ferromagnetic material or the evolution of the alignments in a crystalline substance but becomes a problem when modelling phase separation in a binary alloy for which the total amount of each species in the system must be conserved. Hence we are concerned in this chapter with the following non-local equation

$$\begin{aligned} u_t &= \epsilon \left(\psi(u_x)\right)_x + f(u) - \frac{1}{|\Omega|}\int_\Omega f(u)\,dx, \quad x \in \Omega,\ t > 0, \qquad (5.1)\\ u_x &= 0, \qquad\qquad x \in \partial\Omega, \quad t > 0,\\ u(x,0) &= u_0(x), \qquad x \in \Omega, \end{aligned}$$

where $\Omega = (0, L) \subset \mathbb{R}$, $L > 0$, $|\Omega|$ is the Lebesgue measure of Ω and ϵ, $\psi(s)$ and $f(u)$ are as in previous chapters. The equation does conserve mass since, if we

integrate (5.1) over Ω, we obtain

$$\begin{aligned}\frac{d}{dt}\int_\Omega u(x,t)\,dx &= \int_\Omega u_t\,dx \\ &= \epsilon\int_\Omega \left(\frac{u_x}{\sqrt{1+u_x^2}}\right)_x dx + \int_\Omega f(u)\,dx - \frac{1}{|\Omega|}\int_\Omega\left(\int_\Omega f(u)\,dy\right)dx \\ &= 0, \end{aligned} \tag{5.2}$$

from the Neumann boundary conditions and so we must have that

$$\int_\Omega u(x,t)\,dx = \int_\Omega u_0(x)\,dx \quad \forall t>0.$$

There are various ways to introduce (5.1). One is simply by analogy with the Rubinstein-Sternberg equation (2.13). Another way is as described in Section 2.1.4 where we noted that (5.1) can be viewed as the constrained gradient flow of the free energy functional (2.24) on the linear manifold $\mathcal{M} = \hat{u} + L_0^2(\Omega)$ in the Hilbert space $L^2(\Omega)$ where $\hat{u}$ is some element of $L^2(\Omega)$ and

$$L_0^2(\Omega) = \left\{ v \in L^2(\Omega) \ : \ \int_\Omega v(x)\,dx = 0 \right\}.$$

We will be analysing the stationary problem associated with (5.1) on Ω and so from this point of view, we can also introduce (5.1) by considering the Cahn-Hilliard version of the bistable Rosenau equation (3.1), that is,

$$\begin{aligned} &u_t = -(\epsilon(\psi(u_x))_x + f(u))_{xx}, \ \ x\in\Omega, \ t>0, \\ &u_x = 0 \text{ and } (\epsilon(\psi(u_x))_x + f(u))_x = 0, \ \ x\in\partial\Omega, \end{aligned} \tag{5.3}$$

which can be obtained as the H^{-1}-gradient flow of the free energy functional in (2.25). Note that one can integrate the stationary problem associated with (5.3) twice using the Neumann boundary conditions to obtain the stationary problem associated with (5.1). Hence stationary solutions to (5.1) are stationary solutions to (5.3) and so since we are primarily interested in the stationary problem for (5.1), the fact that (5.1) is nonlocal is not very important. We note that the Cahn-Hilliard version of the non-local integro-differential equation in (2.20) with

Neumann boundary conditions is considered in [4] in which well-posedness of that problem is proven. We conclude this chapter with a study of a mass-conserving numerical scheme for (5.1) and some numerical simulations of (5.1) using this scheme.

5.1 The stationary problem

We are interested in this section in characterising the multiplicity of solutions to the stationary problem associated with (5.1),

$$\begin{aligned} (\psi(u_x))_x + \lambda f(u) - \frac{\lambda}{L}\int_0^L f(u(x))\,dx = 0, \quad x \in (0,L), \qquad (5.4)\\ u_x = 0, \quad \text{at } x = 0,\ L,\\ \frac{1}{L}\int_0^L u(x)\,dx = M, \end{aligned}$$

as the bifurcation parameter $\lambda = \frac{1}{\epsilon}$ varies in $(0,\infty)$. We will see that the solutions to (5.4) depend not only on their average mass M but also on the length L of the space domain. As in previous chapters, we will be taking $f(u) = u - u^3$ however, the arguments below can easily be adapted to handle any bistable nonlinearity.

5.1.1 Liapunov-Schmidt reduction

Just as we did for the non-conserving problem (4.24) in Section 4.3, we use the method of Liapunov-Schmidt reduction described in Section 2.3 to obtain local bifurcation results for (classical) solutions to the non-local equation in (5.4). Note that if $u(x)$ is a solution to (5.4) then $u(L-x)$ is also a solution to (5.4) and so bifurcations from the trivial solution $u(x) = M$ of (5.4) arise as pitchforks.

This work is a quasilinear analogue to work done in [26] which considers the case where $\psi(s) = s$ in (5.4) and uses local bifurcation and path-following methods to

examine the changes in bifurcation diagrams of stationary solutions to the Cahn-Hilliard model of phase separation as the mass constraint is varied.

We set $v = u - M$ and recast problem (5.4) as

$$G(v, \lambda, M) = 0,$$

where

$$G(v, \lambda, M) = \left(\frac{v_x}{\sqrt{1 + (v_x)^2}} \right)_x + \lambda f(v + M) - \frac{\lambda}{L} \int_0^L f(v(x) + M)\, dx. \qquad (5.5)$$

Hence we regard G as an operator $G : D(G) \subset H \to H$ where $D(G)$ is given by

$$D(G) = \left\{ v \in C^2((0, L)) \ : \ v'(0) = v'(L) = 0, \ \frac{1}{L} \int_\Omega v(x)\, dx = 0 \right\},$$

and H is the space

$$H = \left\{ w \in C((0, L)) \ : \ \frac{1}{L} \int_0^L w(x)\, dx = 0 \right\}.$$

The linearisation about the trivial solution $v = 0$ is given by

$$\begin{aligned} (dG)_{0,\lambda,M} \cdot w &= \frac{d}{dh} G(0 + hw, \lambda, M)|_{h=0} \\ &= w_{xx} + \lambda f'(M) w - \frac{\lambda}{L} \int_0^L f'(M) w(x)\, dx \\ &= w_{xx} + \lambda f'(M) w, \end{aligned}$$

since $w \in D(G)$. Hence $\ker(dG)_{0,\lambda,M}$ is one-dimensional when $\lambda = \lambda_k = \dfrac{k^2 \pi^2}{L^2 f'(M)}$ and is spanned by $v_k = \cos\left(\frac{k\pi x}{L}\right)$. Thus in a neighbourhood of a bifurcation point $(\lambda_k, 0)$ of (5.4), we aim to show that solutions of

$$G(v, \lambda, M) = 0$$

on H are in one-to-one correspondence with solutions of the reduced equation

$$h(\lambda, y) = 0, \qquad y \in \mathbb{R},$$

through a Liapunov-Schmidt reduction. Let

$$S = (dG)_{0,\lambda_k,M} : D(G) \to H,$$

with kernel $\mathcal{K}$ and range $\mathcal{R}$ given by

$$\mathcal{K} = \left\{ \text{span} \left[\cos\left(\frac{k\pi x}{L}\right) \right] \right\},$$

and

$$\mathcal{R} = \left\{ w \in H : \int_0^L w(x) \cos\left(\frac{k\pi x}{L}\right) \, dx = 0 \right\}, \tag{5.6}$$

respectively, and let $E : H \to \mathcal{R}$ denote the projection of H onto $\mathcal{R}$. As for the non-conserving problem (4.24), the linearisation S of the equation (5.4) at a bifurcation point $(\lambda_k, 0)$ is self-adjoint and Fredholm of index zero and so, following the steps in Section 2.3, the spaces $D(G)$ and H are decomposed as

$$D(G) = \mathcal{K} \oplus \mathcal{K}^\perp, \qquad H = \mathcal{K} \oplus \mathcal{K}^\perp,$$

since $\mathcal{K} = \mathcal{R}^\perp$ and $\mathcal{K}^\perp = \mathcal{R}$. The coordinates chosen in the Liapunov-Schmidt reduction are then

$$v_k^* = 2\cos\left(\frac{k\pi x}{L}\right), \quad v_k = \cos\left(\frac{k\pi x}{L}\right),$$

and we denote the L^2-inner product on $[0, L]$ by $\langle \cdot, \cdot \rangle$.

We now proceed to calculate the derivatives given in (2.51) of the reduced function $h(\lambda, y)$ in order to determine locally the direction of the pitchfork bifurcations from the trivial solution $u(x) = M$ of (5.4) for a given L and a given M. This is more complicated than for the non-conserving problem (4.24) since unlike the operator Θ defined in (4.12), the operator G in (5.5) is not odd and so terms involving S^{-1} in (2.51) will not necessarily vanish. In order to invert S we will need to solve an ordinary differential equation; see (5.7).

From (2.50) we have

$$\begin{aligned}(d^2G)_{0,\lambda_k,M}(w_1,w_2) &= \frac{\partial^2}{\partial t_1 \partial t_2} G(0+t_1w_1+t_2w_2,\lambda_k,M)\\ &= \lambda_k f''(M)w_1w_2 - \frac{\lambda_k}{L}\int_0^L f''(M)w_1(x)w_2(x)\,dx,\end{aligned}$$

and so

$$\begin{aligned}(d^2G)_{0,\lambda_k,M}(v_k,v_k) &= \lambda_k f''(M)\cos^2\left(\frac{k\pi x}{L}\right) - \frac{\lambda_k}{L}\int_0^L f''(M)\cos^2\left(\frac{k\pi x}{L}\right)\,dx\\ &= \lambda_k f''(M)\cos^2\left(\frac{k\pi x}{L}\right) - \lambda_k\frac{f''(M)}{2}.\end{aligned}$$

Hence by (2.51)

$$\begin{aligned}h_{yy} &= \left\langle v_k^*, d^2G(v_k,v_k)\right\rangle\\ &= \int_0^L 2\cos\left(\frac{k\pi x}{L}\right)\left[\lambda_k f''(M)\cos^2\left(\frac{k\pi x}{L}\right) - \lambda_k\frac{f''(M)}{2}\right]\,dx\\ &= 0.\end{aligned}$$

Set

$$(d^2G)_{0,\lambda_k,M}(v_k,v_k) = \lambda_k f''(M)\cos^2\left(\frac{k\pi x}{L}\right) - \lambda_k\frac{f''(M)}{2} = p(x).$$

so that

$$p'(0) = p'(L) = 0,$$

and

$$\frac{1}{L}\int_0^L p(x)\,dx = 0,$$

therefore $(d^2G)_{0,\lambda_k,M}(v_k,v_k) \in H$.

However,

$$\begin{aligned}&\int_0^L (d^2G)_{0,\lambda_k,M}(v_k,v_k)\cos\left(\frac{k\pi x}{L}\right)\,dx\\ &\qquad = \int_0^L \left[\lambda_k f''(M)\cos^3\left(\frac{k\pi x}{L}\right) - \lambda_k\frac{f''(M)}{2}\cos\left(\frac{k\pi x}{L}\right)\right]\,dx\\ &\qquad = 0,\end{aligned}$$

so that $(d^2G)_{0,\lambda_k,M}(v_k, v_k) \in \mathcal{R}$ by (5.6). Therefore $(d^2G)_{0,\lambda_k,M}(v_k, v_k) \in H$ trivially decomposes as

$$(d^2G)_{0,\lambda_k,M}(v_k, v_k) = (d^2G)_{0,\lambda_k,M}(v_k, v_k) + 0,$$

where $(d^2G)_{0,\lambda_k,M}(v_k, v_k) \in \mathcal{R}$ and of course $0 \in \mathcal{R}^{\perp}$. Thus, since $E : H \to \mathcal{R}$ is the projection of H onto the range of S, we have

$$E[(d^2G)_{0,\lambda_k,M}(v_k, v_k)] = (d^2G)_{0,\lambda_k,M}(v_k, v_k),$$

and we consider

$$\begin{aligned} S^{-1}E[(d^2G)_{0,\lambda_k,M}(v_k, v_k)] &= S^{-1}(d^2G)_{0,\lambda_k,M}(v_k, v_k) = l(x) \\ \Rightarrow (d^2G)_{0,\lambda_k,M}(v_k, v_k) &= Sl(x). \end{aligned}$$

Thus the second order ordinary differential equation that we need to solve for $l(x)$ in order to obtain $S^{-1}E[(d^2G)_{0,\lambda_k,M}(v_k, v_k)]$ is

$$l''(x) + \lambda_k f'(M) l(x) = \lambda_k f''(M) \cos^2\left(\frac{k\pi x}{L}\right) - \lambda_k \frac{f''(M)}{2}, \tag{5.7}$$

which has solution

$$l(x) = \cos\left(\frac{k\pi x}{L}\right) - \frac{1}{6}\frac{f''(M)}{f'(M)} \cos\left(\frac{2k\pi x}{L}\right),$$

so that

$$S^{-1}E[(d^2G)_{0,\lambda_k,M}(v_k, v_k)] = \cos\left(\frac{k\pi x}{L}\right) - \frac{1}{6}\frac{f''(M)}{f'(M)} \cos\left(\frac{2k\pi x}{L}\right).$$

Hence we compute

$$\begin{aligned} &d^2G(v_k, S^{-1}E[d^2G(v_k, v_k)]) \\ &\quad = d^2G\left(\cos\left(\frac{k\pi x}{L}\right), \cos\left(\frac{k\pi x}{L}\right) - \frac{1}{6}\frac{f''(M)}{f'(M)} \cos\left(\frac{2k\pi x}{L}\right)\right) \\ &\quad = \lambda_k f''(M) \left[\cos^2\left(\frac{k\pi x}{L}\right) - \frac{1}{6}\frac{f''(M)}{f'(M)} \cos\left(\frac{2k\pi x}{L}\right) \cos\left(\frac{k\pi x}{L}\right)\right] \\ &\quad\quad - \lambda_k \frac{1}{L}\int_0^L f''(M) \left[\cos^2\left(\frac{k\pi x}{L}\right) - \frac{1}{6}\frac{f''(M)}{f'(M)} \cos\left(\frac{2k\pi x}{L}\right) \cos\left(\frac{k\pi x}{L}\right)\right] dx \\ &\quad = \lambda_k f''(M) \left[\cos^2\left(\frac{k\pi x}{L}\right) - \frac{1}{6}\frac{f''(M)}{f'(M)} \cos\left(\frac{2k\pi x}{L}\right) \cos\left(\frac{k\pi x}{L}\right)\right] - \lambda_k \frac{f''(M)}{2}, \end{aligned}$$

and so we have

$$\begin{aligned}\langle v_k^*, 3d^2G(v_k, S^{-1}E[d^2G(v_k,v_k)])\rangle \\ &= \int_0^L 6\lambda_k f''(M)\left[\cos^3\left(\frac{k\pi x}{L}\right) - \frac{1}{6}\frac{f''(M)}{f'(M)}\cos\left(\frac{2k\pi x}{L}\right)\cos^2\left(\frac{k\pi x}{L}\right)\right]dx \\ &\quad - \int_0^L 3\lambda_k f''(M)\cos\left(\frac{k\pi x}{L}\right)dx \\ &= -\frac{\lambda_k L}{4}\frac{[f''(M)]^2}{f'(M)} = -\frac{k^2\pi^2}{4L}\frac{[f''(M)]^2}{[f'(M)]^2}. \end{aligned} \tag{5.8}$$

In addition to this,

$$\begin{aligned}(d^3G)_{0,\lambda_k,M}(w_1,w_2,w_3) &= \frac{\partial^3}{\partial t_1\partial t_2\partial t_3}G(0+t_1w_1+t_2w_2+t_3w_3,\lambda_k,M)|_{t_1=t_2=t_3=0} \\ &= -3[w_3''w_1'w_2' + w_2''w_1'w_3' + w_1''w_2'w_3'] + \lambda_k f'''(M)w_1w_2w_3 \\ &\quad - \lambda_k f'''(M)\frac{1}{L}\int_0^L w_1(x)w_2(x)w_3(x)\,dx,\end{aligned}$$

so that

$$\begin{aligned}(d^3G)_{0,\lambda_k,M}(v_k,v_k,v_k) &= -9[v_k''(v_k')^2] + \lambda_k f'''(M)v_k^3 - \lambda_k f'''(M)\frac{1}{L}\int_0^L v_k^3(x)\,dx \\ &= \frac{9k^4\pi^4}{L^4}\cos\left(\frac{k\pi x}{L}\right)\sin^2\left(\frac{k\pi x}{L}\right) + \lambda_k f'''(M)\cos^3\left(\frac{k\pi x}{L}\right),\end{aligned}$$

and

$$\begin{aligned}\left\langle v_k^*, d^3G(v_k,v_k,v_k)\right\rangle &= \int_0^L\left[\frac{18k^4\pi^4}{L^4}\cos^2\left(\frac{k\pi x}{L}\right)\sin^2\left(\frac{k\pi x}{L}\right) + 2\lambda_k f'''(M)\cos^4\left(\frac{\pi x}{L}\right)\right]dx \\ &= \frac{3k^2\pi^2}{4L^3}\left(3k^2\pi^2 + L^2\frac{f'''(M)}{f'(M)}\right).\end{aligned} \tag{5.9}$$

Therefore from (2.51), (5.8) and (5.9) we obtain

$$\begin{aligned}h_{yyy} &= \left\langle v_k^*, d^3G(v_k,v_k,v_k) - 3d^2G(v_k, S^{-1}E[d^2G(v_k,v_k)])\right\rangle \\ &= \frac{3k^2\pi^2}{4L^3[f'(M)]^2}\left(3k^2\pi^2[f'(M)]^2 + L^2f'''(M)f'(M) + \frac{L^2}{3}[f''(M)]^2\right).\end{aligned} \tag{5.10}$$

Also,

$$G_\lambda(v,\lambda,M) = f(v+M) - \frac{1}{L}\int_0^L f(v(x)+M)\,dx,$$

so that $G_\lambda(0, \lambda_k, M) = 0$ which implies that

$$(d^2G)_{0,\lambda_k,M}(v_k, S^{-1}E[G_\lambda(0, \lambda_k, M)]) = 0, \tag{5.11}$$

while

$$\begin{aligned}(dG_\lambda)_{0,\lambda_k,M} \cdot w &= f'(M)w - \frac{1}{L}\int_0^L f'(M)w(x)\,dx \\ &= f'(M)w, \end{aligned} \tag{5.12}$$

for any $w \in D(G)$. Therefore, from (2.51), (5.11) and (5.12) we have

$$\begin{aligned} h_{\lambda y} &= \left\langle v_k^*, dG_\lambda(v_k) - d^2G(v_k, S^{-1}EG_\lambda)\right\rangle \\ &= \int_0^L 2\cos\left(\frac{k\pi x}{L}\right) f'(M)\cos\left(\frac{k\pi x}{L}\right)\,dx \\ &= Lf'(M). \end{aligned} \tag{5.13}$$

By the preceding calculations,

$$h = h_y = h_{yy} = h_\lambda = 0,$$

and so we therefore have from Proposition 2.13 that

$h_{\lambda y}h_{yyy} < 0 \Rightarrow$ a supercritical bifurcation from the trivial solution occurs;

$h_{\lambda y}h_{yyy} > 0 \Rightarrow$ a subcritical bifurcation from the trivial solution occurs.

So, for $f(s) = s - s^3$, consider first taking $M = 0$. In this case, $h_{\lambda y} = L > 0$ by (5.13) and we need to determine where h_{yyy} changes sign.

From (5.10), when $M = 0$,

$$h_{yyy} = \frac{3k^2\pi^2}{4L^3}(3k^2\pi^2 - 6L^2),$$

which will be negative for L large enough i.e. for $L > \frac{k\pi}{\sqrt{2}}$ and so we have that the bifurcation from the trivial solution is subcritical if $L < \frac{k\pi}{\sqrt{2}}$ and supercritical

if $L > \frac{k\pi^2}{\sqrt{2}}$. This corresponds with the result obtained in Proposition 4.4 for the non-conserving equation

$$\left(\frac{u'}{\sqrt{1+(u')^2}}\right)' + \lambda f(u) = 0, \qquad (5.14)$$
$$u'(0) = u'(L) = 0,$$

as we would expect since, as we noted in Section 4.1, non-constant classical solutions to (5.14) are represented by a trajectory encircling the origin, starting and ending on the u-axis in the phase plane for the first order system (4.6) associated with (5.14). The symmetry in the phase plane means that a non-constant classical solution $u(x)$ to (5.14) has zero mean, i.e.

$$\frac{1}{L}\int_0^L u(x)\,dx = 0,$$

and, by integrating (5.14) over $\Omega = (0, L)$, we see that

$$\frac{1}{L}\int_0^L f(u)\,dx = 0.$$

Therefore non-constant *classical* solutions to (5.14) are solutions to (5.4) in the case that $M = 0$.

Now suppose $0 < |M| < \frac{1}{\sqrt{5}}$ we again need to determine where h_{yyy} in (5.10) changes sign in order to answer the question of how many stationary solutions there are for a given L and a given M such that $0 < |M| < \frac{1}{\sqrt{5}}$ as λ varies in a neighbourhood of a bifurcation point $(\lambda_k, 0)$. Solving $h_{yyy} = 0$ for L^2 as a function of M gives

$$L^2 = (L^*)^2 := \frac{k^2\pi^2}{2}\frac{[1-3M^2]^2}{(1-5M^2)},$$

and taking the positive square root of this gives

$$L = L^* := \frac{k\pi}{\sqrt{2}}\frac{[1-3M^2]}{\sqrt{1-5M^2}}, \qquad (5.15)$$

which has a vertical asymptote when $|M| = \frac{1}{\sqrt{5}}$ and a turning point when $|M| = \frac{1}{\sqrt{15}}$. We plot the relationship between this critical value of L in (5.15) and M for some $k \in \mathbb{N}$ in Figure 5.1.

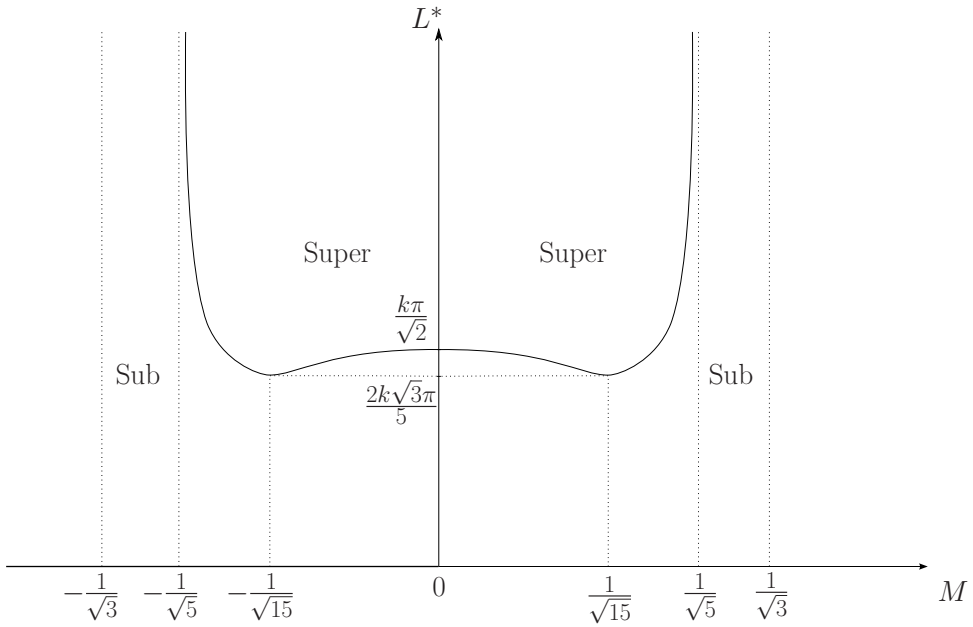

Figure 5.1: Plot of length L^* against mass M for some $k \in \mathbb{N}$, $(k = 1)$.

Consider

$$
\begin{aligned}
h_{yyy} = \frac{3k^2\pi^2}{4L^3[f'(M)]^2}\left(3k^2\pi^2[f'(M)]^2 + L^2f'''(M)f'(M) + \frac{L^2}{3}[f''(M)]^2\right) > 0 \\
\Leftrightarrow 3k^2\pi^2[f'(M)]^2 + L^2f'''(M)f'(M) + \frac{L^2}{3}[f''(M)]^2 > 0 \\
\Leftrightarrow 3k^2\pi^2(1-3M^2)^2 - 6L^2(1-3M^2) + 12L^2M^2 > 0 \\
\Leftrightarrow 3k^2\pi^2(1-3M^2)^2 > 6L^2 - 30L^2M^2 \\
\Leftrightarrow k^2\pi^2(1-3M^2)^2 > 2L^2(1-5M^2) \\
\Leftrightarrow L^2 < \frac{k^2\pi^2}{2}\frac{(3M^2-1)^2}{1-5M^2} = (L^*)^2,
\end{aligned}
$$

since $0 < |M| < \frac{1}{\sqrt{5}}$ so that $1 - 5M^2 > 0$.

Also, we note that for all $L > 0$ with $\frac{1}{\sqrt{5}} < |M| < \frac{1}{\sqrt{3}}$,

$$3k^2\pi^2[f'(M)]^2 + L^2 f'''(M)f'(M) + \frac{L^2}{3}[f''(M)]^2$$
$$= 3k^2\pi^2(1-3M^2)^2 + 6L^2(5M^2-1) > 0,$$

so that from (5.10), $h_{yyy} > 0$ for all for all such L and M. Therefore, since $h_{\lambda y} = f'(M)L > 0$ for all M such that $|M| < \frac{1}{\sqrt{3}}$, we have established:

Proposition 5.1. *For $0 \leq |M| < \frac{1}{\sqrt{5}}$, the k-th bifurcation from the trivial solution of (5.4) is a supercritical pitchfork if $L > L^*$ and a subcritical pitchfork if $L < L^*$ (with L^* given in (5.15)). For $\frac{1}{\sqrt{5}} < |M| < \frac{1}{\sqrt{3}}$, bifurcation from $u(x) = M$ is a subcritical pitchfork for all L. In the parameter regime $|M| \geq \frac{1}{\sqrt{3}}$, no local bifurcations from the constant solution $u(x) = M$ exist for any L.*

Remark: Note that, just as in the non-conserving situation discussed in Section 4.3, it is again possible to have either subcritical or supercritical bifurcations for different values of k.

5.1.2 Nonexistence of classical solutions for λ large enough

For fixed L and $a \in \mathbb{R}$, we consider

$$\left(\frac{u'}{\sqrt{1+(u')^2}}\right)' + \lambda f(u) = \lambda a, \tag{5.16}$$
$$u'(0) = u'(L) = 0,$$

which can be written as the first order system

$$\begin{cases} u' = v, \\ v' = \lambda(a - f(u))(1+v^2)^{\frac{3}{2}}, \end{cases} \tag{5.17}$$

with the first integral given by

$$H(u,v) = \frac{1}{\sqrt{1+v^2}} + \lambda(au - F(u)). \tag{5.18}$$

Integrating (5.16) over $\Omega = (0, L)$ we see that

$$\frac{1}{L}\int_0^L f(u(x))\,dx = a,$$

hence we can think of (5.16) as an ancillary problem for (5.4) and we will use (5.16) to gain insight into the multiplicity of solutions to (5.4). We begin with the following Lemma.

Lemma 5.2. *For a fixed L and any $a \in \mathbb{R}$ such that $|a| < \frac{2}{3\sqrt{3}}$, there is a number $\lambda^*(a, L)$ such that $\forall \lambda > \lambda^*(a, L)$, there are no non-constant classical solutions to (5.16).*

Proof. Suppose $0 < a < \frac{2}{3\sqrt{3}}$ so that the equation $f(u) = a$ has three solutions u_l, c, u_r with $u_l < 0 < c < u_r$ where $(u_l, 0)$ and $(u_r, 0)$ are saddle points for (5.17) and $(c, 0)$ is a centre. From considerations on the first integral (5.18) associated with the ancillary problem (5.16) one can see that for $\lambda < \lambda_h(a)$, there is a homoclinic loop connecting $(u_r, 0)$ to itself which, for a particular $\lambda < \lambda_h(a)$, we have denoted by γ_λ in Figure 5.2. Note that for each a, $\lambda_h(a)$ is obtained through solving

$$H(u_r, 0) = H(c, -\infty),$$

for $\lambda = \lambda_h(a)$. Non-constant classical solutions to (5.16) for $\lambda < \lambda_h(a)$ are represented in the phase plane by trajectories which encircle the centre $(c, 0)$, start and end on the u-axis and which are *contained within* γ_λ.

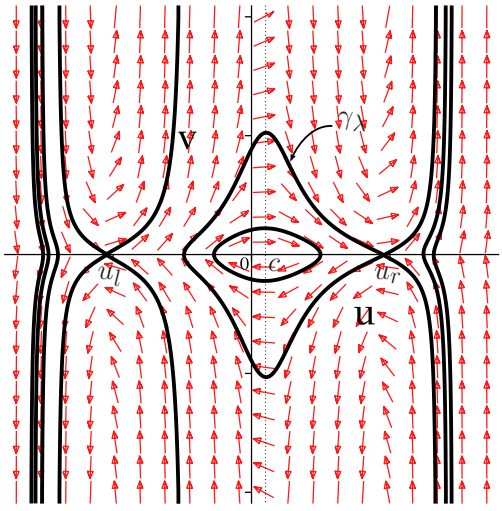

Figure 5.2: Phase portrait for (5.17) with $\lambda < \lambda_h(a)$ ($a = 0.1$, $\lambda = 3 < \lambda_h(0.1) = 6.3426$).

For λ large enough, i.e. for $\lambda = \lambda_h(a)$, the homoclinic loop will break. Through further considerations on $H(u, v)$, one sees that if $\lambda > \lambda_h(a)$, as in Figure 5.3, there exist values $u^*(\lambda)$ and $u^{**}(\lambda)$ such that $u^*(\lambda) < c < u^{**}(\lambda)$,

$$H(u^*(\lambda), 0) = H(u^{**}(\lambda), 0), \tag{5.19}$$

and

$$u^*(\lambda) \to c^-, \ u^{**}(\lambda) \to c^+ \ \text{ as } \lambda \to \infty. \tag{5.20}$$

Note that for each λ, we can find $u^*(\lambda)$ for each $\lambda > \lambda_h(a)$ by solving

$$H(u^*(\lambda), 0) = H(c, \infty),$$

for $u_l < u^*(\lambda) < c$ and then obtain $u^{**}(\lambda)$ via (5.19). Hence non-constant classical solutions to (5.16) are now confined to γ_λ^* as in Figure 5.3 which is the region enclosed by the trajectories through $(u^*(\lambda), 0)$ and $(u^{**}(\lambda), 0)$ in the phase plane.

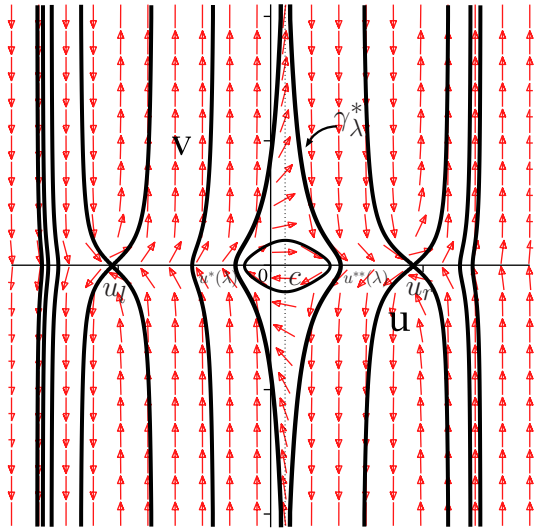

Figure 5.3: Phase portrait for (5.17) with $\lambda > \lambda_h(a)$, ($a = 0.1$, $\lambda = 15 > \lambda_h(0.1) \simeq 6.3426$).

Now assume that for a given λ and a given $n \in \mathbb{N}$, there exists a non-constant classical solution $u(x)$ to (5.16) which has n points of inflection in $(0, L)$. Such a

solution will have period equal to $\frac{2L}{n}$. For λ large enough, because of (5.20), the only possible non-constant Neumann classical solutions to (5.16) will be in a small neighbourhood of the centre, hence we linearise (5.16) around $(c, 0)$ to obtain

$$u'' + \lambda f'(c)u = 0.$$

Thus the period of such a solution is equal to

$$\frac{2\pi}{\sqrt{\lambda f'(c)}}, \tag{5.21}$$

which is well-defined since $0 < c < \frac{1}{\sqrt{3}}$ so that $f'(c) > 0$ but (5.21) will not be equal to $\frac{2L}{n}$ if λ is large enough. This contradiction proves Lemma 5.2 in the case that $0 < a < \frac{2}{3\sqrt{3}}$. The case $-\frac{2}{3\sqrt{3}} < a < 0$ can be treated similarly. Note that in the case that $a = 0$ (in which non-constant classical solutions to (5.16) are also solutions to the non-conserving equation (4.24)), there are heteroclinic loops connecting saddle points which break for λ large enough rather than homoclinic loops but the arguments carry through just as easily. □

Remark: We note that for each $0 < a < \frac{2}{3\sqrt{3}}$, if λ is small enough then the phase portrait for (5.17) contains non-trivial classical solutions to the ancillary problem (5.16) which are also non-trivial classical solutions to (5.4) for some $0 < M < 1$. Similarly, for each $-\frac{2}{3\sqrt{3}} < a < 0$, if λ is small enough then the phase portrait for (5.17) contains non-trivial classical solutions to (5.16) which are also non-trivial classical solutions to (5.4) for some $-1 < M < 0$. If $a = 0$ then for λ small enough, the phase portrait for (5.17) contains non-trivial classical solutions to (5.16) which are also non-trivial classical solutions to (5.4) with $M = 0$.

Just as we did in Chapter 4 for the stationary problem (4.24) associated with the non-conserving equation (3.18), we now concentrate on the multiplicity of *monotone* classical solutions to (5.4) where without loss of generality, $0 \leq M < \frac{1}{\sqrt{3}}$ so that from now on, for $a \in \left[0, \frac{2}{3\sqrt{3}}\right)$, $\lambda^*(a, L)$ represents the value of λ for which there are no monotone classical solutions to (5.16) $\forall \lambda > \lambda^*(a, L)$. We

also note that when $a = 0$, the value $\lambda^*(0, L)$ corresponds to the value arising in Section 4.4 that we denoted by $\lambda^*(L)$, i.e. the value of λ such that monotone classical solutions to (4.24) develop infinite gradient in $(0, L)$ and the bifurcation diagrams for monotone classical solutions to (4.24) stop. Therefore we have that $\lambda^*(a, L) \to \lambda^*(0, L) = \lambda^*(L)$ as $a \to 0$. Also, the value $\lambda^*(a, L)$ must occur after the homoclinic orbit has broken for a fixed a so that $\lambda^*(a, L) \to \infty$ as $a \to \frac{2}{3\sqrt{3}}$.

Let us drop the dependence of $\lambda^*(a, L)$ from Lemma 5.2 on L and denote the value simply by $\lambda^*(a)$ since we will regard L as being fixed. Hence Lemma 5.2 implies that for every $a \in \left[0, \frac{2}{3\sqrt{3}}\right)$, there is a value $\lambda^*(a)$ such that monotone solutions to the ancillary problem (5.16) develop infinite gradient at some $x_0 \in (0, L)$. Therefore for every $\lambda \geq \lambda^*(0)$, there is a value of a corresponding to the inverse of $\lambda^*(a)$ which will be denoted by $a^*(\lambda)$ and be such that $a^*(\lambda) \to \frac{2}{3\sqrt{3}}$ as $\lambda \to \infty$ and $a^*(\lambda) \to 0$ as $\lambda \to \lambda^*(0)^+$. We give a sketch of the function $a^*(\lambda)$ in Figure 5.4 but note that we do not prove that the curve $a^*(\lambda)$ is continuous (see Theorem 5.4).

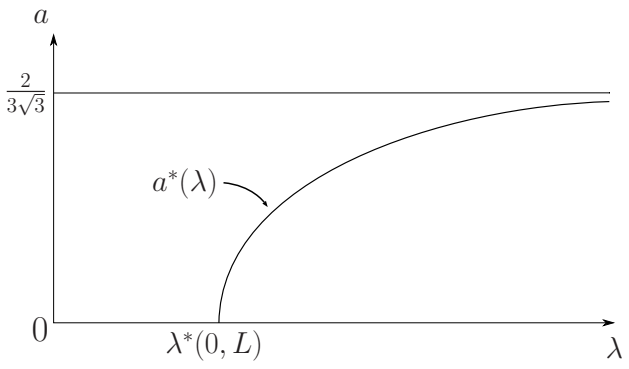

Figure 5.4: Sketch of the curve $a^*(\lambda)$ in the (λ, a)-plane.

Lemma 5.3. *For a fixed L and each $0 \leq M < \frac{1}{\sqrt{3}}$, the bifurcation curve of monotone classical solutions to (5.4) does not exist in the region in the (λ, a)-plane defined by $a^*(\lambda) < a < \frac{2}{3\sqrt{3}}$ for λ large, where $a^*(\lambda)$ is the curve obtained*

from Lemma 5.2.

Proof. Let $\tilde{a}(\lambda)$ denote the bifurcation curve of monotone classical solutions to (5.4) in the (λ, a)-plane and assume the contrary to Lemma 5.3. Then there exists a sequence $(\lambda_n)_{n=1}^{\infty}$ such that $\lambda_n \to \infty$ as $n \to \infty$ and

$$a^*(\lambda_n) < \tilde{a}(\lambda_n) < \frac{2}{3\sqrt{3}},$$

for all $n \in \mathbb{N}$ sufficiently large. Then since $a^*(\lambda_n) \to \frac{2}{3\sqrt{3}}$ as $n \to \infty$ we have by the sandwich theorem that

$$\tilde{a}(\lambda_n) \to \frac{2}{3\sqrt{3}} \text{ as } n \to \infty. \tag{5.22}$$

But M is constant along $\tilde{a}(\lambda)$ and (5.22) implies that M must be equal to $\frac{1}{\sqrt{3}}$ which is a contradiction. □

We now have the following theorem regarding (monotone) classical solutions to the non-local mass-conserving equation (5.4):

Theorem 5.4. *For fixed L and $0 \leq M < \frac{1}{\sqrt{3}}$, there exists a value $\lambda_1(M, L)$ such that for $\lambda > \lambda_1(M, L)$ there cannot exist monotone classical solutions to the non-local mass-conserving equation in (5.4).*

Proof. In the (λ, a)-plane, the curve $a^*(\lambda)$ obtained from Lemma 5.2 separates two regions; a region in which monotone classical solutions to the non-local mass-conserving equation (5.4) can exist for fixed L and $0 \leq M < \frac{1}{\sqrt{3}}$ and a region in which monotone classical solutions to (5.4) cannot exist for such L and M. As in Lemma 5.3, let $\tilde{a}(\lambda)$ denote the bifurcation curve of monotone classical solutions to (5.4). We know by Lemma 5.3, that $\tilde{a}(\lambda)$ *must* intersect the curve $a^*(\lambda)$ at some point since $\tilde{a}(\lambda)$ cannot not exist in the region defined by $a^*(\lambda) < a < \frac{2}{3\sqrt{3}}$ in the (λ, a)-plane for sufficiently large λ and from the Rabinowitz theorem (see [56, Theorem 13.10]), it has to go *somewhere* as λ increases. We want to prove that $\tilde{a}(\lambda)$ intersects $a^*(\lambda)$ at a point of continuity of $a^*(\lambda)$.

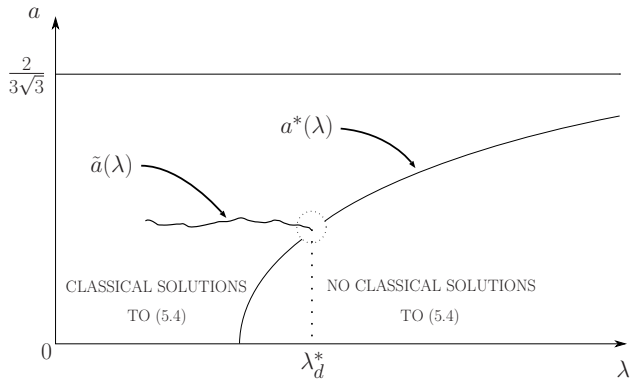

Figure 5.5: The curve $a^*(\lambda)$ and a proposed bifurcation curve $\tilde{a}(\lambda)$ of classical monotone solutions to (5.4) intersecting $a^*(\lambda)$ at a supposed point of discontinuity of $a^*(\lambda)$.

We assume the contrary and consider the bifurcation curve $\tilde{a}(\lambda)$ of monotone classical solutions to (5.4) in the (λ, a)-plane as we have it in Figure 5.5. We assume that the curve $a^*(\lambda)$ is discontinuous at some value λ_d^* and that the bifurcation curve $\tilde{a}(\lambda)$ enters the region of no classical solutions to (5.4) at this point of discontinuity of $a^*(\lambda)$. By the Rabinowitz theorem [56, Theorem 13.10] there must be a classical solution in a neighbourhood of this point λ_d^* and the bifurcation curve of classical solutions can be extended. However, we would then have entered into the region in which there can be no classical solutions to (5.4) and so we have obtained a contradiction. Hence the bifurcation curve must intersect the curve $a^*(\lambda)$ at a point of continuity and the theorem is proven.

□

Remark: Although we established Theorem 5.4 for monotone classical solutions to (5.4), the result can be generalised to non-monotone classical solutions $u(x)$ to (5.4) which have n points of inflection in $(0, L)$ for some $n \in \mathbb{N}$. Thus for *each* $n \in \mathbb{N}$, there exists a value $\lambda_n(M, L)$ such that for $\lambda > \lambda_n(M, L)$, there are no classical solutions to (5.4) with n points of inflection in $(0, L)$. However, we point out that unlike the situation in the (semilinear) Rubinstein-Sternberg equation [26],

there is no obvious way to deduce the behaviour of a particular branch of solutions to (5.4) from that of the monotone one. Also, in the proof of Theorem 5.4 we did not establish that the curve $a^*(\lambda)$ is continuous but we did show that it must be continuous at the point λ_d^* where the bifurcation curve of monotone classical solutions to (5.4) intersects it.

We have not given a precise depiction of the bifurcation curve of monotone classical solutions to the mass-conserving problem (5.4) in the (λ, a)-plane for given L and $0 \leq M < \frac{1}{\sqrt{3}}$. Hence for fixed L and M subcritical and then for fixed L and M supercritical, we numerically obtain the curve $a^*(\lambda)$ from Lemma 5.2 and the bifurcation curve $\tilde{a}(\lambda)$ of monotone classical solutions to (5.4) and plot these in the (λ, a)-plane. With regards to problem (5.4), we know that along the line of trivial solutions, $a = \frac{1}{L}\int_0^L f(u(x))\,dx$ is constant and equal to $M - M^3$. Given L, for each $0 \leq M < \frac{1}{\sqrt{3}}$, bifurcation from the trivial solution of (5.4) occurs when $\lambda = \frac{\pi^2}{L^2 f'(M)}$ which we can rearrange to

$$M = \frac{1}{\sqrt{3}}\sqrt{1 - \frac{\pi^2}{L^2\lambda}},$$

and since bifurcation points appear along the line of trivial solutions (upon which $a = M - M^3$) we can plot a curve of bifurcation points for fixed L in the (λ, a)-plane by considering the function

$$\begin{aligned} a_b(\lambda) &= M - M^3 \\ &= \frac{1}{3\sqrt{3}}\sqrt{1 - \frac{\pi^2}{L^2\lambda}}\left(2 + \frac{\pi^2}{L^2\lambda}\right). \end{aligned}$$

For a given L, we can numerically work out the value of $\lambda^*(a)$ from Lemma 5.2 for various values of $a \in \left[0, \frac{2}{3\sqrt{3}}\right)$ and then plot the curve $a^*(\lambda)$ in the (λ, a)-plane through an analysis of the time map associated with the ancillary problem (5.16) which can be defined in a similar way to the time map for the non-conserving equation (4.24) defined in Section 4.2. Using AUTO [24], we then plot the bifurcation curve $\tilde{a}(\lambda)$ of monotone classical solutions to (5.4) in the (λ, a)-plane for fixed M

and L and obtain the value $\lambda_1(M, L)$ of Theorem 5.4.

Thus we fix $L = 1$ and $M = 0.1$ so that the bifurcation at $\lambda = \frac{\pi^2}{f'(0.1)} = 10.1748500$ from the trivial solution is subcritical and $a = 0.099$ along the line of trivial solutions to (5.4). According to AUTO, the branch of monotone classical solutions to (5.4) for these parameter values stops when $\lambda = \lambda_1(0.1, 1) = 5.657873$ with $\tilde{a}(\lambda_1(0.1, 1)) = a^*(\lambda_1(0.1, 1)) = 0.02890214$ and we have plotted all relevant curves in the (λ, a)-plane in Figure 5.6.

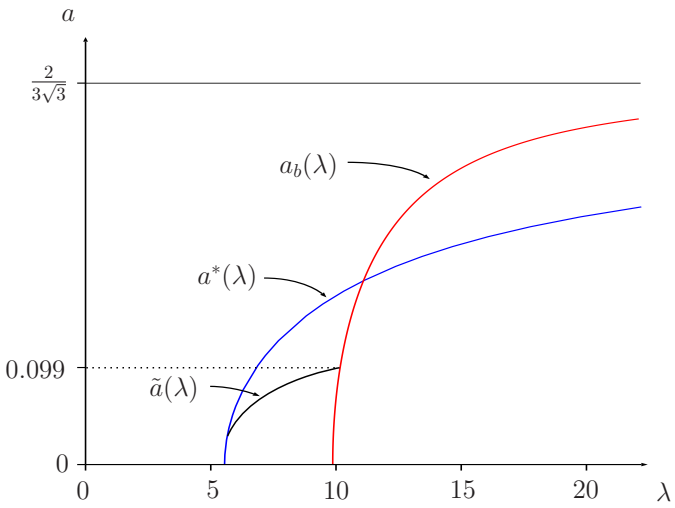

Figure 5.6: The bifurcation curve $\tilde{a}(\lambda)$ of monotone classical solutions to (5.4) for $L = 1$, $M = 0.1$ and the curves $a_b(\lambda)$ and $a^*(\lambda)$ in the (λ, a)-plane.

In the case of large L, $\lambda_h(a) \simeq \lambda^*(a)$ for each a where $\lambda_h(a)$ is the value of λ mentioned in the proof of Lemma 5.2 for which the homoclinic loop connecting the saddle point $(u_r, 0)$ to itself breaks. In Figure 5.7 we plot all relevant curves in the (λ, a)-plane for $L = 2.5$, $M = 0.3$ for which $a = 0.273$ along the line of trivial solutions to (5.4). We have a supercritical bifurcation from the trivial solution when $\lambda = \frac{\pi^2}{2.5^2 f'(0.3)} = 2.163201$ and according to AUTO, the branch of monotone classical solutions in this case stops when $\lambda = \lambda_1(0.3, 2.5) = 4.085973$ with $\tilde{a}(\lambda_1(0.3, 2.5)) = a^*(\lambda_1(0.3, 2.5)) = 0.005144947$.

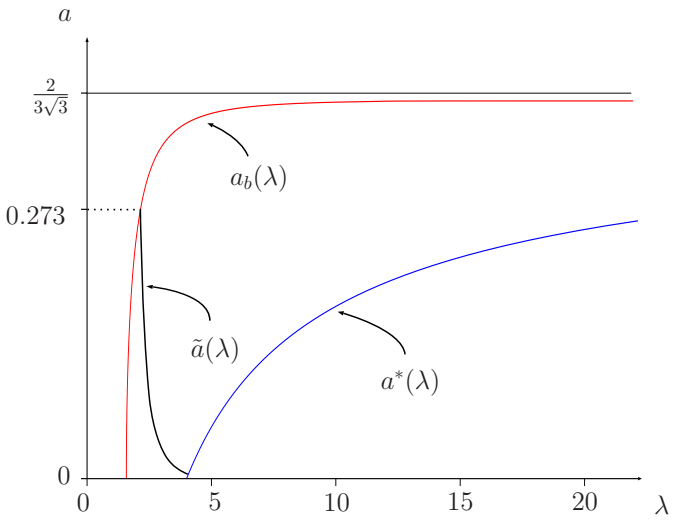

Figure 5.7: The bifurcation curve $\tilde{a}(\lambda)$ of monotone classical solutions to (5.4) for $L = 2.5$, $M = 0.3$ and the curves $a_b(\lambda)$ and $a^*(\lambda)$ in the (λ, a)-plane.

On the basis of the preceding numerical experiments we would conjecture that the bifurcation curve $\tilde{a}(\lambda)$ of classical solutions to (5.4) is monotonic and for given L and M, a is at its largest along the line of trivial solutions i.e. when $a = M - M^3$.

Remark: We have not discussed the case of having $\frac{1}{\sqrt{3}} < |M| < 1$ in (5.4), i.e. what happens in the "metastable" regime in which there are no local bifurcations from the trivial solution and for which the trivial solution is always stable. As $|M| \to \frac{1}{\sqrt{3}}$, $f'(M) \to 0$ and the first and all subsequent bifurcation points $\lambda_k = \frac{k^2\pi^2}{L^2 f'(M)}$ go off to infinity. In the semilinear situation studied in [26], in passing from the spinodal to the metastable regime, they show through spectral approximations and path-following methods that the saddle-nodes which exist for $\frac{1}{\sqrt{5}} \leq |M| < \frac{1}{\sqrt{3}}$, move off to the right as $f'(M) \to 0^+$ but at a speed much slower than that of the bifurcation points. In our case, for all L with M just less than $\frac{1}{\sqrt{3}}$ so that the bifurcation from the trivial solution is subcritical by Proposition 5.1, the classical solutions to (5.4) stop existing *before* we reach a saddle-node. Hence we were not able to perform a two parameter continuation in λ and in M of the saddle-

nodes for $|M|$ beyond $\frac{1}{\sqrt{3}}$. We can however say what happens in the parameter regime $|M| \geq 1$. By the remark after Lemma 5.2 we see that it is not possible to construct a non-trivial classical solution to the ancillary problem (5.16) which will have average mass M such that $|M| \geq 1$. One can also see from phase portraits associated with (5.17) that it is also not possible to construct a non-classical solution to (5.16) for any $|a| < \frac{2}{3\sqrt{3}}$ which will have $|M| \geq 1$. Therefore for $|M| \geq 1$, there are no non-trivial solutions to (5.4) for any $\lambda \in (0, \infty)$ which is also true of the semilinear problem (see [26]).

5.2 Numerical analysis

In this section we carry out some numerical experiments for the non-local mass-conserving equation in (5.1). The MATLAB PDE solver pdepe we used for the numerical experiments on the non-conserving problem (3.1) in Section 3.2 and Section 4.6 is not applicable here as one cannot implement the integral term in (5.1) with this solver. Therefore we first have to derive an explicit numerical method to solve the equation (5.1) and we are grateful to Dr John Mackenzie of The University of Strathclyde for discussions on the numerical scheme we outline in the following subsection.

5.2.1 Numerical approximation

We derive a mass-conserving numerical scheme to solve

$$\begin{aligned} u_t &= \left(\frac{u_x}{\sqrt{1+u_x^2}} \right)_x + \lambda f(u) - \frac{\lambda}{|\Omega|} \int_\Omega f(u)\, dx, \quad (x,t) \in Q_T \equiv \Omega \times (0,T) \\ u_x(0,t) &= u_x(L,t) = 0, \quad (x,t) \in \partial\Omega \times (0,T) \\ u(x,0) &= u_0(x), \qquad\qquad x \in \Omega, \end{aligned} \tag{5.23}$$

where $\lambda \in (0, \infty)$, $\Omega = (0, L)$, $L > 0$, $f(s) = s - s^3$ and $0 < T < \infty$. We obtain (5.23) from (5.1) by multiplying (5.1) by $\frac{1}{\epsilon}$ and scaling time as $t \mapsto \epsilon t$.

By (5.2), the non-local equation (5.23) conserves mass and to hope to have the same at the discrete level we must discretise the equation in conservative form, i.e. in the form given in (5.23).

We discretise the space interval Ω into $N+1$ evenly spaced points

$$0 = x_1 < x_2 < \ldots < x_{N+1} = L,$$

so that $\Delta x = \frac{L}{N}$ and we regard there as being cells $[x_{i-\frac{1}{2}}, x_{i+\frac{1}{2}}]$ of width Δx around each *internal* point x_i, $i = 2, \cdots, N$ while at the boundaries $i = 1$ and $i = N+1$ we use cells $[x_1, x_{\frac{3}{2}}]$ and $[x_{N+\frac{1}{2}}, x_{N+1}]$ of half width $\frac{\Delta x}{2}$ as in Figure 5.8.

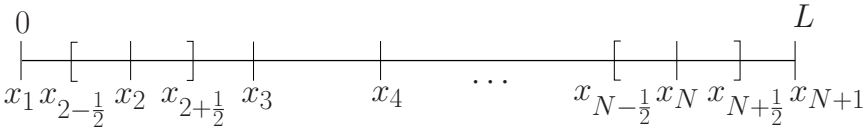

Figure 5.8: Discretisation of the space interval $[0, L]$.

At a particular $x_i \in \Omega = (0, L)$ (hence $i \in \{2 \cdots N\}$), $t_n \in (0, T)$ the equation is given by

$$u_t(x_i, t_n) = \left(\frac{u_x(x_i, t_n)}{\sqrt{1 + u_x^2(x_i, t_n)}} \right)_x + \lambda f(u(x_i, t_n)) - \frac{\lambda}{L} \int_0^L f(u(x, t_n))\, dx.$$

Let $v(x, t)$ denote the flux, i.e.

$$v(x, t) = \frac{u_x(x, t)}{\sqrt{1 + u_x^2(x, t)}}$$

so that at some $x_i \in \Omega = (0, L)$, $t_n \in (0, T)$

$$\begin{aligned} \left(\frac{u_x(x_i, t_n)}{\sqrt{1 + u_x^2(x_i, t_n)}} \right)_x &= v_x(x_i, t_n) \\ &\simeq \frac{v(x_{i+\frac{1}{2}}, t_n) - v(x_{i-\frac{1}{2}}, t_n)}{\Delta x} \end{aligned} \tag{5.24}$$

that is, we approximate the flux term by a first central difference in space at the point x_i with half-spacing.

Now,

$$v(x_{i+\frac{1}{2}},t_n) = \frac{u_x(x_{i+\frac{1}{2}},t_n)}{\sqrt{1+u_x^2(x_{i+\frac{1}{2}},t_n)}} \simeq \frac{(u(x_{i+1},t_n)-u(x_i,t_n))/\Delta x}{\sqrt{1+\left[\frac{u(x_{i+1},t_n)-u(x_i,t_n)}{\Delta x}\right]^2}} \tag{5.25}$$

and

$$v(x_{i-\frac{1}{2}},t_n) = \frac{u_x(x_{i-\frac{1}{2}},t_n)}{\sqrt{1+u_x^2(x_{i-\frac{1}{2}},t_n)}} \simeq \frac{(u(x_i,t_n)-u(x_{i-1},t_n))/\Delta x}{\sqrt{1+\left[\frac{u(x_i,t_n)-u(x_{i-1},t_n)}{\Delta x}\right]^2}} \tag{5.26}$$

so that in (5.25) we approximate the term $v(x_{i+\frac{1}{2}},t_n)$ by a first central difference in space about the point $x_{i+\frac{1}{2}}$ with half-spacing and in (5.26) we approximate the term $v(x_{i-\frac{1}{2}},t_n)$ by a first central difference in space about the point $x_{i-\frac{1}{2}}$ with half-spacing. Therefore by (5.24), (5.25) and (5.26)

$$\left(\frac{u_x(x_i,t_n)}{\sqrt{1+u_x^2(x_i,t_n)}}\right)_x = v_x(x_i,t_n) \simeq \frac{1}{\Delta x^2}\left(\frac{(u(x_{i+1},t_n)-u(x_i,t_n))}{\sqrt{1+\left[\frac{u(x_{i+1},t_n)-u(x_i,t_n)}{\Delta x}\right]^2}} - \frac{(u(x_i,t_n)-u(x_{i-1},t_n))}{\sqrt{1+\left[\frac{u(x_i,t_n)-u(x_{i-1},t_n)}{\Delta x}\right]^2}}\right).$$

We approximate the integral term in (5.23) at some given time t_n using the mid-point rule for numerical integration as follows

$$\begin{aligned}\int_0^L f(u(x,t_n))\,dx &= \int_{x_1}^{x_{\frac{3}{2}}} f(u(x,t_n))\,dx + \int_{x_{\frac{3}{2}}}^{x_{\frac{5}{2}}} f(u(x,t_n))\,dx + \ldots + \int_{x_{i-\frac{1}{2}}}^{x_{i+\frac{1}{2}}} f(u(x,t_n))\,dx \\ &\quad + \ldots + \int_{x_{N-\frac{1}{2}}}^{x_{N+\frac{1}{2}}} f(u(x,t_n))\,dx + \int_{x_{N+\frac{1}{2}}}^{x_{N+1}} f(u(x,t_n))\,dx \\ &\simeq \frac{\Delta x}{2} f(u(x_1,t_n)) + \sum_{j=2}^{N} \Delta x f(u(x_j,t_n)) + \frac{\Delta x}{2} f(u(x_{N+1},t_n)).\end{aligned}$$

Let $u(x_i, t_n) = u_i^n$ so that using the forward Euler method, we approximate (5.23) at interior points $x_i \in (0, L)$, $i = 2, \cdots, N$ by the numerical scheme

$$u_i^{n+1} = u_i^n + \Delta t \Bigg(\frac{1}{\Delta x^2} \left[\frac{u_{i+1}^n - u_i^n}{\sqrt{1 + \left(\frac{u_{i+1}^n - u_i^n}{\Delta x} \right)^2}} - \frac{u_i^n - u_{i-1}^n}{\sqrt{1 + \left(\frac{u_i^n - u_{i-1}^n}{\Delta x} \right)^2}} \right] + \lambda f(u_i^n) - \frac{\lambda}{L} \left[\frac{\Delta x}{2} f(u_1^n) + \sum_{j=2}^{N} \Delta x f(u_j^n) + \frac{\Delta x}{2} f(u_{N+1}^n) \right] \Bigg), \tag{5.27}$$

for $i = 2, \ldots, N$. At the boundary points $x = 0$ and $x = L$ we consider the discretisation in the half-cells $[x_1, x_{\frac{3}{2}}]$ and $[x_{N+\frac{1}{2}}, x_{N+1}]$ respectively, so that we have

$$u_1^{n+1} = u_1^n + \Delta t \Bigg(\frac{2}{\Delta x^2} \frac{u_2^n - u_1^n}{\sqrt{1 + \left[\frac{u_2^n - u_1^n}{\Delta x} \right]^2}} + \lambda f(u_1^n) - \frac{\lambda}{L} \left[\frac{\Delta x}{2} f(u_1^n) + \sum_{j=2}^{N} \Delta x f(u_j^n) + \frac{\Delta x}{2} f(u_{N+1}^n) \right] \Bigg), \tag{5.28}$$

and

$$u_{N+1}^{n+1} = u_{N+1}^n + \Delta t \Bigg(- \frac{2}{\Delta x^2} \frac{u_{N+1}^n - u_N^n}{\sqrt{1 + \left[\frac{u_{N+1}^n - u_N^n}{\Delta x} \right]^2}} + \lambda f(u_{N+1}^n) - \frac{\lambda}{L} \left[\frac{\Delta x}{2} f(u_1^n) + \sum_{j=2}^{N} \Delta x f(u_j^n) + \frac{\Delta x}{2} f(u_{N+1}^n) \right] \Bigg). \tag{5.29}$$

For the above numerical scheme to approximately (5.23) reasonably it must also conserve mass. Therefore we have the following theorem.

Theorem 5.5. *The explicit numerical scheme contained in (5.27), (5.28), (5.29) conserves mass.*

Proof. We multiply (5.27) by Δx and sum over $i = 2, 3, \cdots, N$ to obtain

$$\begin{aligned}\sum_{i=2}^{N} u_i^{n+1}\Delta x = \sum_{i=2}^{N} u_i^n \Delta x + \Delta t\Bigg(\sum_{i=2}^{N} \frac{1}{\Delta x}\left[\frac{u_{i+1}^n - u_i^n}{\sqrt{1+\left(\frac{u_{i+1}^n - u_i^n}{\Delta x}\right)^2}} - \frac{u_i^n - u_{i-1}^n}{\sqrt{1+\left(\frac{u_i^n - u_{i-1}^n}{\Delta x}\right)^2}}\right] \\ + \lambda \sum_{i=2}^{N} f(u_i^n)\Delta x - \sum_{i=2}^{N} \Delta x \frac{\lambda}{L}\left[\frac{\Delta x}{2} f(u_1^n) + \sum_{j=2}^{N} \Delta x f(u_j^n) + \frac{\Delta x}{2} f(u_{N+1}^n)\right]\Bigg) \\ = \sum_{i=2}^{N} u_i^n \Delta x + \Delta t\Bigg(\frac{1}{\Delta x}\left[\frac{u_{N+1}^n - u_N^n}{\sqrt{1+\left[\frac{u_{N+1}^n - u_N^n}{\Delta x}\right]^2}} - \frac{u_2^n - u_1^n}{\sqrt{1+\left[\frac{u_2^n - u_1^n}{\Delta x}\right]^2}}\right] \\ + \lambda \sum_{i=2}^{N} f(u_i^n)\Delta x - \sum_{i=2}^{N} \Delta x \frac{\lambda}{L}\left[\frac{\Delta x}{2} f(u_1^n) + \sum_{j=2}^{N} \Delta x f(u_j^n) + \frac{\Delta x}{2} f(u_{N+1}^n)\right]\Bigg)\end{aligned} \tag{5.30}$$

Now we multiply both of the boundary terms in (5.28) and (5.29) by $\frac{\Delta x}{2}$ and add the resulting equations to (5.30) to give

$$\left[\frac{u_1^{n+1}}{2} + \sum_{j=2}^{N} u_i^{n+1} + \frac{u_{N+1}^{n+1}}{2}\right]\Delta x = \left[\frac{u_1^n}{2} + \sum_{j=2}^{N} u_i^n + \frac{u_{N+1}^n}{2}\right]\Delta x$$

and so mass is conserved at the discrete level as required. □

5.2.2 Numerical experiments

We present the results of some numerical simulations for the non-local mass-conserving equation (5.23) using the explicit mass-conserving numerical scheme described in Section 5.2.1. For $0 < M < \frac{1}{\sqrt{5}}$ fixed, we choose both sub- and supercritical lengths L (see Proposition 5.1). In the subcritical case (Experiment 5.6) we use AUTO to plot the bifurcation diagram for monotone classical solutions to (5.4) and find the value $\lambda_1(M, L)$ of Theorem 5.4 for these values of M and L. Then we solve (5.23) using (5.27), (5.28), (5.29) for $\lambda < \lambda_1(M, L)$ and for $\lambda > \lambda_1(M, L)$ with monotone initial data satisfying the mass constraint and present the initial data with the final equilibrium state in each case. In the supercritical case (Experiment 5.7), we use AUTO to plot the bifurcation diagram for monotone classical

solutions to (5.4) and also for non-monotone classical solutions to (5.4) which have two inflection points in $(0, L)$. We find $\lambda_1(M, L)$ and $\lambda_2(M, L)$ the values of λ such that for all $\lambda > \lambda_i(M, L)$, there are no classical solutions to (5.4) with i inflection points in $(0, L)$ for $i = 1, 2$ respectively. We then run experiments solving (5.23) in the cases $\lambda > \lambda_1(M, L)$ and $\lambda > \lambda_2(M, L)$ using (5.27), (5.28), (5.29) for particular initial data $u_0(x)$.

Experiment 5.6. We fix $M = 0.2$ so that $L^* = 2.185609418$ from (5.15) and so, to have a subcritical L, we can take $L = 1.7$ in this case. We use path-following methods of AUTO to plot the bifurcation diagram for monotone classical solutions to (5.4) for these values of L and M in Figure 5.9. We have a subcritical bifurcation from the trivial solution $u(x) = M$ when $\lambda = \dfrac{\pi^2}{1.7^2 f'(0.2)} = 3.880782$ and according to AUTO, the bifurcation diagram for monotone classical solutions to the stationary problem stops when $\lambda = \lambda_1(0.2, 1.7) \simeq 4.303221$ as in Figure 5.9.

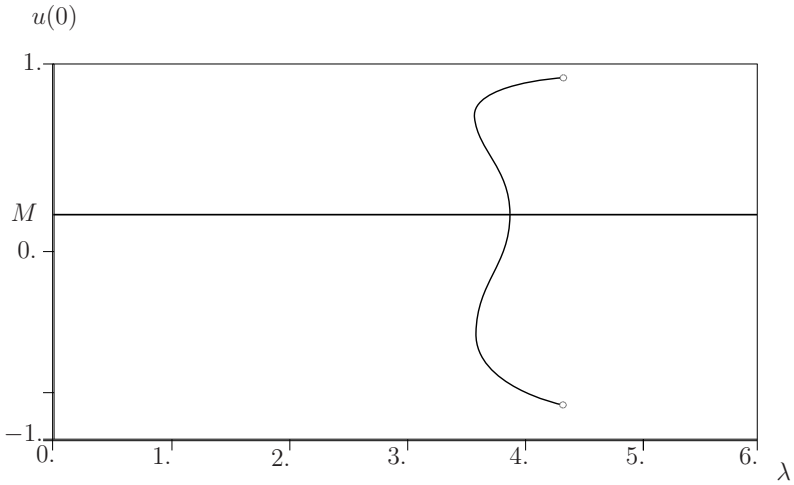

Figure 5.9: Bifurcation diagram for monotone classical solutions to (5.4) with $M = 0.2$, $L = 1.7$ where $\lambda_1(M, L) \simeq 4.043293$.

We take the following initial data

$$u_0(x) = 0.3 - 0.5 \tanh\left(1000\left[\frac{x}{L} - 0.4\right]\right), \tag{5.31}$$

which satisfies the mass constraint, i.e.

$$\frac{1}{L}\int_0^L u_0(x)\,dx = M = 0.2.$$

Hence we present the equilibrium solutions to the time-dependent problem (5.23), (5.31) in Figure 5.10 for $\lambda = 4 < \lambda_1(M, L)$ (left) and $\lambda = 5 > \lambda_1(M, L)$ (right) obtained using the scheme in (5.27), (5.28), (5.29) with $N = 500$.

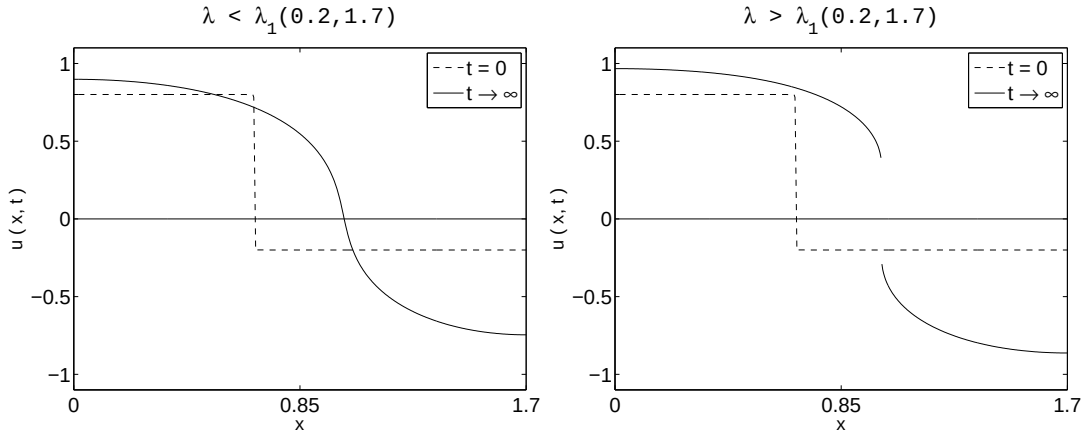

Figure 5.10: Initial data and equilibrium solutions to (5.23), (5.31) for $\lambda < \lambda_1(0.2, 1.7)$ (left) and $\lambda > \lambda_1(0.2, 1.7)$ (right).

Experiment 5.7. Suppose we now consider the case $M = 0.2$ with $L = 2.5$. We have a supercritical bifurcation from the trivial solution $u(x) = M$ when $\lambda = \dfrac{\pi^2}{2.5^2 f'(0.2)} = 1.794474$ and according to AUTO, the bifurcation diagram for monotone classical solutions to the stationary problem stops when $\lambda = \lambda_1(0.2, 2.5) \simeq 4.043293$. There is also a subcritical bifurcation from the trivial solution when $\lambda = \dfrac{4\pi^2}{2.5^2 f'(0.2)} = 7.177894$ and a curve of non-monotone classical solutions to (5.4) which stops when $\lambda = \lambda_2(0.2, 2.5) \simeq 4.987213$ just after it has reached a saddle-node at $\lambda = \lambda_{sn} \simeq 4.971442$ as in Figure 5.11.

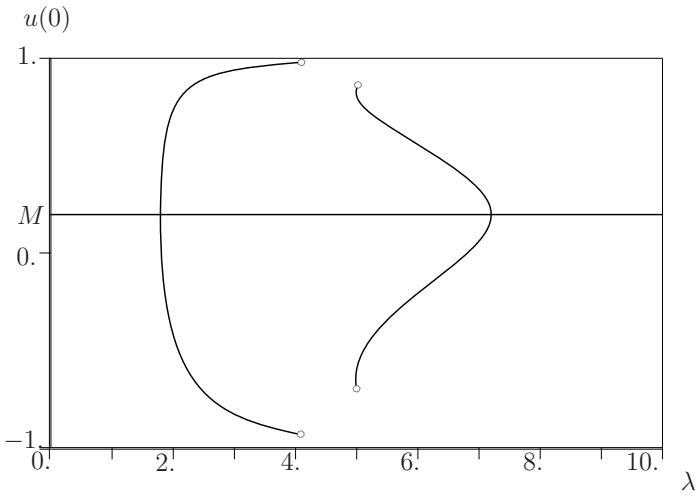

Figure 5.11: Bifurcation diagram for classical solutions to (5.4) with at most two inflection points in $(0, L)$ where $M = 0.2$, $L = 2.5$, $\lambda_1(M, L) \simeq 4.043293$, $\lambda_2(M, L) \simeq 4.987213$ and there is a saddle-node at $\lambda = \lambda_{sn} \simeq 4.971442$.

Suppose we solve (5.23) for $L = 2.5$, $M = 0.2$ and fixed $\lambda > \lambda_1(M, L)$ with initial data given by

$$u_0(x) = \beta + 0.5 \tanh\left(1000\left(\frac{x}{L} - \gamma\right)\right), \tag{5.32}$$

and we vary the position $x_0 = \gamma L$ of the interface in (5.32) but ensure that

$$\frac{1}{L}\int_0^L u_0(x) = M, \tag{5.33}$$

still holds by changing β accordingly. The results of taking $L = 2.5$, $M = 0.2$ with $\lambda = 8 > \lambda_1(0.2, 2.5) \simeq 4.043293$ and solving (5.23) for various values of γ (and β) are plotted in Figure 5.12 where one sees that modifying the initial data while ensuring that (5.33) holds has an effect on the equilibrium state to which the solution converges as $t \to \infty$ which is not the case for $\lambda < \lambda_1(M, L)$. This suggests that, as for the non-conserving situation (4.24) discussed in Section 4.6, the discontinuous equilibria for (5.1) existing for $\lambda > \lambda_1(M, L)$ are **normally** stable in the sense of [51].

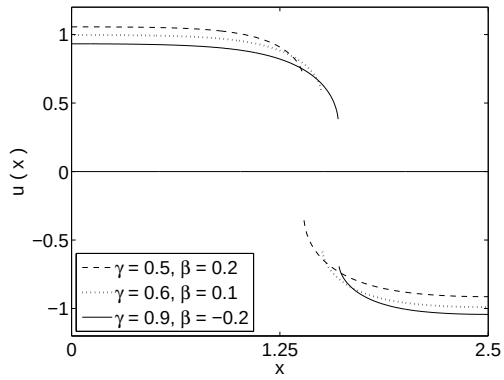

Figure 5.12: Equilibrium solutions to (5.23), (5.32) with $(\gamma, \beta) = (0.5, 0.2),\ (0.6, 0.1),\ (0.9, -0.2)$ solved using (5.27), (5.28), (5.29) with $N = 500$.

Finally we take $\lambda > \lambda_2(0.2, 2.5)$ with the following non-monotone initial data we define piecewise as follows

$$u_0(x) = \begin{cases} 0.32 - 0.6 \tanh\left(1000\left[\frac{x}{L} - 0.2\right]\right) & 0 \leq x < \frac{L}{2} \\ 0.32 + 0.6 \tanh\left(1000\left[\frac{x}{L} - 0.8\right]\right) & \frac{L}{2} \leq x < L, \end{cases} \tag{5.34}$$

which satisfies the mass constraint (5.33). In Figure 5.13 we show this initial data and the final equilibrium state to which the solution converges as $t \to \infty$ for $\lambda = 8 > \lambda_2(0.2, 2.5)$.

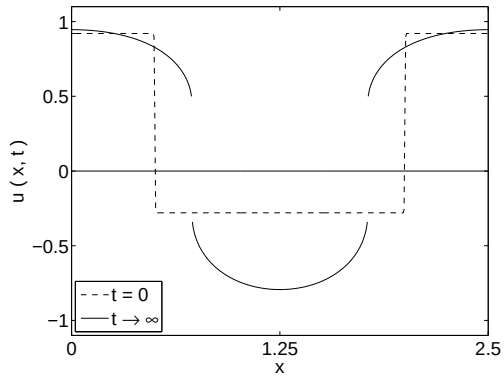

Figure 5.13: Non-monotone non-classical equilibrium solution to (5.23), (5.34) for $\lambda > \lambda_2(0.2, 2.5) \simeq 4.987213$ solved using (5.27), (5.28), (5.29) with $N = 500$.

5.3 Conclusions

The equation (5.1) we have introduced in this chapter can be viewed as a one-dimensional quasilinear version of the Rubinstein-Sternberg equation (2.13) and we have considered its associated stationary problem. We have shown in Proposition 5.1 that unlike the situation for the bifurcation diagrams of stationary solutions to the one-dimensional Cahn-Hilliard equation [26], the bifurcation behaviour for classical stationary solutions to (5.1) as λ is varied depends on the length L of the space interval Ω as well as on the average mass M of a solution. Just as we did for the stationary problem for the quasilinear version (3.1) of the Allen-Cahn equation, we have proved (Theorem 5.4) that for each $n \in \mathbb{N}$ there is a value of $\lambda = \lambda_n(M, L)$ such that for any $\lambda > \lambda_n(M, L)$ there cannot exist classical stationary solutions to (5.1) with n points of inflection in $(0, L)$. We have presented some numerical results using AUTO which illustrate Proposition 5.1 and Theorem 5.4 and we derived a mass-conserving numerical scheme for (5.1). There is numerical evidence (see Figure 5.12) to suggest that for $\lambda > \lambda_1(M, L)$, there exist a continuum of *stable* (again in the sense of [51]) non-classical monotone stationary solutions to (5.1) with a discontinuity at some $x_0 \in (0, L)$. We have also presented numerical evidence which suggests that there are also *stable* non-monotone non-classical stationary solutions to (5.1) for λ large enough (see Figure 5.13).

An understanding of what happens in the "metastable" regime $\left(\frac{1}{\sqrt{3}} < |M| < 1\right)$ is required. We were not able to perform a two parameter continuation in λ and in M of the saddle-nodes arising in the $\frac{1}{\sqrt{5}} < |M| < \frac{1}{\sqrt{3}}$ parameter regime since for M large enough, the classical solutions to (5.4) stop existing in the bifurcation diagrams before the saddle-nodes are reached. One can show however through an analysis of the phase plane associated with the ancillary problem for (5.4) that for $|M| \geq 1$, there are no non-trivial solutions to (5.4).

Chapter 6

Conclusions and further work

In Chapter 3 we introduced a one-dimensional model (3.1) for solid-solid phase transitions to replace the Allen-Cahn equation (2.7) in the case of large spatial gradients in the order parameter. We defined a BV solution to this problem via a variational inequality and proved a well-posedness result for the equation in the space of functions of bounded variation. There remains much analysis to be done on the bistable Rosenau equation (3.1). Everything concerning the asymptotic behaviour of the solutions to (3.1) is open. We were able to produce some numerical evidence which suggests that if the diffusion coefficient is small enough then solutions to (3.1) cannot coarsen to either of the two stable solutions of the kinetic equation (2.22) and that if the diffusion coefficient is large enough then solutions of the bistable Rosenau equation are asymptotic to solutions of (2.22). We have not proven a stabilisation result for (3.1). In the case of the semilinear Allen-Cahn equation (2.7), which generates a gradient system on $L^2(\Omega)$, such a stabilisation result follows from the general theory of such systems (see for example, [40]). It would perhaps be useful to have other notions of solution to (3.1) since issues such as stabilisation are best approached if one can obtain some integral representation of the solution with estimates, which seems out of reach of the variational inequalities framework. Questions of stabilisation are best considered in the framework of semigroup theory since this affords representation formulae (such as the (nonlin-

ear) variation of constants formula) for the solution and estimates on decay - see for example [50]. However, we are not aware of a semigroup theory that applies to non-accretive perturbations of accretive operators in a BV set-up such as the one we have in (3.1).

We dealt with the stationary problem (4.3) associated with (3.1) in Chapter 4 and defined BV solutions to this problem via the time-independent version of the variational inequality associated with solutions to (3.1). We have shown through a Liapunov-Schmidt reduction that the local bifurcation structure for (4.3) is dependent not only on the bifurcation parameter (which corresponds to the reciprocal of the diffusion coefficient) but also on the length L of the space interval. A physical interpretation of the dependence of the bifurcation diagrams on L is required. We proved that the non-constant classical solutions to (4.3) are unstable by showing that any non-constant classical solution of (4.3) is not a local minimum of the associated free energy functional (2.28). We have also shown through a phase plane analysis and a discussion of the time map associated with (4.3) that for each L, as the bifurcation parameter is increased, the non-constant classical solutions to (4.3) develop infinite gradient in $\Omega = (0, L)$ and the classical solutions to the problem stop existing. We concluded Chapter 4 with a discussion of non-classical solutions to (4.3) which are discontinuous in the interior of the space interval. We began with a formal construction of non-classical solutions to (4.3) by connecting different level curves of the Hamiltonian in the phase plane such that the values of the time maps at the boundary points sum to L. We then proved that this formal construction gives rise to a continuum of solutions satisfying the variational inequality associated with the stationary problem (4.3). Numerical experiments on non-classical solutions revealed that there is an intimate connection between discontinuity and stability of solutions to (4.3). That is, the loss in continuity of solutions to (4.3) appears to coincide with a gain in stability (in the sense of [51]) and an illumination as to how this stability is generated remains an open problem.

The numerical experiments also suggest that a result for convergence to equilibria for the full evolution problem (3.1) does hold and we also saw that if there was a discontinuity present in the initial data then in order for the discontinuity to move, the solution to (3.1) became continuous first. The result of this experiment suggests that the bistable Rosenau equation (3.1) generates a C_0-semigroup in BV.

Chapter 5 was concerned with a nonlocal mass-conserving version (5.1) of the bistable Rosenau equation (3.1) which can also be viewed as a quasilinear analogue of the Rubinstein-Sternberg equation (2.13). We were mainly interested in the corresponding stationary problem (5.4) for (5.1) and we proved through a Liapunov-Schmidt reduction that the bifurcation structure also depends on the length L of the space interval as well as on the average mass M of a solution and on the bifurcation parameter which was taken to be the reciprocal of the diffusion coefficient. The result holds only for M in the spinodal region, i.e. for $M \in \left(-\frac{1}{\sqrt{3}}, \frac{1}{\sqrt{3}}\right)$ since for $|M| \geq \frac{1}{\sqrt{3}}$ there are no local bifurcations from the trivial solution of (5.4). We introduced an ancillary problem (5.16) for (5.4) in order to obtain further results on classical solutions to (5.4). Using (5.16), we were able to prove that for a fixed L and $|M| < \frac{1}{\sqrt{3}}$, the non-constant classical solutions to (5.4) cease to exist once the bifurcation parameter is sufficiently large. We were able to illustrate these results using AUTO but we were not able to perform a two parameter continuation in λ and in M of the saddle nodes arising in the $\frac{1}{\sqrt{5}} < |M| < \frac{1}{\sqrt{3}}$ parameter regime since for $|M|$ large enough and close to $\frac{1}{\sqrt{3}}$, the classical solutions would stop existing before we reached a saddle node. An explanation of what happens in the metastable regime $\frac{1}{\sqrt{3}} < |M| < 1$ is required. We saw through arguments in the phase plane associated with the first order system corresponding to (5.16) that there are no non-trivial solutions to (5.4) for $|M| \geq 1$. We concluded the chapter by deriving a mass-conserving numerical scheme to solve the dynamic problem (5.1) and we were able to produce numerical evidence for the existence of stable non-monotone non-classical solutions to (5.4).

The numerical method outlined in Chapter 5 is used primarily to illustrate Theorem 5.4 and because the in-built MATLAB solver pdepe is not able to implement the integral term $\frac{\lambda}{L}\int_0^L f(u(x))\,dx$. We were restricted somewhat in the number N of space mesh points we were allowed to take. For finite difference schemes solving linear partial differential equations, there are usually restrictions on the time and space step-sizes that one can choose as one usually has to ensure that Δt and Δx satisfy a certain property in order for the numerical scheme to be stable. For example, in the case of the (parabolic) heat equation, the corresponding numerical scheme requires that

$$r = \frac{\Delta t}{\Delta x^2} \leq 0.5. \tag{6.1}$$

We cannot be sure what the equivalent statement would be for our scheme but, since our equation is also parabolic, we worked to ensure that (6.1) also held for the numerical scheme in (5.27), (5.28), (5.29). This meant that when it came to choosing a space mesh with $N+1$ mesh points and $\Delta x = \frac{L}{N}$, we were limited in our choice of times T to which we could let the scheme run because the size of $\Delta t = \frac{T}{M}$ was determined by choosing the number of time-steps M so that (6.1) was satisfied. For example, for $N = 500$ and $L = 2.5$, if we wanted the scheme to run to a final time of $T = 20$ then, from (6.1), we would need to take

$$M \geq \frac{N^2 T}{L^2 0.5} = 1600000.$$

So even for 500 space mesh points we needed to take an computationally costly number of time-steps in order to reach a final time T at which we can measure "convergence to equilibria" in the manner described in the remark at the end of Section 3.2. This discussion perhaps motivates the need for a more efficient numerical method to solve (5.23).

Bibliography

[1] R. Adams. *Sobolev Spaces*. Academic Press, New York, (1975).

[2] S. M. Allen and J. W. Cahn. A microscopic theory for antiphase boundary motion and its application to antiphase domain coarsening. *Acta Metallurgica*, **27**:1085–1095, (1979).

[3] L. Ambrosio, N. Fusco, and D. Pallara. *Functions of Bounded Variation and Free Discontinuity Problems*. Oxford University Press, (2000).

[4] P. Bates and J. Han. The Neumann boundary problem for a nonlocal Cahn-Hilliard equation. *J. Differ. Equ.*, **212**:235–277, (2005).

[5] P. W. Bates and A. Chmaj. An integrodifferential model for phase transitions: stationary solutions in higher dimensions. *J. Stat. Phys.*, **95**:1119–1139, (1999).

[6] P. W. Bates, P. C. Fife, X. Ren, and X. Wang. Traveling waves in a convolution model for phase transitions. *Arch. Rat. Mech. Anal.*, **138**:105–136, (1997).

[7] S. Bhowmik, D. B. Duncan, M. Grinfeld, and G. J. Lord. Finite to infinite steady state solutions, bifurcations of an integro-differential equation. *Disc. Contin. Dyn. Syst. B*, **16**:57–71, (2011).

[8] J. J. Binney, N.J. Dowrick, A. J. Fisher, and M. E. J. Newman. *The Theory of Critical Phenomena*. Clarendon Press-Oxford, (1992).

[9] D. Bonheure, P. Habets, F. Obersnel, and P. Omari. Classical and non-classical solutions of a prescribed curvature equation. *J. Differ. Equ.*, **243**: 208–237, (2007).

[10] N. D. Brubaker and J. A. Pelesko. Non-linear effects on canonical MEMS models. *Euro. J. App. Math.*, (2011). doi: 10.1017/S0956792511000180.

[11] M. Burns and M. Grinfeld. On a bistable quasilinear parabolic equation: well-posedness and stationary solutions. *Comm. Appl. Anal.*, (2011) (*to appear*).

[12] M. Burns and M. Grinfeld. Steady state solutions of a bi-stable quasi-linear equation with saturating flux. *Euro. J. App. Math.*, **22**:317–331, (2011). doi: 10.1017/S0956792511000076.

[13] J. W. Cahn and J. E. Hilliard. Free energy of a nonuniform system. I. Interfacial free energy. *J. Chem. Phys.*, **28**:258–267, (1958).

[14] J. Carr and R. L. Pego. Metastable patterns in solutions of $u_t = \epsilon^2 u_{xx} - f(u)$. *Comm. Pure Appl. Math.*, **42**:523–576, (1989).

[15] J. Carr, M. Gurtin, and M. Slemrod. One-dimensional structured phase transformations under prescribed loads. *J. Elasticity*, **15**:133–142, (1985).

[16] R. Casten and C. Holland. Instability results for reaction-diffusion equations with Neumann boundary conditions. *J. Differ. Equ.*, **27**:266–273, (1978).

[17] N. Chafee. Asymptotic behavior for solutions of a one-dimensional parabolic equation with homogeneous Neumann boundary conditions. *J. Differ. Equ.*, **18**:111–134, (1975).

[18] A. Chertock, A. Kurganov, and P. Rosenau. Formation of discontinuities in flux-saturated degenerate parabolic equations. *Nonlinearity*, **16**:1875–1898, (2003).

[19] R. Chill. On the Łojasiewicz-Simon gradient inequality. *J. Funct. Anal.*, **201**: 572–601, (2003).

[20] A. Chmaj and X. Ren. The nonlocal bistable equation: stationary solutions on a bounded interval. *Elec. J. Diff. Eqns.*, **2002**:1–12, (2002).

[21] E. Conway, D. Hoff, and J. Smoller. Large time behavior of solutions of systems of nonlinear reaction-diffusion equations. *SIAM J. Appl. Math.*, **1**: 1–16, (1978).

[22] L. Dascal, S. Kamin, and N. Sochen. A variational inequality for discontinuous solutions of degenerate parabolic equations. *Revista de la Real Academia de Ciencias Exactas, Fisicas y Naturales. Serie A: Matemáticas (RACSAM)*, **99**: 243–256, (2005).

[23] E. Demengel and R. Temam. Convex functions of a measure and applications. *Indiana Univ. Math. J.*, **33**:673–709, (1984).

[24] E. Doedel, R. Paffenroth, A. Champneys, T. Fairgrieve, Y. A. Kuznetsov, B. Sandstede, and X. Wang. Continuation and bifurcation software for ordinary differential equations (with HomCont). *Technical Report, Caltech*, (2001).

[25] D. B. Duncan, M. Grinfeld, and I. Stoleriu. Coarsening in an integro-differential model of phase transitions. *Euro. J. App. Math.*, **11**:561–572, (2000).

[26] J. C. Eilbeck, J. E. Furter, and M. Grinfeld. On a stationary state characterization of transition from spinodal decomposition to nucleation behaviour in the Cahn-Hilliard model of phase separation. *Phys. Lett. A*, **135**:272–275, (1989).

[27] L. C. Evans and R. F. Gariepy. *Measure Theory and Fine Properties of Functions*. CRC Press, Boca Raton, (1992).

[28] D. J. Eyre. Systems of Cahn-Hilliard equations. *SIAM J. Appl. Math.*, **53**: 1686–1712, (1993).

[29] P. C. Fife. Models for phase separation and their mathematics. *Elec. J. Differ. Equ.*, **2000**:1–26, (2000).

[30] P. C. Fife. An integro-differential analog of semilinear parabolic PDEs. in *Partial Differential Equations and Applications,* Marcel Dekker, pages 137–145, 1996.

[31] P. C. Fife and J. B. McLeod. The approach of solutions of nonlinear diffusion equations to travelling front solutions. *Arch. Rat. Mech. Anal.*, **65**:335–361, (1977).

[32] G. Fusco and J. K. Hale. Slow-motion manifolds, dormant instability, and singular perturbations. *Dyn. Diff. Equ.*, **1**:74–95, (1989).

[33] R. Glauber. Time-dependent statistics of the Ising model. *J. Math. Phys*, **4**: 294–307, (1963).

[34] M. Golubitsky and D. G. Schaeffer. *Singularities and Groups in Bifurcation Theory,* Vol. I. Springer-Verlag, New York, (1985).

[35] C. Grant. Slow motion in one-dimensional Cahn-Morral systems. *SIAM J. Math. Anal.*, **20**:21–34, (1995).

[36] M. Grinfeld, G. Hines, V. Hutson, K. Mischaikow, and G. T. Vickers. Non-local dispersal. *Diff. Int. Equ.*, **11**:1299–1320, (2005).

[37] P. Habets and P. Omari. Multiple positive solutions of a one-dimensional prescribed mean curvature problem. *Comm. in Contem. Math.*, **9**(5):1–30, (2007).

[38] J. K. Hale. *Asymptotic Behavior of Dissipative Systems,* Mathematical Surveys and Monographs, volume **25**. American Mathematical Society, (1988).

[39] J. K. Hale. Large diffusivity and asymptotic behavior in parabolic systems. *J. Math. Anal.*, **118**:455–466, (1986).

[40] D. Henry. *Geometric Theory of Semilinear Parabolic Equations,* LNM, volume **840**. Springer-Verlag, New York, (1981).

[41] K. Kawasaki. Diffusion constants near the critical point for time-dependent Ising models I. *Phys. Rev.*, **145**:224–230, (1960).

[42] A. Kurganov and P. Rosenau. On reaction processes with saturating diffusion. *Nonlinearity*, **19**:171–193, (2006).

[43] O. A. Ladyženskaja, V. A. Solonnikov, and N. N. Ural'ceva. *Linear and Quasilinear Equations of Parabolic Type*. Translations of Mathematical Monographs, American Mathematical Society: Providence RI, (1968).

[44] L. D. Landau and E. M. Lifshitz. *Statistical Physics*. Pergamon Press, Oxford, 1969.

[45] H. Matano. Asymptotic behavior and stability of solutions of semilinear diffusion equations. *Publ. RIMS, Kyoto Univ.*, **15**:401–454, (1979).

[46] F. Obersnel. Classical and non-classical sign changing solutions of a one-dimensional autonomous prescribed curvature equation. *Adv. Nonlin. Stud.*, **7**:671–682, (2007).

[47] H. Pan. One-dimensional prescribed mean curvature equation with exponential nonlinearity. *Nonlin. Anal.*, **70**:999–1010, (2008).

[48] H. Pan and R. Xing. Time maps and exact multiplicity results for one-dimensional prescribed mean curvature equations. *Nonlin. Anal.*, **74**:1234–1260, (2011).

[49] H. Pan and R. Xing. Time maps and exact multiplicity results for one-dimensional prescribed mean curvature equations. II. *Nonlin. Anal.*, **74**:3751–3768, (2011).

[50] A. Pazy. *Semigroups of Linear Operators and Applications to Partial Differential Equations,* Appl. Math. Sci, volume **44**. Springer-Verlag, New York, (1983).

[51] J. Prüss, G. Simonett, and R. Zacher. On convergence of solutions to equilibria for quasilinear parabolic problems. *J. Differ. Equ.*, **1246**:3902–3931, (2009).

[52] P. Rosenau. Free-energy functionals at the high-gradient limit. *Phys. Rev. A*, **41**:2227–2230, (1990).

[53] P. Rosenau, P. S. Hagan, R. L. Northcutt, and D. S. Cohen. Delayed diffusion due to flux limitation. *Phys. Lett. A*, **142**:26–30, (1989).

[54] J. Rubinstein and P. Sternberg. Nonlocal reaction-diffusion equations and nucleation. *IMA J. Appl. Math.*, **48**(3):249–264, (1992).

[55] R. Schaaf. *Global Solution Branches of Two Point Boundary Value Problems,* LNM, volume **1458**. Springer-Verlag, (1991).

[56] J. Smoller. *Shock Waves and Reaction-Diffusion Equations*, volume **258**. Springer-Verlag, (1994).

[57] J. Smoller and A. Wasserman. Global Bifurcation of Steady State Solutions. *J. Differ. Equ.*, **39**:269–290, (1981).

[58] A. I. Vol'pert and S. I. Hudjaev. *Analysis in Classes of Discontinuous Functions and Equations of Mathematical Physics.* Martinus Nijhoff. Dordrecht, (1985).

[59] J. M. Yeomans. *Statistical Mechanics of Phase Transitions.* Clarendon Press-Oxford, (1992).

[60] W. P. Ziemer. *Weakly Differentiable Functions,* GTM 120. Springer-Verlag, (1989).